How plant cells explore geometry

The polarity induction and geometry sensing in BY-2 tobacco protoplasts

Zur Erlangung des akademischen Grades eines

DOKTORS DER NATURWISSENSCHAFTEN

(Dr. rer. nat.)

Der Fakultät für Chemie und Biowissenschaften
Karlsruher Institut für Technologie (KIT) - Universitätsbereich
genehmigte

DISSERTATION
von

Beatrix Zaban

aus
Karlsruhe

Dekan: Prof. Dr. Peter Roesky
Referent: Prof. Dr. Peter Nick
Korreferent: Prof. Dr. Reinhard Fischer
Tag der mündlichen Prüfung: 24.10. 2014

Die vorliegende Dissertation wurde am Botanischen Institut des Karlsruher Instituts für Technologie (KIT), Abteilung Molekulare Zellbiologe, im Zeitraum von März 2011 bis September 2014 angefertigt.

Hiermit erkläre ich, dass ich die vorliegende Dissertation, abgesehen von der Benutzung der angegebenen Hilfsmittel, selbständig verfasst habe. Alle Stellen, die gemäß Wortlaut oder Inhalt aus anderen Arbeiten entnommen sind, wurden durch Angabe der Quelle als Entlehnungen kenntlich gemacht.

Diese Dissertation liegt in gleicher oder ähnlicher Form keiner anderen Prüfungsbehörde vor.

Beatrix Zaban

Karlsruhe, 05. September 2014

DANKSAGUNG

An erster Stelle möchte ich mich bei Herr Professor Dr. Nick für das in mich gesetzte Vertrauen bedanken. Ihre Kompetenz in sämtlichen Fragen, Begeisterungsfähigkeit wie auch innovativen Lehrmethoden motivieren mich seit dem ersten Tag meines Studiums. Die Impulse zu dieser Dissertation sind wesentlich durch Ihr Engagement und ihren Ideenreichtum gesetzt worden. Durch ihr Verständnis und ihre Herzlichkeit gaben Sie mir in schwierigen Zeiten während dieser Dissertation viel Kraft und ließen mich neuen Mut schöpfen. Vielen Dank, dass Sie mir all dies ermöglicht haben.

Herzlichen Dank an Herrn Professor Dr. Fischer für die Koreferenz. Ein aufrichtiges Dankeschön auch an die Prüfungskommission vertreten durch Herrn Professor Dr. Puchta, Herrn Professor Dr. Bastmeyer, Herrn Professor Dr. Taraschewski sowie Herrn Professor Dr. Fischer und Herrn Professor Dr. Nick. Vielen Dank für die Korrekturarbeiten, die bei dieser Dissertation anfielen.

Vielen Dank an unseren Kooperationspartner in Beijing, China. Durch die vom *CAS Key Lab for Biological Effects of Nanomaterials and Nanosafety* gelieferten Mikrofluidik Kanäle wurde es überhaupt erst möglich, diese Dissertation zu realisieren. Besonderer Dank geht hierbei an Dr. Wenwen Liu und Professor Dr. Xingyu Jiang.

Ein großer Dank geht an Herrn Dr. Jan Maisch, der mir immer gute Ratschläge bezüglich aller wissenschaftlichen Fragen gegeben hat und mich während der Anfertigung dieser Dissertation stets unterstützte. Vielen Dank auch an Dr. Kai Eggenberger und Dr. Michael Riemann, die immer für reibungslose Arbeitsabläufe in den Laboren und an den Mikroskopen sorgten.

Herzlicher Dank für die hervorragende technische Unterstützung durch die Laboranten und technischen Assistenten des Instituts. Insbesondere an Sabine Purper, Ernst Heene und Sybille Wörner sowie an die Auszubildenden Anna, Olivia, Anne, Julia, Bianca, Isolde, Lukas und Nadja. Ohne euch wäre diese Arbeit in dieser Zeit nicht möglich gewesen.

Den Alltag im Büro versüßten mir mit vielen sehr informativen und natürlich auch lustigen Gesprächen Frau Dr. Annette Häser, Frau Dr. Gabriele Jürges und alle Mitdoktoranden: Natalie, Qiong, Rita, Holger, Sebastian, Annabelle, Viktoria und Sahar. Ich möchte mich an dieser Stelle ganz herzlich für eure Freundschaft bedanken!

Für die tolle Arbeitsatmosphäre und das gute Miteinander möchte ich mich bei allen anderen Doktoren, Doktoranden, Hiwis, Studenten und Austauschwissenschaftlern des Botanischen Instituts sowie den Gärtnern des Botanischen Gartens bedanken.

Großer Dank geht an meine Freunde, die mich während meines Studiums und der Dissertation begleitet haben und immer für mich da waren. Danke Alex, Paola, Bianca und Dennis!

Mein größter Dank gilt meiner Familie, vor allem meinen Eltern und meinen Omas. Durch Eure Liebe wie auch der moralischen und finanziellen Unterstützung habt ihr mir ermöglicht, diese Dissertation anzugehen. Ihr seid mein Auffangnetz und seid immer für mich da. Ohne euch wäre ich nicht!

Parts of this work have been supported by a collaborating grant from the SinoGerman Science Center (project GZ614 “Probing self-organization by microfluidics”).

Parts of this work have been published in

- JIPB 55, Issue 2, *Dynamic actin controls polarity induction de novo in protoplasts,* 2013
- Scientific Reports 4, *Plant Cells Use Auxin Efflux to Explore Geometry, 2014*

Table of Content

LIST OF ABBREVIATIONS

2,4-D: 2, 4-Dichlorophenoxyacetic acid

AFs: Actin filaments

BY-2: Tobacco *Nicotiana tabacum* L. cv. Bright Yellow 2

CaMV: Cauliflower Mosaic Virus

CESA: Cellulose-synthases

CF: Calcofluor White

CPD: l- 2-carboxyphenyl

DIC: Differential Interference Contrast

GFP: Green Fluorescent Protein

IAA: Indolyl-3-acetic acid

LatB: Latrunculin B

MFs: Microfilaments

MS-Medium: Murashige and Skoog medium

MTs: Microtubules

NAA: 1-Naphthaleneacetic acid

NPA: 1-N-naphthylphthalamic acid

PBA: 1-Pyrenoylbenzoic acid

PIN: *pin-formed* protein

RGD: Arg-Gly-Asp amino acid sequence

TIBA: 2,3,5-Triiodobenzoic acid

WT: Wild type

LIST OF TABLES AND FIGURES

Tables

Figures

Introduction

Materials and Methods

Results

Discussion

ABSTRACT

In this thesis two aspects were examined: the induction of plant polarity and the geometry sensing of plant cells. To study how polarity and axes are induced de novo, protoplasts of tobacco *Nicotiana tabacum* L. cv. BY-2 expressing fluorescently tagged cytoskeletal markers are investigated. A standardized system was developed to generate and integrate quantitative data on the temporal patterns of regeneration stages. Hereinafter this system was integrated into a microfluidic platform to study the impacts of chemical and geometrical stimuli during the establishment of polarity.

Cell polarity and axis development are central for plant morphogenesis. Cell movement as central mechanism for animal morphogenesis does not play a role in the walled cells of higher plants. Plant development rather relies on flexible alignment of cell axis adjusting cellular differentiation with respect to directional cues. As central input, vectorial fields of mechanical stress, but also gradients of the phytohormone auxin have been discussed. In a tissue context mechanical and chemical signals will always act in concert, which makes it experimentally difficult to dissect their individual roles. To overcome this limitation, a novel approach, based on cells where directionality has been eliminated by removal of the cell wall, was designed in this work.

The synthesis of a new cell wall marks the transition to the first stage of regeneration and proceeds after a long preparatory phase within a few minutes. During this preparatory phase (about 0.5 d), the nucleus migrates actively and cytoplasmic strands remodel vigorously. Cell wall formation is followed by the induction of a new cell pole (stage 1), requiring dynamic actin filaments. The new cell axis (stage 2) is manifested as elongation growth perpendicular to the orientation of the aligned cortical microtubules.

This system was probed for the effect of anticytoskeletal compounds, inducible bundling of actin, RGD-peptides, and temperature. The suppression of actin dynamics at an early stage leads to aberrant tripolar cells, whereas suppression of microtubule dynamics produces aberrant sausage-like cells with asymmetric cell walls. These data were integrated into a model, where the microtubular cytoskeleton conveys positional information between the nucleus and the membrane controlling the release or activation of components required for cell wall synthesis.

For studying the chemical and geometrical impacts acting on this system, a new cell axis, using a microfluidic set-up to generate auxin gradients where rectangular microvessels are integrated orthogonally with the gradient, was imposed. Cells in these microvessels align their new axis with microvessel geometry before touching the wall. This alignment depends

on the position in the auxin gradient. Auxin efflux is necessary for this touch-independent exploration of geometry. A model, where auxin gradients can be used to align cell axis in tissues in a manner as to minimize mechanical tensions, was accomplished in this dissertation.

ZUSAMMENFASSUNG

In dieser Dissertation wurden zwei Aspekte, nämlich die Induzierung von Polarität und die Orientierung von pflanzlichen Zellen bezüglich ihrer Umgebung untersucht. In einem ersten Schritt wurde ein Modellsystem zur Polaritätsinduktion erarbeitet und im Folgenden wurde dieses System in einer mikrofluidischen Plattform angewandt um die Umgebungserkundung von Pflanzenzellen besser zu verstehen.

Die Entstehung von Zellpolarität sowie die Entwicklung einer Zellachse sind die zentralen Elemente der pflanzlichen Morphogenese. Die Entwicklung von Pflanzen beruht auf der flexiblen Anordnung der Zellachse, einzelnen Zelldifferenzierungsprozessen und Zellteilungen innerhalb eines Gewebes, sowie anderen richtungsgebenden Aspekten der systemischen Polarität. Bei den mit Zellwand umgebenen Zellen der höheren Landpflanzen spielen Zellbewegungen innerhalb eines Gewebes keine signifikante Rolle. Bei der tierischen Morphogenese hingegen beruht die Entwicklung neben Zelldifferenzierungen und Zellteilungen zum Großteil auf Zellmigrationen oder anderen zellulären Bewegungen. Als zentrale Elemente der Polaritätsausbildung bei pflanzlichen Geweben stehen seit langer Zeit mechanischer Druck sowie Gradienten des Pflanzenhormons Auxin zur Debatte.

Um zu untersuchen, wie Polarität und Zellachse de novo induziert werden, wurden in dieser Arbeit Protoplasten von *Nicotiana tabacum* L. cv. BY-2 untersucht. Die hierbei verwendeten Zellkulturen waren mit fluzoreszenten Cytoskelettmarkern versehen. Des Weiteren wird in dieser Dissertation mittels des entwickelten mikrofluidischen Systems gezeigt, wie Auxingradienten von pflanzlichen Zellen im Gewebekontext genutzt werden, um mechanische Spannungen generell zu vermeiden und zu minimieren.

Nach der BY-2 Tabakprotoplastenisolation ist die Zellwand komplett abgebaut, die Zellen sind isodiametrisch rund und die Cytoskelettelemente liegen zufällig angeordnet vor. Innerhalb des ersten Tages nach der Isolation verändert sich die Anordnung der Cytoplasmastränge und es findet ein verstärkter Vesikeltransport entlang dieser statt. Die Aktinfilamente und Mikrotubuli richten sich neu aus. Zeitgleich mit dieser Neuausrichtung ist eine aktive Kernwanderung zu einer Seite des Protoplasten zu beobachten. Nach dieser Vorbereitungsphase findet die Neusynthese der Zellwand statt. Die Zellwandsynthese geschieht innerhalb weniger Minuten und markiert den Übergang vom Protoplastenstadium (stage 0) zum ersten Regenerationsstadium (stage 1). Nach der Ausbildung der Zellwand erfolgt die Induktion eines neuen Zellpols. Dieser Prozess erfordert dynamische Aktinfilamente. Die Festlegung der Zellachse (stage 2) erfolgt hingegen über das Elongationswachstum der Zelle im rechten Winkel zur Orientierung der kortikalen

Mikrotubuli. Um ein besseres Verständnis des BY-2 Tabakprotoplastenregenerationsprozesses zu erhalten, wurden die Auswirkungen von verschiedenen Faktoren mit Hilfe des in dieser Dissertation entwickelten Systems ermittelt. Hierbei wurden die Effekte von verschiedenen Cytoskelettinhibitoren, induzierbarer Aktinfilamentbündelung, sowie die Auswirkung von RGD Peptiden und der Temperatureffekt untersucht. Wird während eines frühen Stadiums der Regeneration die Aktindynamik inhibiert, führt dies zur anormalen tripolaren Zellentwicklung. Die Hemmung der Mirkotubulidynamik ruft dahingegen eine Häufung von anormalen, wurstförmigen Zellen mit asymmetrisch angelegten Zellwänden hervor. Mikrotubuli sind wichtig für die Positionierung des Zellkerns und der Verankerung dessen an der Membran. Durch die Mikrotubuli wird die Aktivierung beziehungsweise das Freisetzen der für die Zellwandsynthese notwendigen zellulären Komponenten kontrolliert. Dynamische Aktinfilamente hingegen sind für die Induktion der Polarität *de novo* in BY-2 Tabakproplasten notwendig.

Während der Entwicklung eines Gewebes ist es schwierig, die einzelnen Effekte mechanischer und chemischer Signale voneinander zu trennen. Bei der Untersuchung dieses Sachverhaltes traten in der Vergangenheit oftmals experimentelle Schwierigkeiten auf. Um diese zu umgehen, wurde eine neue Herangehensweise entwickelt. BY-2 Tabakprotoplasten, also Zellen ohne festgelegte Richtung und Polarität, wurden innerhalb eines mikrofluidischen Systems untersucht. In einem mikrofluidischen Kanal wurden Mikrogefäße, die orthogonal zu einem induzierbaren Auxingradient angeordnet sind, mit Protoplasten befüllt. Dabei wurde die Festlegung der Zellachse während des Regenerationsprozesses untersucht. Die regenerierenden Zellen in den Mikrogefäßen richten ihre neue Zellachse entlang der Geometrie der Mikrogefäße aus. Die beginnende Zellachsenausrichtung erfolgt bereits bevor die Zelle die Begrenzung des Gefäßes berührt. Die sich entwickelnde Pflanzenzelle erkundet über den Auxin Efflux die geometrischen Gegebenheiten ihrer Umgebung und legt somit berührungsunabhängig ihre zukünftige Zellachse fest.

1. INTRODUCTION

Every multicellular organism has a direction and a special arrangement of its tissues, organs and even cells, which are shaping the geometrical structures and maintain the proper functionality of the organism. This so called polarity is determing the position of head or extremities in animals or where the roots, shoots and flowers are evolving in plants. The polarity of single cells is laid down very early in the organism's development and once the polarity or direction is determined, it cannot be easily reversed or changed. Polarity and a direction on the organism's level is determined during cell differentiation, caused i.a. by activations and interactions of different developmental genes. These mechanisms are especially well understood in *Drosophlia melanogaster* (Maung and Jenny 2011, Bayly and Axelrod 2011). Multicellularity allows assigning different functions to individual cells. Cell differentiation implies that individual cells have to upregulate specific functions balanced by down regulation of other functions. The reduced functions must be compensated by neighboring cells culminating in a situation where the individual cells cannot survive isolated from the organism context (Lintilhac 1999). The primordial form of cell differentiation is developmental dichotomy characteristic for the first formative cell division of zygotes or spores in many algae, mosses and ferns, and in the first division of the Angiosperm zygote. Developmental dichotomy stems are forming a gradient of developmental determinants within the progenitor cell that are then differentially partitioned to the daughter cells. This process is called formative cell division. Since the eighteenth century, the development of such gradients along an originally more or less homogeneous axis has been termed "polarity". This concept simply designates the specific orientation of activity in space and involves no assumptions whatsoever as to its causes (Bloch 1965).

Further phyllotaxis has been intensively studied as a model for morphogenetic responses through axis adjustment. In the growing meristem, new leaf primordia are laid down in a certain distance from preexisting leaves, leading to characteristic patterns that are under genetic control. This phenomenon has long been explained on a biophysical base: the older primordia would, due to increase tissue tension, suppress the formation of new primordia in their neighborhood. On the base of this mechanism, the position of incipient primordia could be predicted by the modeled stress-strain patterns (for a classical review see Green 1980).

This biophysical explanation was supported by work, where local release of tension using beads coated with extensin, a protein that softens the cell-wall, inverted the phyllotactic pattern (Fleming et al. 1997). Moreover, in-vivo imaging of GFP-tagged microtubules (as early readout of cell axis adjustment), in combination with ablation of meristem layers produced responses that were matched by stress-strain modeling (Hamant et al. 1998). However, there exist concurrent models, where the preexisting primordia drain their neighborhood from diffusible auxin such that no further primordia can be initiated (Reinhardt et al. 2003). This chemical model is supported by experiments, where apical meristems had been freed from any primordia by treatment with inhibitors of auxin transport, such that it was possible to generate and manipulate de-novo patterns of phyllotaxis by local application of either auxin or auxin-transport inhibitors (Reinhardt et al. 2000). The central player in the chemical model is the auxin-efflux regulator PIN1, although the observation of a residual pattern in the pin1 mutant suggests that additional factors participate in patterning (Guenot et al. 2012). A temporal separation between induction and manifestation of directionality has also been found for the *Fucus* zygote (Goodner and Quatrano 1992). The *Fucus* system has been for long time the best understood model for polarity induction, but it illustrates the general feature of symmetry break, although the phaeophycean algae do not fall into the ancestral line of terrestrial plants and therefore probably have developed polarity induction by convergent evolution.

Polarity establishment and perception of the geometry and space respecting the surrounding environment are essential mechanisms for the proper development of organisms.

Polarity can be found within the whole organism's level but also within single cells. Every cell inherits polarity information from its mother cell and thus the right polarity information is necessary for the proper generation of cell axis and later the tissue development. Exceptions for this inheritated information regarding direction are protoplasts of fungi, bacteria or plant cells and of course the famous example of the *Fucus* zygote.

Can already a single plant cell sense its surrounding geometry? In respect to the geometry and surrounding environment- how does a plant cell establish its polarity? And which cellular mechanisms are necessary for establishing this polarity? These questions are tried to be understood by the experiments, accomplished in this work.

In the following chapter a short outline is given about polarity generation in some selected model organisms.

1.1. What causes polarity? A view on selected model organisms: differences and commonalities regarding polarity

How cells acquire polarity and axis remains a central question of development. In animals, the basic structures are laid down early in development. In some cases, maternal factors have been found in complementation to the DNA, providing a kind of morphogenetic inheritance for the embryo. For example there is a gradient of maternal, untranslated mRNA encoding transcription factors such as BICOID or NANOS, determining the anterior-posterior polarity in the *Drosophila* embryo (Nüsslein-Volhard 1995). In the amphibian embryo, which provides a classical model for epigenetic morphogenesis (Spemann 1936), the dorsiventral polarity of the frog egg is established by autocatalytic feedback of polarizing signals like gravity or sperm entrance upon inherited patterns. Preformed morphogenetic movements, but also transport and translation of maternal mRNA coding for cytoskeletal proteins and polar determinants are included in these hereditable patterns (Elinson and Rowning 1988). In animals, the set up of polarity during development is laid down early, often prior to cellularisation, and furthermore a differentiation proceeds from the level of the entire organism down to the level of individual cells.

A classical system for polarity induction has been the zygote of *Fucus* (for review see Goodner and Quatrano 1993; Hable and Hart 2010). This spherical cell divides asymmetrically giving rise to a rhizoid and a thallus progenitor cell. The orientation of this division can be aligned by unilateral blue light inducing a calcium influx at the shaded flank, where later the rhizoid will emerge (Jaffe, 1966). Subsequently, a cap of fine actin filaments is observed at the rhizoid pole attracting a pronounced flow of vesicles carrying cell-wall material causing a bulge as first manifestation of the incipient rhizoid. The polarity seen in response to blue light is produced by reorientation of a preformed polarity, but truly generated *de novo*, demonstrated by induction with strong plane- polarized blue light producing a high fraction of birhizoidal twins. This beautiful system has enabled a wealth of phenomenological, physiological, and cell- biological insights into polarity induction, but it suffers from limited molecular accessibility. Comparable systems, where spherical cells undergo formative divisions, are rare in higher plants. The closest version, developing microspores, are quite different, in that they harbor a distinct preformed polarity that becomes manifest as nuclear movements as well as asymmetric cell fate of the daughter cells: the generative daughter will inherit immortality, whereas the vegetative cell is doomed to death at fertilization, giving a neat illustration of Weismann's germ line/ soma concept (Weismann 1893). By colchicine or other antimicrotubular drugs, this developmental asymmetry can be eliminated (Twell et al. 1998).

Polarized growth is also realized in fungi and there it is the dominant growth form, especially in filamentous fungi like *Aspergillus nidulans* or *Neurospora crassa*. Polarized growth in fungi is studied by genetic, molecular biological, cell biological and biochemical methods. One of the most polarized cells in nature is indeed the growing hyphae of filamentous fungi, which are widely spread in nature and cause repeatedly problems in agriculture and food production. For that they are quite interesting regarding the molecular analysis of polarized growth to identify new targets for antifungal drugs. It is also assumed that some hydrolytic proteins are secreted via the same machinery as the enzymes required for polarized growth (Pel et al. 2007).

First, within the germination process, spores start to swell and then start to polarize. Fungal hyphae are composed of compartments, which are separated by septae. One can say that the mycelium is the body of the fungus and that such complex mycelia are generated via new polarized hyphae by the way of lateral branching. Therefore the polarity of hyphal growth is an important process for fungal development. A continuous flow of secretion vesicles from the hyphal body towards the hyphal tip causes the cell wall and membrane extension. In single cell yeasts, like brewer's yeast, actin- mediated vesicle trafficking is sufficient for polar cell extension and no microtubules seem to be needed for the polarized growth of the emerging bud, but in filamentous fungi also microtubules could contribute to long- distance vesicle movement. The microtubules deliver the "cell-end marker proteins" to the cell pole, which in turn polarize the actin cytoskeleton (Fischer et al. 2008).

Well understood cell end markers are Tea1 or Tea2 of *Schizosaccharomyces pombe* (tip elongation aberrant), which are transported to microtubules plus ends and which are crucial for the formation of a protein complex that organizes the actin cytoskeleton. Tea mutants as well as mutants with abnormal microtubules show deficits in polarized growth and exhibit bent- or T- shaped cells. Besides Tea1 contributing to cell polarity, also actin cable organization via the interaction with e.g. For3 (a formin, which nucleated actin assembly) or Bud6 (an actin-binding protein), even the interphase arrangement of the microtubules is necessary for the signaling of polarity information to the cell ends. Recent studies have shown that cell end marker proteins also contribute to the polarity in e.g. *Aspergillus nidulans*. A mutation of TeaA, a Tea1 orthologue, causes a zigzag hyphal morphology (Fischer and Takeshita 2011). TeaA is delivered to the cortex by growing microtubules. Summarized it can be stated that for polarity establishment and maintenance in fungi the cytoskeleton arrangement and its organization as well as the continuous vesicle flow from the cell bogy to the growing tip and the interaction of cytoskeleton related sustaining proteins like Bud or Tea are crucial.

Plants are different from other organisms in many aspects. Plants have to sense, due to their sessile lifestyle, their position in space and their environment in a different way as animals, bacteria or fungi. The next section will give a closer view to the peculiarities concerning plant development and the generation of polarity there.

1.2. Why plants are different: Aspects of polarity establishment and geometry sensing in plant cells

Plants are different regarding their development. The genetic determination of the plant shape depends strongly on the environment and is not as strict as in animal development. As a central feature for plant morphogenesis, growth is not confined during early development, but takes place throughout the whole life cycle. The ability for adjusting growth in response to the environment is central for the individual plant adaptation towards the challenges of the habitat. Cellular movements, a central mechanism in animal development are, as consequence of the rigid cell walls, not relevant for plant morphogenesis. The basic morphogenetic unit in plant development is the individual cell. The differentiation in plants initiates from the level of individual cells and subsequently spreads to the level of the entire organism. This causes the ability to regenerate entire plants from almost any plant cell, called totipotency. In animals, totipotency is limited to the fertilized egg cell and, in some cases to its immediate descendants (Spemann 1936).

In other words, plant morphogenesis cannot rely on cell movement, because plant cells are encased by a cellulosic wall. Therefore, plants use a flexible alignment of their cell axis as major mechanism for morphogenetic changes. As they face a hypotonic environment, they expand by uptake of water and are pressed against the cell wall. This so called turgor pressure can accumulate to considerable tissue tensions, which on the one hand can be used as signal for integration of the body plan (for review see Niklas and Spatz 2004), but on the other hand have to be minimized in order to ensure tissue stability. A simple and elegant mechanism to release mechanical tension would be to orient cell axis with respect to force. In fact, the compression of plant cells in tissue culture aligns the new cell plates with the force vector (Lintilhac and Vesecky 1984). Whereas polarity in animals is usually systemic in nature and generated through interaction of different cell types, plant polarity seems to be rooted directly in the individual cell. Although polarity of individual cells can be adjusted in a flexible manner, the global polarization of an organ represents the integration of these individual polarities and therefore is relatively stable (Vöchting 1878).

Cell polarity in higher plants has been associated with the directional flux of the plant hormone auxin linked with the polar distribution of auxin- efflux carriers such as the PIN proteins (for a recent review see Peera et al. 2011). Efflux carriers are dynamically recycled between their active site at the plasma membrane and intracellular stores. This recycling differs between the different flanks of the cell such establishing a polar distribution (Dhonukshe et al. 2008). The interference with this recycling, for instance by manipulation of the Rab5 GTPase pathway, can cause an aberrant distribution of auxin and even a redetermination of organs resembling homeotic mutations. Direction- dependent recycling as mechanism to build polarity relies on a dynamic directional lattice. This lattice seems to be the actin cytoskeleton (for review see Nick 2010).

In higher plants, spherical cells that undergoing formative divisions are rare. Even developing pollen show a clear preformed directionality that during gametophytic development becomes manifest as directional movements of nucleus and organelles and as asymmetric cell fate of the daughter cells (immortal generative cells, and mortal vegetative cell). This innate directionality seems to be linked with the cytoskeleton, because the assignment of different cell fates to the daughter cells can be equalized by anti- microtubular drugs (Twell et al. 1998). In regenerating protoplasts of the moss *Physcomitrella patens* it was possible to follow how calcium channels (visualized by a fluorescent channel antagonist) redistributed during regeneration and were assigned asymmetrically to one daughter cell giving rise to the protonema (Bhatla et al. 2002). By addition of artificial auxin or inhibition of auxin efflux, but also by inhibition of channel activity, both the polar redistribution of these channels as well as the formative cell division could be blocked.

Thus, protoplasts can generate axis and polarity *de novo*. They resemble *Fucus* zygotes in this aspect. However, even a round protoplast can still maintain innate directionality. This became evident, when in a spectacular experiment, entire maize plants were regenerated after *in-vitro* fertilization of a protoplasted egg cell by an isolated sperm cell (Lörz and Kranz 1993). Regeneration in this system was only successful, when the sperm cell was fused in a specific site of the oocyte adjacent to the nucleus indicating that the preformed polarity of the egg cell had persisted during cell isolation. Despite this caveat, initial symmetry can be observed in regenerating protoplast providing an alternative to the *Fucus* system.

The following sections 1.3. and 1.4. will resume the use of BY-2 protoplast for understanding polarity establishment *de novo* in plant cells. The described *tabula rasa* approach below was developed during my diploma thesis and was the base for the following work of this dissertation.

1.3. The *tabula rasa* approach: How polarity is established in BY-2 tobacco protoplasts

To study polarity induction *de novo* in plant cells, a loss of polarity can be caused artificially by digesting the cell wall with cellulase. These protoplasts correspond to a tabula- rasa situation and lack any axis and polarity, but retain the ability to regenerate complete plants as shown in spectacular experiments on tobacco (Nagata and Takebe, 1970). The tabula- rasa approach yields protoplasts that, in most cases, are round and apparently have lost axis and polarity. Thus, protoplasts resemble the zygotes of *Fucus* with respect to *de novo* generation of polarity. The observation that regenerating protoplasts of the moss *Physcomitrella patens* show a redistribution of calcium channels, visualized by a fluorescent channel antagonist (Bhatla et al., 2002) indicate that the underlying mechanisms might be similar.

Tobacco BY-2 cells have been widely used as classical system for plant cell biology, mainly because mitosis can be readily synchronized allowing biochemical approaches to the cell cycle (Nagata et al. 1992). This cell line is more than a mere plant version of the famous “HeLa” culture, because the pluricellular files produced after subcultivation behave as a very simple organism visible as clear axis and polarity of the cell file and a temporal pattern of individual cell divisions that are synchronized by a directional flow of auxin through the cell file (Maisch and Nick 2007; review in Nick 2010). Protoplasts of this cell line therefore represent a beautiful system to study the generation of axis and polarity *de novo*. In addition, fluorescently tagged marker lines can be easily generated in this model, which allows for life-cell imaging of the morphogenetic process.

1.3.1. Staging of protoplast regeneration

Using a protocol modified from Wymer and Cyr (1992), protoplast regeneration could be observed with a high degree of developmental homogeneity, which allowed defining distinct stages of regeneration (Figure 1.3). Based on obvious or readily detectable differences in cell shape and cell- wall reformation, the vast majority of cells could be clearly assigned to one of four stages schematically represented in Figure 1.3 A: Stage 0, prevailing at the end of digestion defined as t = 0, comprised round, completely symmetrical protoplasts lacking any indications for axis or polarity (Figure 1.3 B, day 0). About 12- 24 h later, a new cell wall is synthesized, which is accompanied by vivid cytoplasmic streaming. The presence of a cell wall as visualized by staining with Calcofluor White defines stage 1. Although these cells still show radial symmetry, they already slightly deviate from a spherical shape expressed as local flattening (Figure 1.3 B, day 1). Between day 1 and day 2 of regeneration, cell shape changes distinctly, and a clear cell axis emerges leading to an ovoid shape. This cell axis represents the criterion for stage 2 (Figure 1.3 B, day 2). Subsequently, this axis becomes manifest as anisotropic expansion leading to cells, where the long axis is more than twice as long as the short axis, marking stage 3 (Figure 1.3 B, day 3). At this stage, some of the cells begin to divide axially producing pluricellular files characteristic for tobacco suspension cells. These files are indistinguishable from those deriving from walled cells. This general pattern of regeneration was observed in around 80% of the cells. However, a small but significant fraction of cells (around 20%) deviated from this canonical sequence (Zaban et al. 2013).

This experimental setup was established during my diploma thesis for the qualitative comparison of the different stages. In this dissertation, this system was extended to investigate non- directional, scalar factors and furthermore it was integrated into a microfluidic platform for testing possible manipulations and vectorial impacts.

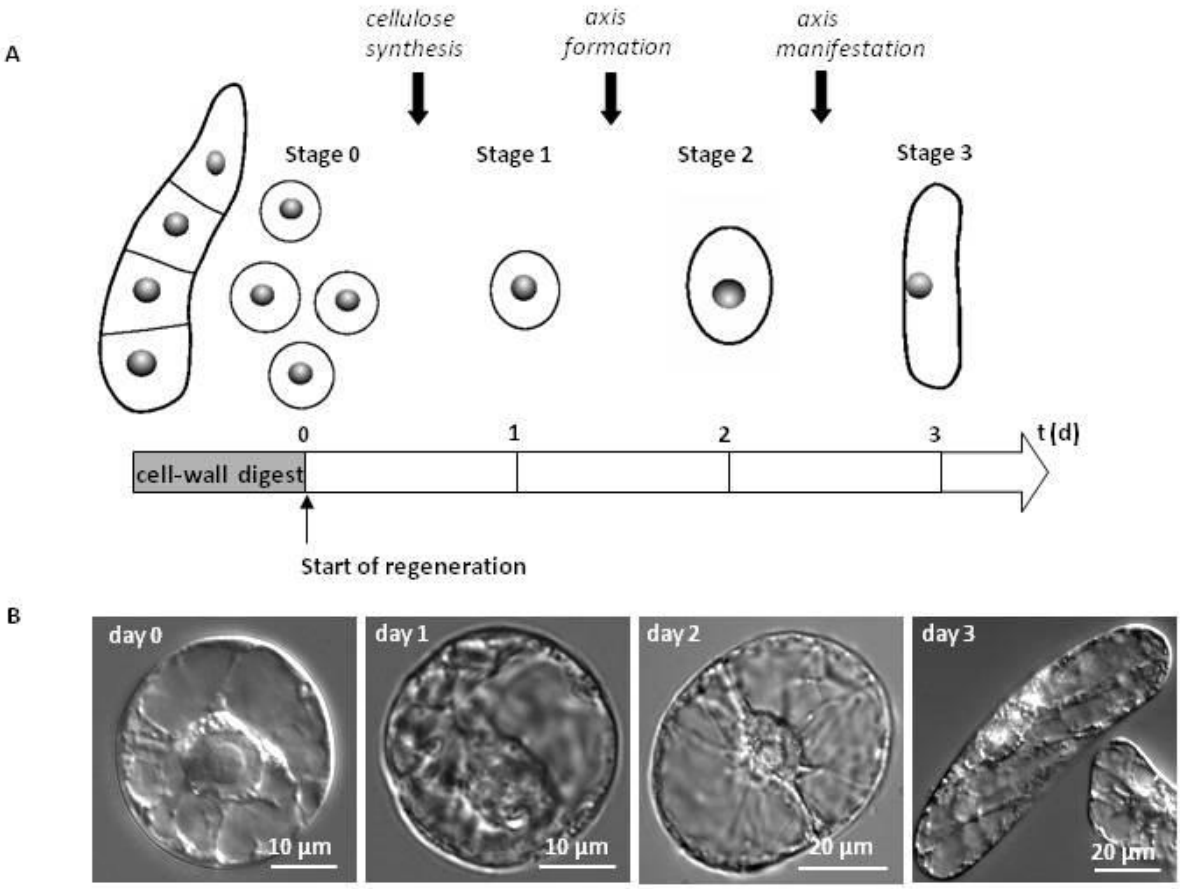

Figure 1.1.: Regeneration of tobacco BY-2 protoplasts. (A) Experimental design and definition of the stages. Suspension cultures of tobacco BY-2 are digested by treatment with cellulase YC and pectolyase Y- 23, washed to remove the enzymes, and transferred at t = 0 into regeneration medium containing synthetic auxin (NAA) and cytokinin (BAP). Regeneration can be subdivided into four distinct stages. Stage 0 is defined by radial symmetry and the absence of cellulose, stage 1 is defined by radial symmetry, but presence of cellulose, stage 2 is defined by a break of radial symmetry, stage 3 is defined by the manifestation of cell axis. (B) Representative differential- interference contrast images of BY-2 cells recorded at different time points of regeneration. Figure from Zaban et al. (2013).

1.4. The main players in the regeneration process of BY-2 tobacco cells - a view on the cellular components

In order to ensure that the process of the polarity establishment runs properly, a lot of factors within the cell must act in concert. In addition to elements of the cytoskeleton like actin filaments or microtubules, the cell- wall formation and auxin efllux are playing obviously important roles during polarity formation. This chapter will give a insight into already known facts concerning the roles of above mentioned factors towards plant cell development.

The filaments of the cytoskeleton pervade through the cytoplasm and they are significant for the structural and functional organization of the cell. Especially in animal cells, which possess no cell wall, the cytoskeleton holds the cell shape maintained. The cytoskeleton elements are anchoring many cell organelles and even cytosolic enzyme molecules. Due to the dome- like structure, the cytoskeletal elements stabilize each other via force impact and thereby these structures are extremely strong and resistant. In contrast, the cytoskeleton has amazing dynamic properties like decomposition within a short time in one part and the contemporaneous new composition in another part of the cell. The cytoskeleton interacts with several cell movement compounds. Local changes of cytoskeletal elements as well as the displacement of organelles within the cell are caused by such compounds. These movements are enabled by close interaction with cytoskeleton motor proteins, e.g. dyneins and myosins, which act in concert with actin and microtubules. In plant cells, the cytoplasmic streaming is driven by the actomyosin system.

1.4.1. The contribution of actin and auxin respecting polarity aspects in plant cells

In plants, the cytoskeleton has, compared to animal cells, further functions: for example actin is significantly necessary for the polar auxin transport (Waller and Nick 1997) and for vesicle transport. Furthermore actin mediates cell polarity, like tip growth e.g. in pollen tubes and root hairs (Fu et al. 2001). Actin filaments intercept tensions in the cytoskeleton, whereat in animal cells they are associated with proteins beneath the plasma membrane, which are also contributing to the maintenance of the cell shape. As the main players for muscle contraction, actin filaments are meanwhile well understood in almost all their functions within animal cells. In plants, however, the cell shape is determined by the cell wall and the role of actin therefore differs from animal cells.

Actin plays a role in polar auxin transport (Maisch and Nick 2007). At the apical cell membrane auxin is deprotonated and it has to be actively pumped out of the cell by efflux carriers, like e.g. PIN proteins (for review, see Chen and Masson 2006). Actin enables the cycling of PIN proteins and facilitates in this way the auxin efflux mechanism. In the absence of auxin or light actin filaments are bundled, in the presence of auxin or in darkness they are present as fine cortical structures. Fine actin filaments are transporting the PIN proteins more effectively, whereby more auxin can flow through the cell (Paciorek et al. 2005 and Nick 2010). Interestingly, more auxin in the cell causes again finer actin filaments. This is a self amplifying, so- called Turing system (Turing 1952).

Indole- acetic acid (IAA), the most common natural auxin, is astonishingly small and simple. It combines three molecular properties: it is a small organic acid and therefore easily moves through the acidic environment of the apoplast. It carries a lipophilic indole ring and so it can permeate the cell membrane from any direction, which allows a cell to “explore” the auxin levels in its neighborhood. Finally, auxin is a weak acid and thus readily trapped in the neutral cytoplasm. It has to be actively exported by carriers, which allows establishing a directionality of auxin efflux. It is uncharged in the acidic environment at the outer surface of plant cells and can permeate through the membrane even without the help of influx carriers. Auxin is deprotonated in the more or less neutral cytoplasm and acquires a negative charge that will prevent its spontaneous exit from the cell. Therefore auxin accumulates in the cell due to this ion- trap mechanism (for review, see Lomax et al. 1995).

The combination of the non- directional influx and the directional efflux produces a reciprocal competition of individual cells for free auxin and a directional flow in the direction of cell polarity. If there are either more active or more auxin exporters localized at the basal part of the cell, the cell will transport more auxin than the neighbor cells. Therefore, more auxin is deducted from the neighbor cells and so a drainage of auxin is caused. This lateral inhibition

mechanism is furthermore combined with an autocatalytic feedback, whereby e.g. the differentiation from the ground state into a vascular cell fate is induced via auxin flux passing through the cell. *Vice versa*, this differentiation promotes cell polarity resulting in a stronger gradient of auxin exporters and stimulates further the auxin drainage of the neighbor cells.

Auxin- efflux carriers undergo, like mentioned above, dynamic cycling between intracellular compartments and the plasma membrane. Treatment with the fungal toxin brefeldin A is trapping the carriers in intracellular compartments (Geldner et al. 2001). This trapping can be suppressed by cytochalasin D, an inhibitor of actin assembly. Actin is therefore involved in the cycling of auxin- efflux carriers and auxin controls the conformation of actin, whereby the massive bundles prevalent in the absence of auxin are rapidly detached into finer filaments after addition of auxin (for review see Nick 2010). Thus, auxin stimulates its own transport by improving the polar localization of the auxin- efflux carriers at the cell poles (Paciorek et al. 2005), suggesting that these transporters are more efficiently moved along the finer actin filaments in response to auxin. Therefore a model of a regulatory circuit between polar auxin transport and actin organization can be set up, where auxin promotes its own transport by shaping actin filaments (Figure 1.2).

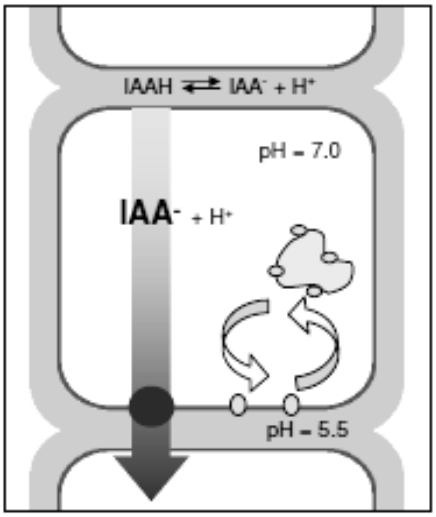

Figure 1.2.: Model for polar auxin transport and ion- trap mechanism of a plant cell. The arrows imply the cycling of the PIN proteins along the actin filaments (from Maisch 2007).

1.4.2. Microtubules are guiding the new cell-wall formation and connecting a variety of cellular processes

Cell axis is a prerequisite for polarity. It is laid down by independent mechanisms in higher plants. Here, it is not actin, but cortical microtubules that define the biophysical properties of the yielding cell wall and thus the geometry of expansion.

Microtubules are involved in the formation of the cell wall and the orientation of cellulose fibrils as well as for cell growth and cell division (Paredez et al. 2006). The cytoskeleton is also involved in cell biochemistry (Nick 1999). Mechanical stimuli acting on the surface can be transmitted via cytoskeletal elements to the nucleus and induce there a specific gene activation. It has even been possible to predict the reorganization of microtubules due to an applied pressure at certain points of the cell surface (Hamant et al. 2008).

Microtubules are straight hollow rods with a diameter of about 25 nm and they are found *inter alia* in the cytoplasm of all eucaryotic cells. Microtubules are pervading the cell and form the shape e.g. in animal cells. They act similar like rails, where organelles can glide along due to motor proteins. In animal cells secretory vesicles from the Golgi apparatus are conducted towards the plasma membrane via these rails. In plants, however, the ER and the Golgi apparatus are under the control of the actomyosin system (Hawes et al. 1999). Microtubules are one of the main players for the protoplast regeneration process. It is known, that they first are presented in a randomly arranged network in the protoplast`s cortex. Regenerated cells from protoplasts possess a transverse arrangement of cortical microtubules. This transverse arrangement of the microtubules could arise on two ways from the originally random arranged cortical network. One possibility could be a restructuring of existing microtubules; the second option would be a total depolymerization of the randomly arranged microtubules followed by a new polymerization. To test these two hypotheses, the microtubules of the protoplasts have been stabilized with taxol (Kuss-Wymer and Cyr 1992). The taxol-treated protoplasts regenerated the cell wall faster and also the process of the transverse arrangement of microtubules was accelerated. Because taxol is blocking the depolymerization of microtubules, the above mentioned second option was excluded with this experiment. So it has been proved that there is a reorganization of the microtubules within the regeneration process.

The cellulose fibrils are oriented along microtubules. Paul Green demanded already in 1962 the existence of "micro-tubules". Only one year later, these "micro- tubules" were discovered and a protracted discussion on the interaction of cellulose fibrils with the microtubules followed. The classical model assumes that cortical microtubules define the orientation in which newly synthesized cellulose microfibrils are laid down (reviewed in Geitmann and Ortega 2009; Nick 2011). In fact, fluorescently tagged cellulose synthases have been shown to move in tracks adjacent to the subtending cortical microtubules (Paredez et al. 2006), and a protein interacting with cellulose synthases (CSI1) has been shown to bind microtubules directly (Li et al. 2012).

The cell wall is the shaping element for the plant cell – with the removal during protoplast isolation the obtained cells are round and without direction. A plant cell wall is composed of individual cellulose fibrils which are embedded in a matrix of pectins, hemicelluloses, proteins, and partially lignin. The orientation of the cellulose fibrils defines the direction of growth of the cell. The cell wall is the factor that limits the expansion of the cell. In plants the cell wall has two main functions, stabilizing the cell and compensating the turgor pressure. With the removal of the cell wall, plant cells lose their polarity and the ability for anisotropic growth. The texture and the orientation of the cellulose fibrils thus determine the cell shape, like the length or width of a cell, and therefore also the axis of the cell. This alignment can be observed using polarity microscopy (Ziegenspeck 1948). If the fibrils are orientated longitudinally, the cell grows in width; in a transverse orientation the cell elongates (Nick et al. 1990). In cylindrical cells, where isotropic action of turgor pressure is predicted to produce only half of the strain in longitudinal relative to the transverse direction, a transverse orientation of cellulose microfibrils maintains the lateral reinforcement needed to drive elongation (Green 1980). Based on situations, where a transverse cellulose orientation persisted although microtubules had been eliminated by drug treatment or temperature-sensitive mutations, a self organization of cellulose has been proposed. During cell elongation, microtubules would sustain cellulosic self organization by constraining the secretion of non- cellulosic polysaccharides (Fujita et al. 2011). Irrespective of the underlying mechanisms, which are not mutually exclusive, the cell axis is linked to microtubules rather than actin filaments.

The orientation of cortical microtubules defines the orientation of division- related microtubule structures like the preprophase band or the spindle phragmoplast. In contrast to microtubules, the organization of actin filaments mostly persists during cell division. Therefore, axis and polarity of the daughter cells are mostly inherited from the maternal cell (for review see Nick 2011), stimulating the question of how polarity and axis are established *de novo*. To address this question, systems are required, where polarity is induced outside of

a tissue context. Since the cytoskeleton seems to control axis and polarity of plant cells, the cytoskeleton is expected to undergo a dynamic remodeling during protoplast regeneration. In fact, microtubules can be aligned by mechanic force in regenerating BY-2 protoplasts followed by an alignment of cell elongation and division (Wymer et al. 1996).

1.5. Scope of the dissertation

The phyllotaxis case shows exemplarily that mechanical and chemical signals probably act in concert on the adjustment of cell axis. This calls for systems that are simpler than a multilayered tissue, such that these signals can be investigated separately. This consideration was the motivation to design a system, where generation of axis and polarity can be generated *de novo* in single cells. To return to a *tabula-rasa* state, the axis and polarity was eliminated by removal of the cell wall in tobacco BY-2 cells, and then triggered the formation of a new axis and polarity (Zaban et al. 2013). In the current thesis the bulk remodeling of the cytoskeleton in regenerating protoplasts of BY-2 using cells expressing fluorescently tagged cytoskeletal markers was followed. Upon standardization of the system it was able to generate quantitative data on the temporal patterns of regeneration and the effect of anti- cytoskeletal compounds, inducible bundling of actin, RGD-peptides, and temperature. The occurrence of specific aberrations from the standard process allows defining the sensitive stages of the process.

Furthermore, the *tabula-rasa* approach was integrated into a microfluidic platform (Zaban et al. 2013), which provides directional chemical cues by the flow of auxin-containing medium through the system and mechanical cues by the preformed geometries of the rectangular microvessels. Based on this approach, the cell axis alignment with the geometry of the micro vessel was observed to gain insight into the underlying mechanisms of geometry sensing. The system was interfered either by providing a perpendicular flux of auxin, or by inhibition of auxin efflux through the specific inhibitor 1-N-naphthyl-phthalamic acid (NPA). A better understanding on how plant cells are exploring the geometry of their environment and how they align their axis at an early stage such that during subsequent expansion the mechanical tension in the tissues is minimized, was targeted.

2. MATERIAL AND METHODS

2.1. Buffers, solutions and chemicals

Buffers and solutions were solved in demineralized water (ddH2O) using a milipore device and were autoclaved for 20 minutes at 121 °C with a pressure of about 1 bar. Heat sensitive chemicals like antibiotics were filtered sterile using a 0.22 µm grid size PVDF filter set. All solutions were produced sterile under a laminar flow bench.

2.2. Equipment and tools

Equipment was autoclaved for 20 minutes at 121 °C with a pressure of 1 bar or sterilized for 1 h at the clean bench under UV light. A detailed list of all equipments, tools, as well as electronically devices and software is given below. Besides the bellowed mentioned software, images acquirement was processed for better presentation with respect to size, contrast and brightness via the Photoshop software® (Adobe Systems, San Jose, CA, USA). A detailed list for Equipment, tools and software see on the following page.

Equipment, tools and software	Company
Autoclave device	Systec GmbH, Type VE-95, Wettenberg, Germany
Axio-Cam MRm	Carl Zeiss AG, Jena, Germany
AxioObserver Z.1	Carl Zeiss AG, Jena, Germany
AxioVision Rel. 4.8 Software	Carl Zeiss AG, Jena, Germany
Centrifuge	Hettich Zentrifugen, Typ 1 300,Tuttlingen, Germany
Cleanbench	Hera guard Thermo scientific, Heraeus, Hanau, Germany
Falcons, Eppendorf tubes and plastic ware	Greiner Bio-One GmbH, Frickenhaussen, Germany
Flasks and other glass ware	Schott AG, Mainz, Germany or VWR International GmbH, Darmstadt, Germany
Fuchs- Rosenthal counting chamber	Carl Roth GmbH, Karlsruhe, Germany
Leica Diaplan	Leitz, Bad Dürkheim, Germany
Microfluidic devices	CAS Key Lab for Biological Effects of Nanomaterials and Nanosafety, National Center for NanoScience and Technology, Bejing, China
Microfluidic pump MS-CA 4/820	Ismatec, Wertheim; Germany
Millipore device	SG Wasseraufbereitung und Regenerierstation GmbH, Barsbüttel, Germany
MS Office 2007 Software	Microsoft Cooperation, Redmond, USA
Nescofilm	Carl Roth GmbH, Karlsruhe Germany
Orbital shaker	KS 250 basic, IKA Labortechnik, Staufen, Germany
pH-meter	pH510, Eutech Instruments, Nijkerk, The Netherlands
Rotilabo sterile filter	Carl Roth GmbH, Karlsruhe, Germany

Table 1: Required equipment, tools and software

2.3. Tobacco cell cultures

BY-2 (*Nicotiana tabacum* L. cv Bright Yellow 2) suspension cell lines (Nagata et al. 1992) were cultivated in liquid medium containing 4.3 g/L Murashige and Skoog (MS) salts, 30 g/L sucrose, 200 mg/L KH_2PO_4, 100 mg/L (myo)- inositol, 1 mg/L thiamine, and 0.2 mg/L 2,4-D, pH 5.8. In addition to the non-transformed BY-2 line (wild-type, WT), transgenic lines were used in this study that expressed the actin-binding domain 2 of plant fimbrin (FABD2) in fusion with GFP under the control of the constitutive cauliflower mosaic virus (CaMV) 35S promoter (AtFABD2, Sano et al. 2005), the actin-bundling LIM-domain in fusion with GFP under the control of a glucocorticoid- inducible promoter (Thomas et al. 2007), or a transgenic line expressing the β-tubulin AtTuB6 from Arabidopsis thaliana in fusion with GFP driven by the CaMV 35S promotor (Hohenberger et al. 2011). The cells were subcultivated weekly, inoculating 1.0 to 1.5 mL of stationary cells into 30 mL fresh medium in 100 mL Erlenmeyer flasks. The cells were incubated in darkness at 26 °C under constant shaking on a KS260 basic orbital shaker at 150 rpm. The media for the transgenic WLIM 1A- GFP and AtFABD2- GFP cell lines were complemented with either 30 mg/L hygromycin or with 50 mg/L kanamycin for the AtTuB6- GFP cell line, respectively. Stock BY-2 calli were maintained on media solidified with 0.8 % (w/v) agar and subcultured monthly. For a synoptical table of used cell lines see below.

Name	Antibiotics	Vector	Source
BY-2 WT	none	none	Nagata et al. 1992
BY-2 AtFABD2	30 mg/L hygromycin	pCAMBIA 1300	Sano et al. 2005
BY-2 AtTuB6	50 mg/L kanamycin	pK7WGF2	Hohenberger et al. 2011
BY-2 WLIM 1A	30 mg/L hygromycin	pTA/NtWLIM-GFP	Thomas et al. 2007

Table 2: List of non- transformed and transgenic tobacco cell lines used in this work

2.4. Generation and regeneration of protoplasts

The protocol was adapted from Kuss-Wymer and Cyr (1992) with minor modifications.

3 mL aliquots of cells were harvested under sterile conditions 3 d after subcultivation and digested for 6 h at 25 °C in 1% (w/v) cellulase YC (Yakuruto, Tokyo, Japan), as well as with 0.1% (w/v) pectolyase Y-23 (Yakuruto, Tokyo, Japan) in 0.4 M mannitol (Carl Roth GmbH, Karlsruhe, Germany) at pH 5.5 under constant shaking on a KS260 basic orbital shaker at 100 rpm in petri dishes of 90 mm diameter. For the non- transformed WT, 1.3 mL enzyme solution per mL of suspension was used. For the BY-2 AtFABD2- GFP and BY-2 WLIM- 1A 3 mL were used, for the BY-2 AtTuB6 6 mL.

After digestion, protoplasts were collected by 500 rpm for 5 min at 25 °C into fresh reaction tubes. The protoplast sediment was carefully resuspended in 10 mL of FMS wash medium containing 4.3 g/L MS-salts (Duchefa Biochemie, Haarlem, The Netherlands), 100 mg/L (myo) inositol (Carl Roth GmbH, Karlsruhe, Germany), 0.5 mg/L nicotinic acid (Carl Roth GmbH, Karlsruhe, Germany), 0.5 mg/L pyroxidine- HCl (Sigma Aldrich, St. Louis, USA), 0.1 mg/L thiamin (Sigma Aldrich, St. Louis, USA) and 10 g/L sucrose (Carl Roth GmbH, Karlsruhe, Germany) in 0.25 M mannitol (Carl Roth GmbH, Karlsruhe, Germany); see Kuss-Wymer and Cyr 1992 and Wymer et al. 1996. After three washing steps, protoplasts were transferred into 1.5 mL FMS- store medium, which is the same like FMS wash medium but complemented with 0.1 mg/L 1- naphthaleneacetic acid (NAA, Sigma Aldrich, St. Louis, USA) and 1 mg/L benzylaminopurine (BAP, Sigma Aldrich, St. Louis, USA) .

Protoplasts were incubated in the dark at 26 °C without shaking in petri dishes (50 mm diameter), if not stated otherwise. The densitiy was determined via a Fuchs- Rosenthal counting chamber and was about 105 protoplasts/ mL store medium.

To prevent evaporation, the petri dishes were sealed with nescofilm. In some experiments, the FMS- store medium was complemented with 1 µM of oryzalin, taxol, latrunculin B or phalloidin. Cytoskeleton inhibitors were obtained from Sigma Aldrich, St. Louis, USA. Latrunculin B binds at actin monomers and prevents actin from polymerizing. Phalloidin is locking adjacent F- actin subunits together and prevents the depolymerization of actin filaments. Taxol stabilizes the microtubule polymer against disassembly. Oryzalin sequesters the dimers of plant tubulin at the plus end and depolymerizes the growth of the microtubules at the minus ends.

Alternatively, the pentapeptides YGRGDSP and YGDGRSP (PANATecs Gmbh Tübingen, Germany) with a purity of > 75% were added at 1– 10 µg/L to interfere with the extracellular matrix. Actin- bundling was induced in the BY-2 WLIM 1A cell line by addition of 100 µg/mL dexamethasone (Sigma-Aldrich, Neu Ulm, Germany) into the FMS- store medium (Zaban et al., 2013).

For cellulose staining, 0.1% w/v Calcofluor White (Sigma Aldrich, St. Louis, USA) was directly added to the protoplast suspension.

2.5. Fabrication of microfluidic devices

The microfluidic devices were fabricated by the CAS Key Lab for Biological Effects of Nanomaterials and Nanosafety (National Center for NanoScience and Technology, Beijing, China). According to the requirements of this thesis the microfluidic structures were set up and designed together with the researchers of the CAS Key Lab.

The microchannels and microvessels were produced in polydimethylsiloxane (PDMS) using soft lithography and replica molding. A layer of photoresist SU- 8 2100 (MicroChem Corp., MA, USA) was patterned on a silicon wafer by photolithography, resulting in a positive relief pattern of channels and a series of relief patterns of microvessels. For channels, a prepolymer mixture of Sylgard 184 (Dow Corning, MI, USA) was cast and cured against the positive relief master to obtain a negative replica- molded piece. After curing for 2 h at 70 °C, the PDMS was peeled off the master. The inlets and outlets of the channel were punched with a sharpened needle. For microvessels, a spin coater (1000 rpm, 10 s) was used to cure a prepolymer mixture of Sylgard 184 (Dow Corning, MI, USA) against the positive relief master to obtain a negative replica- molded membrane. After curing again for 10 min at 70 °C, the membrane was peeled off the master. The upper surface with no pattern was adhered to glass using UV light for sealing. The patterned surfaces of channels and microvessels were treated with oxygen plasma for 1 min with 50 mW, and, subsequently, the microchannel was assembled on top of the microvessels to form an integrated device. The dimensions of an individual microvessel were 72.8±1.36 µm in length and 52.5±0.38 in width, the filled channel kept 9.5 µl in volume in total. A model for the channel's design and a photo is given on the next page (Fig. 2.1.).

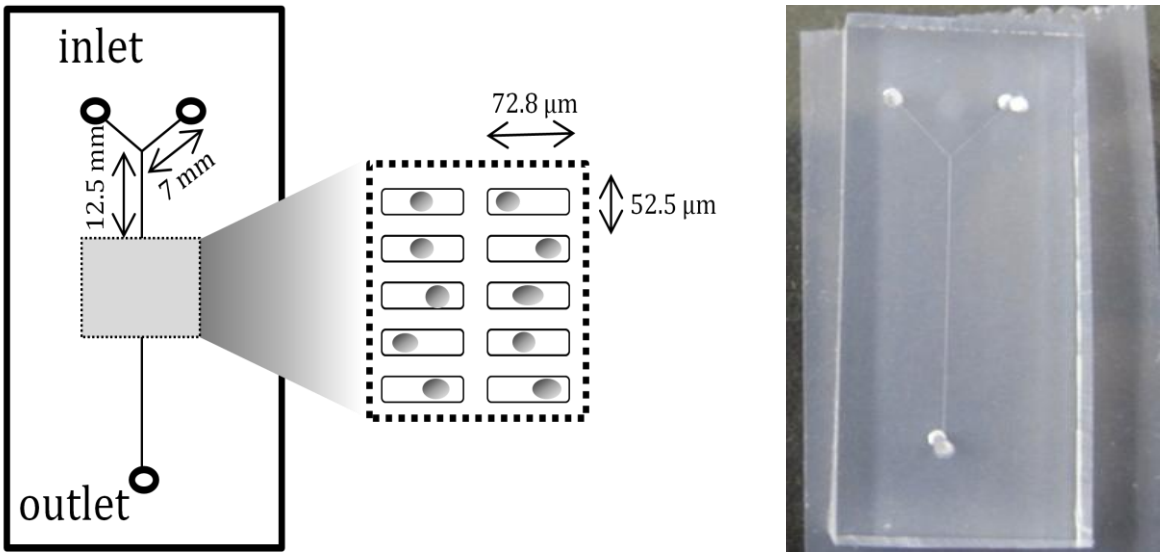

Figure 2.1.: Microfluidic chamber for regeneration of protoplasts in microvessels. Design of the channel and microvessels and right a photo of the microfluidic channel after delivery.

2.6. Charging and compartimentation of microchannels

First some preliminary work was done for the following charging of the microchannels. The microchannels were fixed onto a microscopic slide and filled with a micropipette with FMS store medium. Subsequently, the microchannels were degased by generating a vacuum in an exsiccator using a water- jet vacuum pump.

Subsequently 5 µL of protoplast suspension were filled into the left inlet of the microchannel via a microfluidic pump (MS-CA 4/820, Ismatec, Wertheim; Germany) with a slow flow rate (0.021 ml/h). A model for the experiment's setup is shown in Figure 2.2. In Figure 2.3. a photo from the setup is shown.

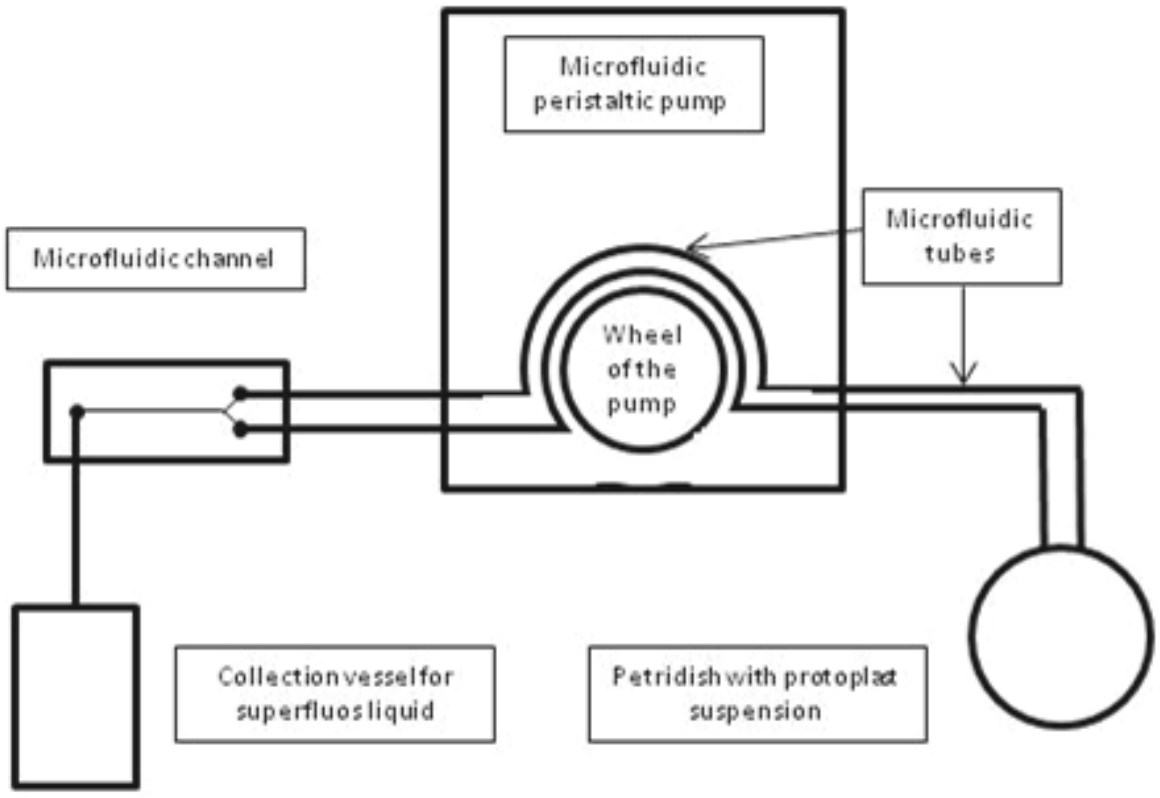

Figure 2.2.: Model for the experiment's setup. The container containing the protoplast suspension is connected via microfluidic hoses with the microfluidic pump. From there protoplasts are filled via the same hoses into the microfluidic channel.

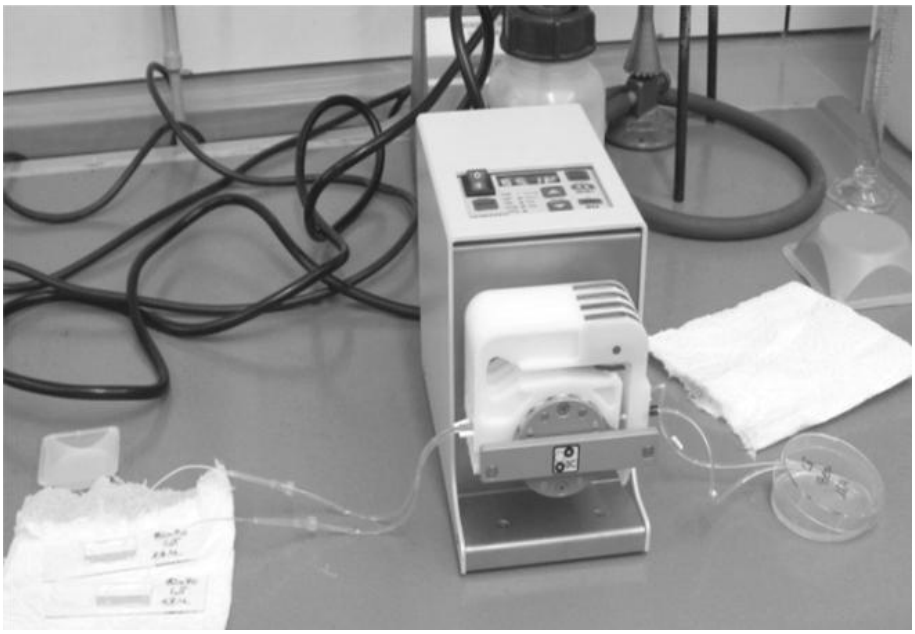

Figure 2.3: Real experimental set up for charging the protoplasts into the microchannels via the micropump

For generating auxin gradients, the channel was first loaded with protoplasts and then the flow was stopped. Subsequently, 2 µl of 1 µM NAA or 2, 4- D in FMS store medium were administered into the right inlet such that a diffusion gradient developed along the axis of the channel. To score the response, the channel was subdivided equally into 4 sections designated A to D, with A located nearest to the inlets upstream in the gradient (see Figure 2.4.). The temporal dynamics of the auxin gradient was calculated based on Fick's second law in one dimension based on a diffusion coefficient for auxin D = 7.10^{-6} cm^2 /s (Goldsmith et al.1981).

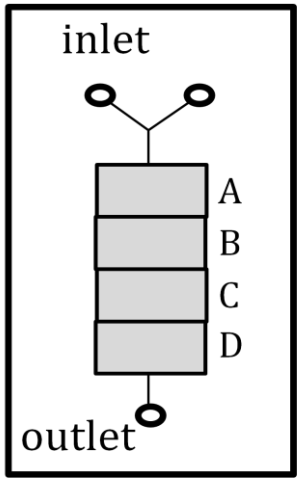

Figure 2.4.: Model for the subdivision of the microchannels into section A - section D

2.7. Microscopy, quantifications and image analysis

2.7.1. Staging protoplasts via *tabula rasa* approach

For staging (Zaban et al. 2013) 15 µL of protoplast suspension were carefully mounted on slides using silicone- made imaging spacers (Secure- Seal, Sigma- Aldrich, Neu- Ulm, Germany) to avoid protoplast bursting. Cellulose was stained by Calcofluor White according to Maeda and Ishida (1967), and Nagata and Takebe (1970) (Figure 3.1.).

Cells were examined under an AxioImager Z.1 microscope (Zeiss, Jena, Germany) equipped with an ApoTome microscope slider for optical sectioning and a cooled digital CCD camera (AxioCam MRm) recording the GFP signal through the filter set 38 HE (excitation at 470 nm, beamsplitter at 495 nm, and emission at 525 nm) and the Calcofluor White signal through the filter set 49 (excitation at 365 nm, beamsplitter at 395 nm, and emission at 445 nm). In some cases, stacks of optical sections were acquired at different step sizes between 0.4 and 0.8 µm. Images were processed and analyzed using the AxioVision software (Rel. 4.8.2) (Zeiss, Jena, Germany). To ensure unbiased acquisition of images, the MosaiX- module sampling system (Zeiss, Jena, Germany) was employed automatically recording individual cells and assembling a large panel of cells covering an area of 5 x 5 mm consisting of 266 individual images. The individual stages as defined in Figure 3.1. were scored from those composite images. For the staging (Figure 3.3.), 5.000- 7.500 individual cells from 30 independent experimental series were pooled.

Stages were defined as follows: stage 0 round, no cell wall; stage 1 cell wall present upon staining with Calcofluor White, nucleus central; stage 2 ovoid shape with a ratio of longer axis to shorter axis of >1.2 (Figure 3.1.), stage 3 elongate with a ratio of longer axis to shorter axis of >2.0.

For the drug, peptide, and temperature studies (Figures 3.7., 3.8., 3.9., 3.11.), typically between 500 and 1.500 individual cells from 2- 3 independent experiments were scored. Mortality (Figure 3.10.) was determined from loss of membrane integrity (e.g. loss of shape and rough outline due to cytoplasm leaking out) and breakdown of cytoplasmic structure visible in the differential- interference contrast. 500- 2.000 individual cells were scored thereby for a single experiment. Each data point represents the mean and standard error from at least 3 independent experimental series. The results were tested for significance using Student's t-test for 95 % and 99% confidence level.

2.7.2. Geometry sensing via microfluidics

For geometry sensing, the loaded microvessels were covered with a coverslip and examined under an Axioskop microscope (Zeiss, Jena, Germany), equipped with a 32x long distance objective (Zeiss Neofluar, Jena, Germany) and a digital CCD camera (AxioCam MRm). The Calcofluor White signal was detected through the filter set 49 (excitation at 365 nm, beamsplitter at 395 nm, and emission at 445 nm). For the viability assays (see Zaban et al. 2013), 100- 250 cells were observed per data point. Between 181- 350 cells were scored for testing the geometry sensing of regenerating protoplast as well as the loss of geometry sensing by inhibition of auxin efflux (Figure 3.13.). For the auxin- gradient analysis (Figure 3.16.) and cell geometry alterations by auxin gradient 62- 186 cells were counted per area and time point. A total population of 408- 688 individual cells per time point was counted for the experiment.

3. RESULTS

This dissertation deals with the induction of polarity *de novo* in plant cells and also with geometry sensing of plant cells. As already mentioned, since plants are sessile organisms, it is very important for them to grow and develop in the right direction. The first step for this is the proper establishment of polarity in each single cell. Many different factors influence the manifestation of the cell axis and almost all of these factors are closely linked and interact with each other. Especially discussed are mechanical and chemical signals, for example the influence of the phytohormone auxin on the polarity establishment. To understand the individual roles of signals influencing the regeneration process, protoplasts of tobacco *Nicotiana tabacum* L. cv. BY-2 were observed and manipulated during their regeneration.

Three approaches were followed in this work.

First, a experimental system for monitoring protoplast regeneration was designed to investigate the regeneration process. This so- called *tabula-rasa* approach includes the classification of stages and deviant stages, the formation of the new cell wall and the analysis of the re- organization of cytoskeletal elements during the regeneration process.

Second, the *tabula-rasa* approach was manipulated with scalar, non- directional factors, like temperature, RGD- peptides and cytoskeletal inhibitors to test their influence on protoplast regeneration. For testing the effect of actin bundling an inducible actin marker cell line was used for investigating the role of the actinfilaments in polarity establishment of tobacco BY-2 protoplasts.

Since cells have to perceive their environment in some way before they assign the new cell axis, the geometry sensing of regenerating protoplasts was considered in a third approach via the integration of the above mentioned system into a microfluidic setup. Here, the effects of mechanical restriction as well as the influence of different auxin gradients on plant cell development were investigated.

3.1. Protoplast regeneration based on the *tabula rasa* approach

Protoplasts pass through different stages while they are regenerating. They determine a new cell axis, manifest it and become finally elongated cells. To understand this process, in the course of my diploma thesis, an experimental system had been developed that allowed to eliminate the innate polarity and to follow regeneration of a new polarity *de novo*. This so called *tabula rasa* approach could now be exploited in the current dissertation to analyze the impact of different factors such as cytoskeletal inhibitors, induced expression of actin-bundling proteins, temperature, or RGD- peptides - also on a quantitative level. The regeneration process could be subdivided into different stages: In the first stage 0 protoplasts have neither polarity nor a cell axis and no cell wall. During the first step of regeneration, the transition from stage 0 to stage 1, the cell wall formation occurs. This is done by cellulose synthase, which is transported towards the membrane by vesicles. The final manifestation of the cell axis takes place in stage 2.

The stages of protoplast regeneration are described in the following sub- paragraphs in detail. To get insight into the cellular mechanisms that drive regeneration and axis formation, the organization of microtubules and actin filaments was followed in protoplasts derived from cells expressing GFP- tagged markers for microtubules and actin filaments (Figure 3.1).

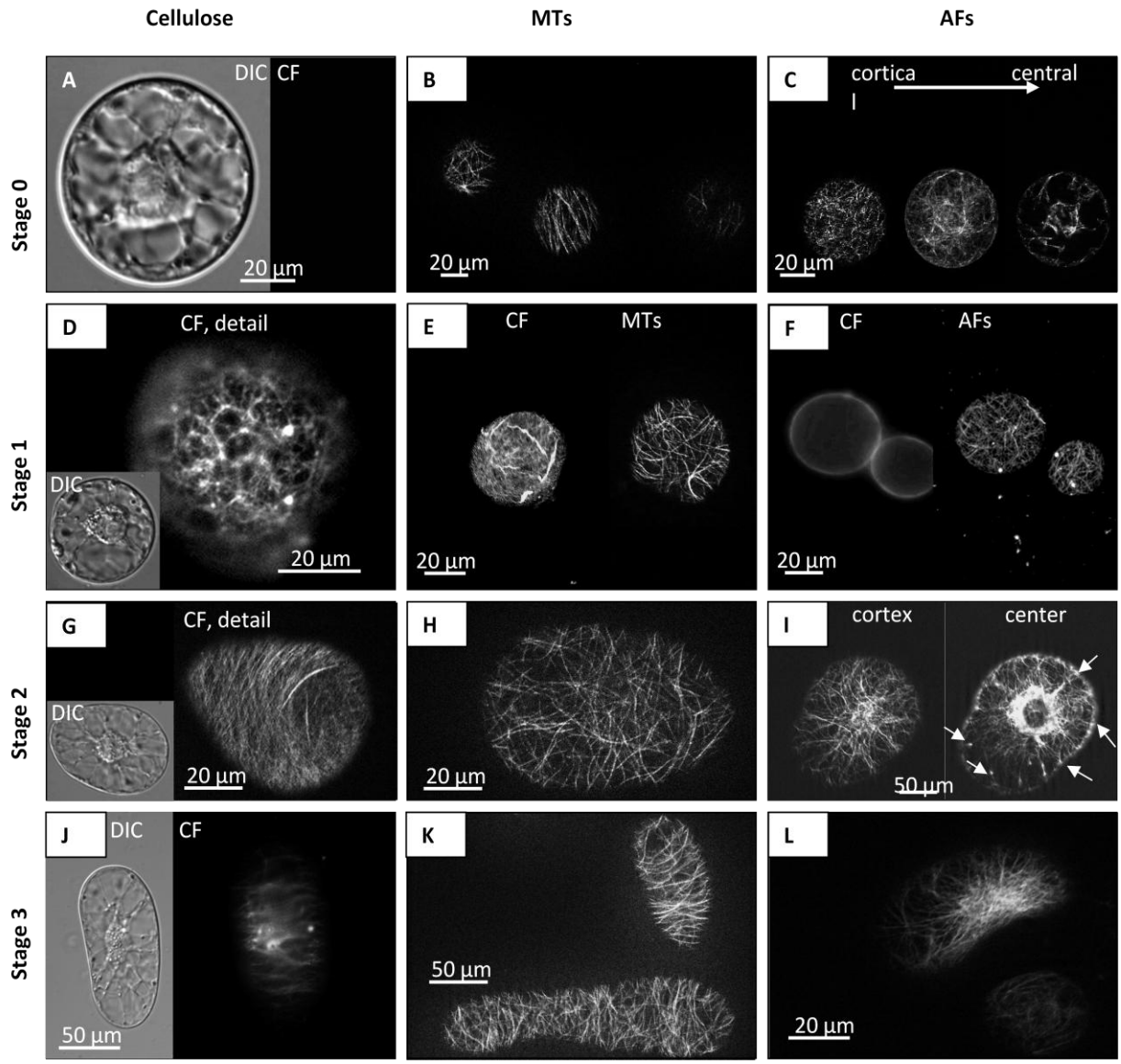

Figure 3.1.: Cellular details of protoplast regeneration

(A–C) *Stage 0*, (D–F) *stage 1*, (G–I) *stage 2*, (J–L) *stage 3*. (A), (D), (G), and (J) show cell morphology (differential interference contrast, DIC), and cellulose (Calcofluor White, CF). (B), (E), (H), and (K) show microtubules (MTs, GFP-AtTuB6), and (C), (F), (I), and (L) show actin filaments (AFs, GFP-FABD2). White arrows in (I) indicate adhesion sites for actin cables at the cell membrane.

Stage 0: By staining with Calcofluor White, no fluorescence can be detected, which indicates that cellulose is completely absent (Figure 3.1. A). Differential interference contrast (DIC) illumination shows that the nucleus is seen to be positioned in the cell center. It is tethered to distinct transvacuolar cytoplasmic strands. The MTs have lost their alignment in most protoplasts. They can be found in a random network in the cortex close to the membrane. However, in some cells, where microtubules appear to be slightly more bundled, the alignment persisted throughout the digestion of the cell wall (Figure 3.1. B).The actin filaments are also randomly oriented in the cell cortex. The cortical network is connected with the nucleus by transvacuolar actin cables. The nucleus is encased by a perinuclear actin network (Figure 3.1 C).

Stage 1: The staining with Calcofluor White shows the reformation of cellulose. The reformation of cellulose can be used as a diagnostic marker for this stage (Figure 3.1. D- E). As visible in the DIC illumination (Figure 3.1. D) in most, but not in all cells, the nucleus begins to shift from the cell center towards one of the lateral walls. As it is visible from confocal sections, which were collected from the cortex, (Figure 3.1. E) the cellulose is not deposited homogenously. The cellulose is either arranged like a meshwork (Figure 3.1. D) or in thick fibers that often follow the direction of the underlying microtubular array. Nevertheless, the thick cellulose fibers cannot be attributed to individual microtubules yet (Figure 3.1. E). Although the microtubules are showing a local alignment, they still do not reveal a clear global orientation. The microtubules of different orientations are often intersected differently (Figure 3.1. E). A cortical network of fine actin filaments still does not reveal any preferential orientation (Figure 3.1. F), but first some filaments appear more distinct and thicker than others.

Stage 2: A clear axis is laid down in these cells. The nucleus is positioned closer to one “basal” cell pole (Figure 3.1. G). The cellulose is now organized in parallel fibrils that cover the complete surface of the cell. The most of them are aligned in a direction perpendicular to the long axis of the cell. However, this alignment is not detected in the cell poles. The cortical microtubules are still randomly organized, but they begin to align in a transverse direction. This alignment initiates in the region around the nucleus (Figure 3.1. H). Nonetheless it is, similar to cellulose microfibrils, not observed in the cell poles. Cortical actin filaments are now prominent. Distinct attachment sites of the actin filaments at the cell periphery can be observed (Figure 3.1. I). The perinuclear actin cage is now very distinct and brightly labeled.

Stage 3: The cells have undergone expansion along with the longer cell axis. Cellulose microfibrils are now clearly aligned in bundles perpendicular to this elongation axis (Figure 3.1. J). The nucleus is tethered to transvacuolar strands and has become elliptic. Its longer axis is parallel to the elongation axis. Cortical microtubules have increased in density, and

they are clearly aligned in parallel bundles perpendicular to the elongation axis (Figure 3.1. K). Compared to stage 2, the cortical network has become finer and less dense. However, the network around the nucleus is more dense and linked by numerous transvacuolar strands with the cell cortex (Figure 3.1. L).

To get a better insight for the polarity establishment and processes in the beginning regeneration process of protoplasts, the transition between stages 0 and 1 was studied in more detail on the base of time- lapse series (Figure 3.2.). This transition is a very dynamic process and involves vivid reorganization of cytoplasmic architecture. This includes a rotation and the repositioning of the nucleus, culminating in a progressively lateral position (Figure 3.2. A). The new synthesis of the cellulosic wall is a rapid process that proceeds within a few minutes (Figure 3.2. B). This occurs almost exclusively in cells where the nucleus has already acquired a lateral position. The exact timing of this event differs between individual regenerating protoplasts, but the majority of cells go through this transition during the first 12-24 h after protoplast isolation.

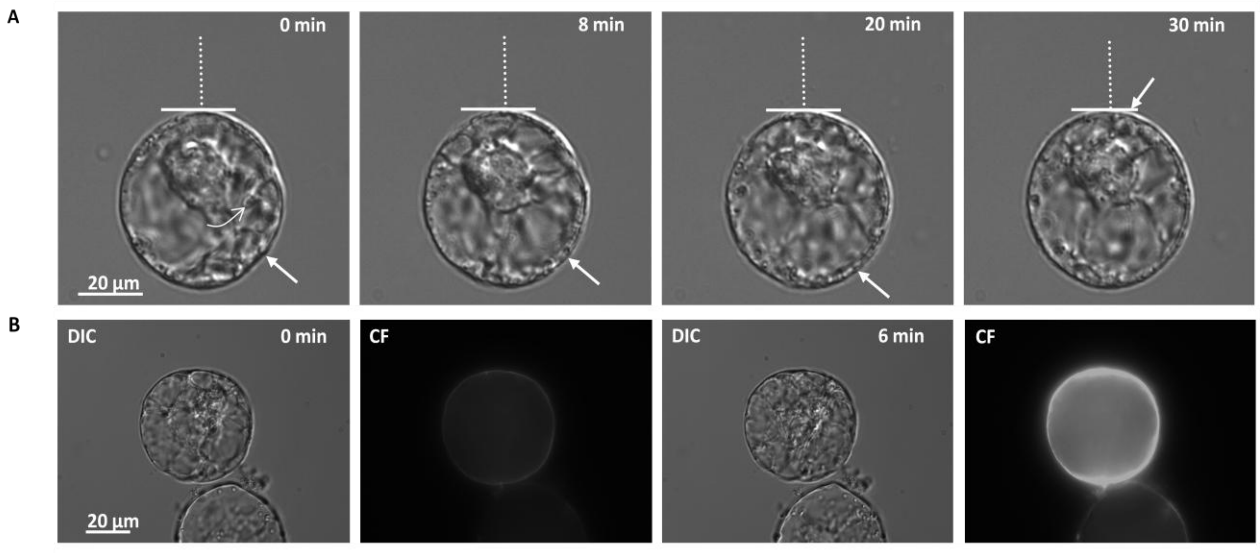

Figure 3.2.: Time-lapse series of the transition from stage 0 to stage 1.
(A) Time series of nuclear movements in a protoplast during stage 0. Strong cytoplasmic streaming converges towards the sites indicated by arrows. The bent arrow indicates the direction of rotational movement, and the white line shows the position of the nuclear diameter with respect to the symmetry axis of the protoplast (dotted line).
(B) Time series of a protoplast at the transition from stage 0 to stage 1. Note the strong increase in the Calcofluor White signal (CF) within a time interval of only 6 min.

With the *tabula- rasa* approach it is possible to control the regeneration process to such a degree that a quantitative treatment became feasible. To validate the results from staging, different, non- transformed BY-2 cell lines at different time points, originating from different labs, were compared. In addition to the non- transformed BY-2 cell line (Figure 3.3. A), the tubulin marker line AtTuB6 (Figure 3.3. B), and the actin marker line FABD2 (Figure 3.3. C) were analyzed. The relative frequency of the stages was then charted over time (Figure 3.3.) Time courses of protoplast regeneration were drawn up for each BY-2 cell line.

The overall regeneration pattern was similar, but it had some specific differences for the marker lines that are described in the following.

After the first day of regeneration, the majority of protoplasts had left stage 0 and reached stage 1. Some of them have even developed further to stage 2 (Figure 3.3. A). At the second day of regeneration, cells in stage 2 were predominant. Therefore, stage 0 had decreased to a residual frequency of 5%, and stage 1 had decreased to 30%. At day 3, more than 20% of cells have reached stage 3, whereas stage 2 had decreased to a frequency of about 30% and stage 1 had decreased to less than 20%.

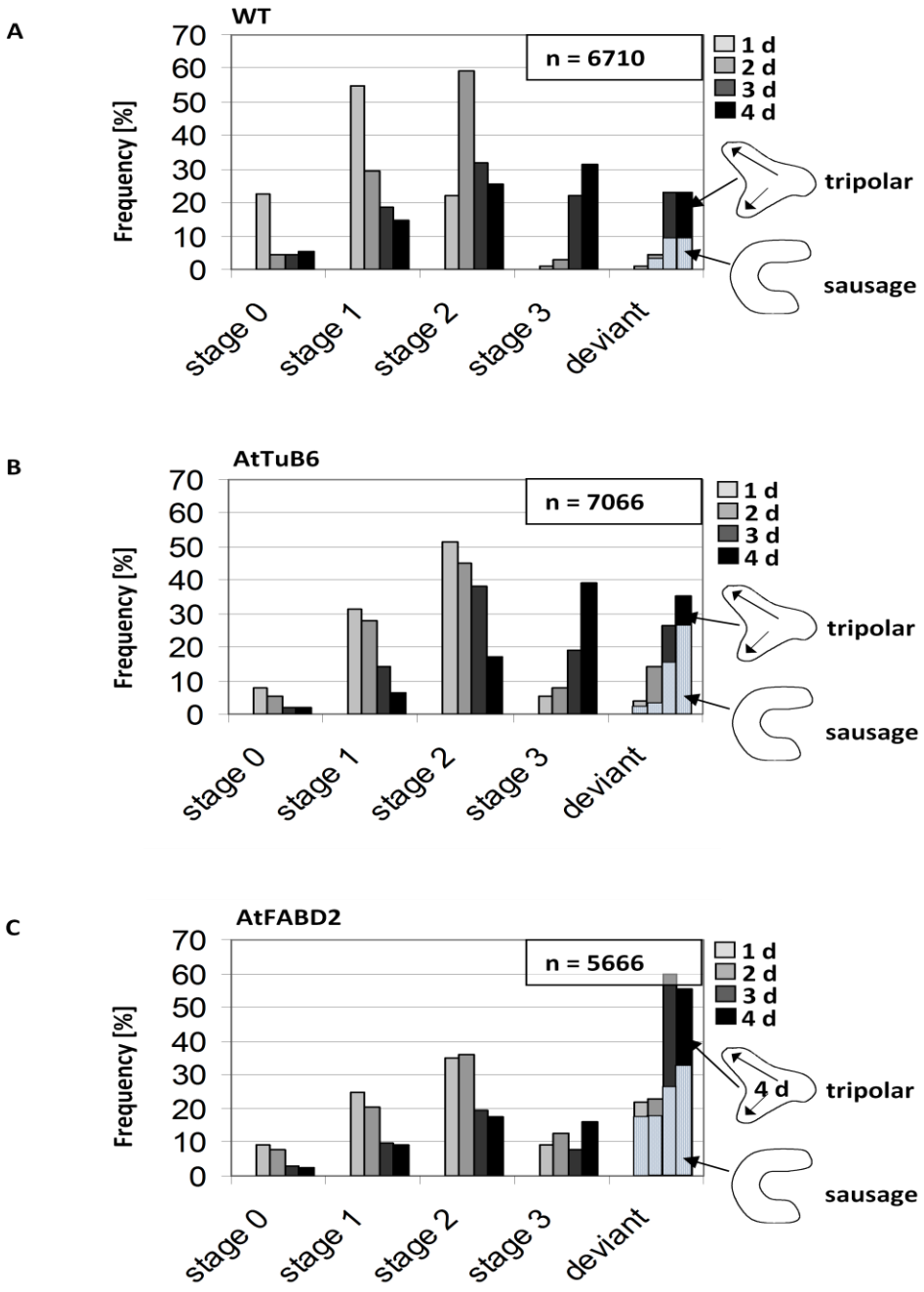

Figure 3.3.: Time courses of regeneration stages.

The relative frequencies of each stage are shown for different time points in non- transformed BY-2 cells (WT, A), cells expressing GFP in fusion with the microtubule marker AtTuB6 under control of the CaMV-35S promoter (AtTuB6, B), and cells expressing GFP in fusion with the actin marker AtFABD2 under control of the CaMV-35S promoter (AtFABD2, C). The frequency of cells deviating from the normal pattern is plotted as “deviant cells”. These included sausage- shaped cells and tripolar cells with branched polarity. The proportion of sausage- shaped cells is represented by the dotted bars. The frequency distributions have been calculated from 5.500 to 7.000 individual cells pooled from 30 independent experimental series.

3.1.1. Deviant stages – loss of polarity during regeneration

A fraction of cells diverged from the normal regeneration pattern of development. In some cells, the cell wall was laid down asymmetrically and was much thicker at the flank site adjacent to the nucleus. This resulted in an asymmetric elongation producing a sausage-shaped bending of the cell (Figure 3.4. A). In the remaining cells, a second competing axis was laid down, leading to a tripolar situation whereby microtubules and cellulose fibers are aligned perpendicular to the adjacent cell pole (Figure 3.4. B).

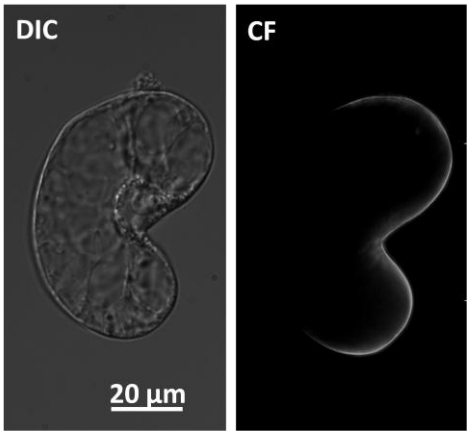

Figure 3.4.: Detail of a deviant sausage- shaped cell as frequently observed in the AtTuB6 cell line.

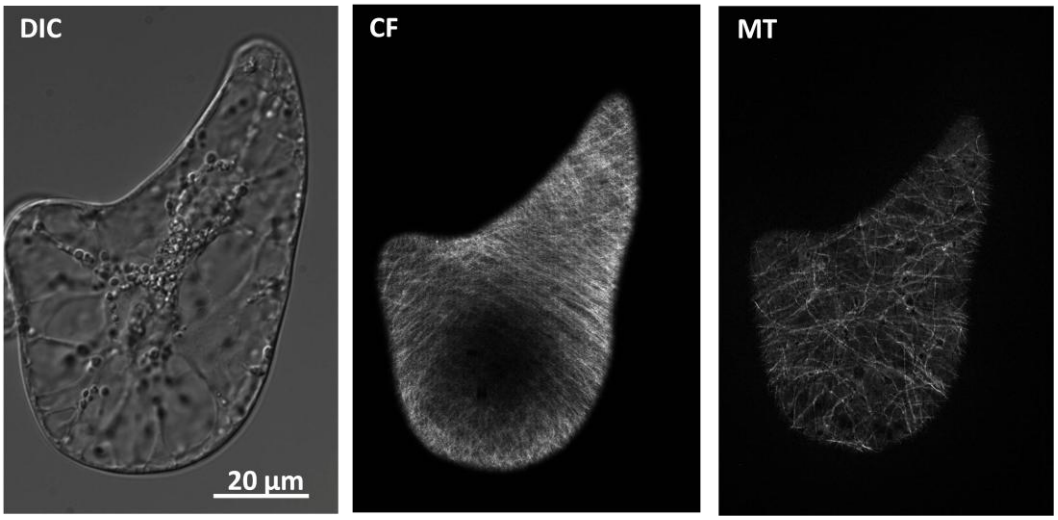

Figure 3.5.: Detail of a deviant binuclear and bipolar cell at stage 2 (day 2) of the AtTuB6 cell line. DIC, differential interference contrast; CF, Calcofluor White signal; MT, microtubules.

3.1.2. The impact of actin filaments and microtubules on the regeneration of BY-2 tobacco cells

In general, the temporal pattern of regeneration in the AtTuB6 line (Figure 3.3. B) is comparable to the situation in the non- transformed WT cell line. However, a closer look revealed that the early phases of regeneration are clearly promoted in the AtTuB6 line. After 1 d, more than 50% of the cells have advanced to stage 2 (as compared to about 20% in the non-transformed cell line). The transition from stage 2 to 3 was not promoted until day 3, which means that the cells remained trapped in stage 2. Then against during day 4, the fraction of the sausage- shaped cells with asymmetric elongation (Figure 3.5.) is increasing drastically compared to that deviant stage observed in the non- transformed WT cell line.

Similar to the AtTuB6 line, the early phases of regeneration were promoted in the AtFABD2 line (Figure 3.3. C). In addition, a significant proportion of cells did not produce a normal stage 3 cell, but instead they are also producing deviant sausage-shaped cells. The frequency of deviant tripolar cells is increased there, driving the fraction of deviant cells to roughly 60%.

To test whether the high frequency of tripolar cells in the AtFABD2 line might be linked to the slight stabilization of actin filaments reported for this marker (Holweg 2007, Wang et al. 2008), the WLIM- 1A cell line was tested and the regeneration process was regarded there. In this cell line the actin- bundling LIM domain could be expressed under the control of a dexamethasone- inducible promoter (Thomas et al. 2007). When the inducer was added 1 d after the onset of regeneration, the pattern recorded at day 3 was the same as that in the non- induced WT control (Figure 3.6. B).

However, when the inducer was added at the beginning, right after protoplasts isolation, the frequency of deviant cells increased significantly. Although the frequency of deviant cells remained at around 35%, which is much lower than the 60% observed deviant cells in the AtFABD2 line in Figure 3.3. C. This increase was due in equal parts to an increase of sausage- shaped and tripolar cells.

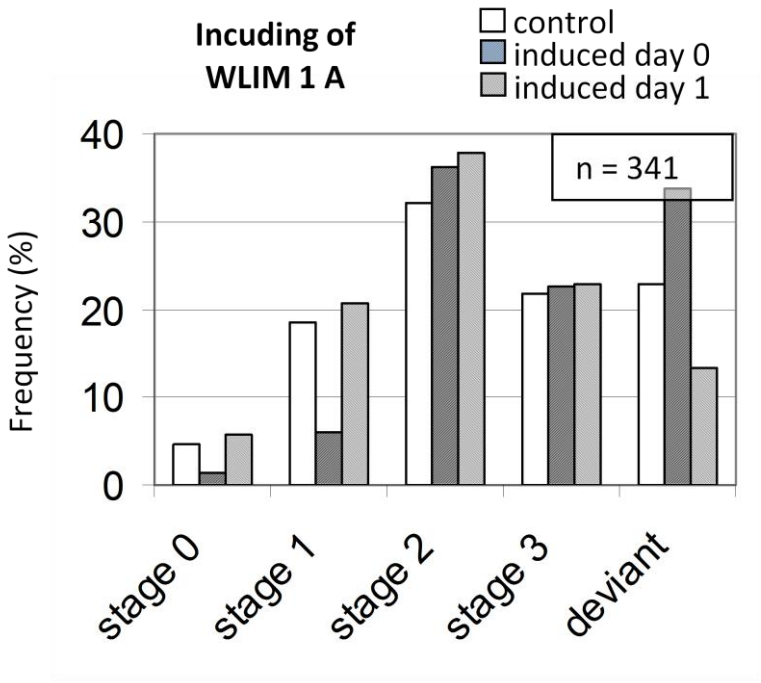

Figure 3.6.: Effect of dexamethasone- inducible actin bundling on the frequency of individual regeneration stages in the WLIM- 1 A line scored at day 3. Dexamethasone was either added at time 0 or 1 day later. Note the decrease of normal stage 1 and the increase of deviant cells for induction at time 0.

3.2. Effects of cytoskeletal drugs, temperature, and RGD- peptides on the protoplast regeneration

3.2.1. Cytoskeletal drugs effect the regeneration process

Since both, microtubules as well as actin filaments, undergo a characteristic reorganization over the course of regeneration (Figure 3.1.), and since expression of proteins binding to microtubules (AtTuB6, Figure 3.3. B) and actin filaments (FABD2, Figure 3.3. C; LIM-domain, Figure 3.6.) leads to specific morphogenetic aberrations, the effects of the cytoskeletal inhibitors (taxol, phalloidin, oryzalin and latrunculin B) on protoplast regeneration were tested (Figure 3.7.).

Treatment of the non- transformed BY-2 WT cell line with 1 µM of taxol, a microtubule stabilizer, clearly promoted the transition from stage 0 to stage 1 (Figure 3.7. A). The frequency of stage 2 was not significantly increased by taxol. The frequency of sausage-shaped cells doubled compared to the sausage- shaped cells observed in the control. Thus, the taxol treatment phenocopies several aspects observed in the AtTuB6 line (Figure 3.3. B). A treatment with 0.5 µM of taxol caused a similar response, but at a lower amplitude.

A treatment of the non- transformed BY-2 WT line with 1 µM of phalloidin, a stabilizer for actin, promoted the early transitions visible as a lower frequency of stage 1 and a higher frequency of stage 2 (Figure 3.7. D). However, this was not followed by an increased frequency of stage 3. Instead, a much higher frequency of deviant cells was observed. In the cells, which were treated with 1 µM phalloidin, there is a raise from 14% of deviant cells in the control to 36%; the treatment with 0.5 µM phalloidin produced 32% deviant cells. Thus, the phalloidin treatment phenocopies the AtFABD2 line in several aspects (Figure 3.7. C).

The early phases of regeneration were promoted in the AtTuB6 line compared to the non-transformed WT control (Figure 3.3. B). Since the integration of AtTuB6 might interfere with the dynamicity of microtubules by conferring a slight stabilization, it was tested whether a wild- type pattern could be restored in the AtTuB6 line by a mild treatment with 1 µM of oryzalin (Figure 3.7. B) that was sufficient to eliminate microtubules shifting the nucleus to one cell pole (Figure 3.7. E). In fact, oryzalin treatment slowed down the transition from phase 1 to phase 2 and consequently decreased the appearance of stage 3 cells. Specifically, oryzalin treatment restored the characteristic frequency peak of stage 2 at day 2 of regeneration found in the non- transformed WT (compare the line “Ory” in Figure 3.7. B with the line “control” in Figure 3.7. A). Thus, a mild oryzalin treatment can rescue towards a normal regeneration pattern in the AtTuB6 line.

In the AtFABD2 line, the early phases of regeneration were found to be promoted (Figure 3.3. C). However, the later phases, and most prominently the transition from stage 2 to stage 3, were impaired. This is leading to a high frequency of deviant cells. Analogous to the oryzalin experiment, it was tested whether this cell line could be rescued by a mild treatment with 1 µM of latrunculin B with respect to the incidence of stage 2 and stage 3. Latrunculin B sequesters G- actin monomers and by that it eliminates actin filaments depending on their innate turnover. This treatment removed the cortical actin network and the transvacuolar strands that tether the nucleus to the cortex (Figure 3.7. E). The perinuclear actin cage persisted, but the nucleus was again shifted to one cell pole similar to the situation after treatment with oryzalin. The latrunculin B treatment increased the frequency of stage 2 cells (Figure 3.7. D) and clearly rescued the incidence of stage 3 to more than 30%, which is the value that was observed in the non-transformed WT cell line (compare the line “Latrunculin B” in Figure 3.7. D with the line “control” in Figure 3.7. A). The frequency of deviant cells, which were around 60% observed at day 4 in the untreated AtFABD2 line, was reduced by about half to 32%. Thus, a mild treatment with latrunculin B can rescue towards a normal regeneration pattern in the AtFABD2 line.

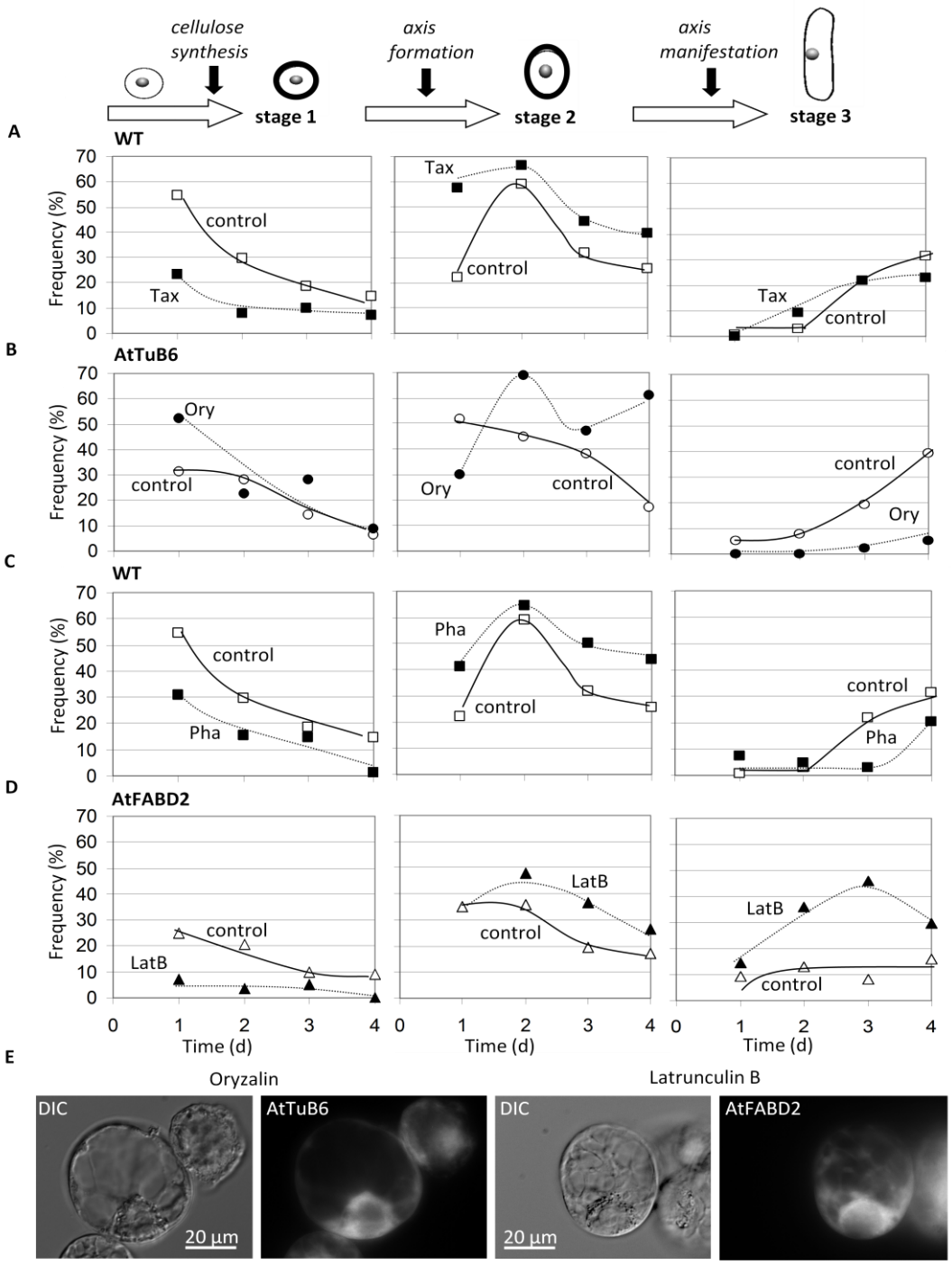

Figure 3.7.: Effect of the cytoskeletal inhibitors on the temporal pattern of regeneration stages. Stages 1 to 3 in non-transformed BY-2 cells (WT, A, C), cells expressing GFP in fusion with the microtubule marker AtTuB6 under control of the CaMV-35S promoter (AtTuB6, B), and cells expressing GFP in fusion with the actin marker AtFABD2 under control of the CaMV-35S promoter (AtFABD2, D). Open symbols: non- treated cells. Closed symbols: 1 µM of taxol (A), oryzalin (B), phalloidin (C) or latrunculin B (D). The data represent populations of 500- 1.000 individual cells. (E) Representative cells treated with 1 µM oryzalin (AtTuB6) or latrunculin B (AtFABD2) at day 2.

3.2.2. The regeneration process is temperature dependent

The interaction with the cell wall renders the cytoskeleton resistant against cold (Akashi et al. 1990). If the interaction of the cytoskeleton with an extracellular matrix is driving individual steps of the regeneration, this should therefore become evident in the temperature dependency of the respective step. For testing this subject, time courses of regeneration for different temperatures ranging from 17 °C to 30 °C are followed, using intervals of 3 °C (Figure 3.8.). These temperatures were selected because they cover the physiological potency of BY-2 cells over which they remain viable. From these time courses, transition rates could be deduced. They show the changes of frequency in % over time (Figure 3.9. B).

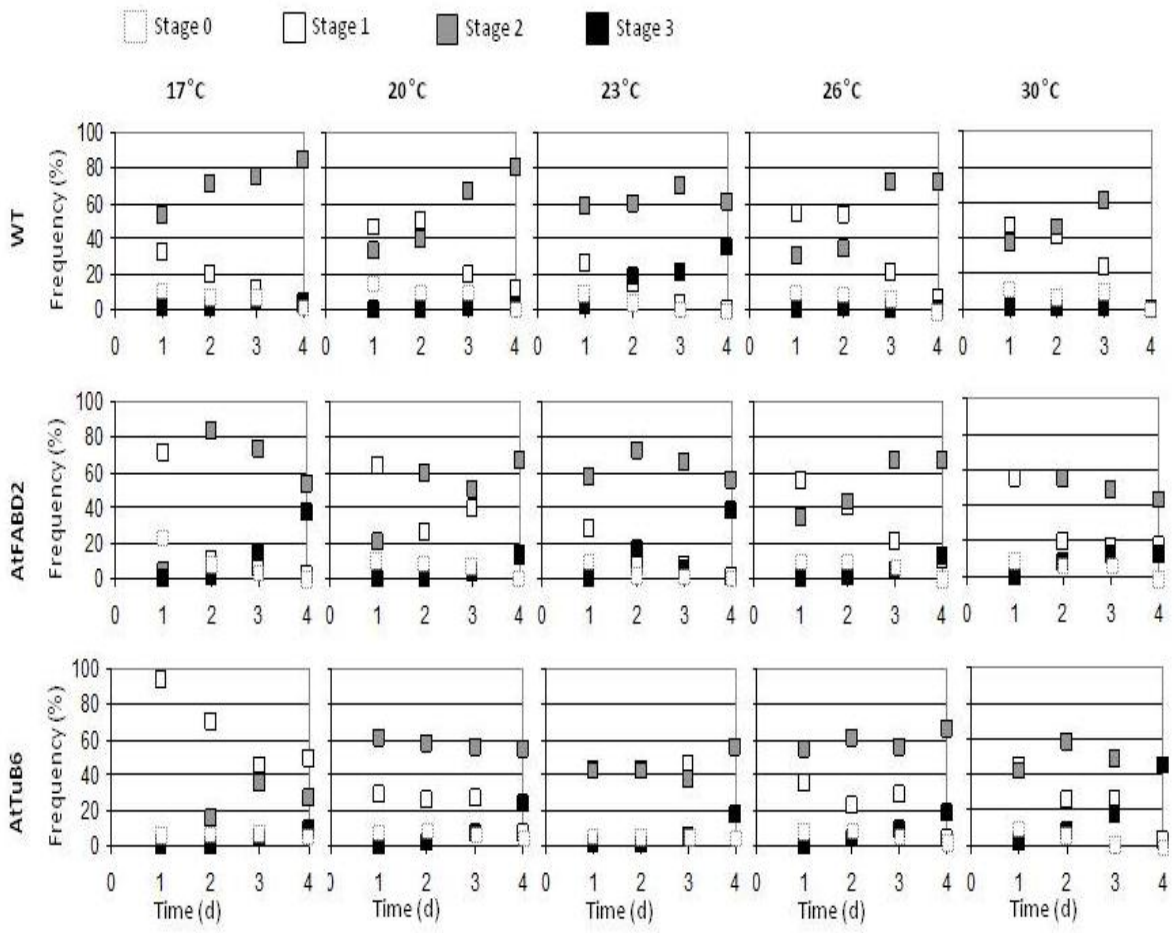

Figure 3.8.: Time course for the incidence of individual stages at different temperatures from 17°C till 30°C in non- transformed BY-2 cells (WT, white bars), cells expressing GFP in fusion with the actin marker AtFABD2 under control of the CaMV- 35S promoter (AtFABD2, grey bars), and cells expressing GFP in fusion with the microtubule marker AtTuB6 under control of the CaMV- 35S promoter (AtTuB6, black bars). Relative frequencies were determined from populations ranging between 1.250 till 3.000 individual cells.

The transition from stage 0 to stage 1, i.e. the regeneration of a cellulosic wall, is fairly independent of temperature in all three lines (Figure 3.9. B, left graph). In contrast, the transition from stage 1 to stage 2, i.e. the induction of a cell axis, is clearly dependent on temperature (Figure 3.9. B, central graph).

For the non- transformed WT cell line, the transition rate was slow at temperatures of up to 20 °C, but the rate doubled when the temperature was raised from 20 °C to 26 °C and remained high between 26 °C and 30 °C.

For the AtTuB6 and the AtFABD2 lines, the transition rates were high at low temperatures. They decreased to the level of non- transformed WT cells at temperatures of 20 °C to 23 °C and increased again at higher temperatures, similar to the non- transformed WT cell line. The transition from stage 2 to stage 3, i.e. cell elongation, showed a pronounced temperature window for non- transformed WT cells (Figure 3.9. B, right graph) and the AtFABD2 line exhibited a maximal rate at 23 °C but had low rates for temperatures that were lower or higher. In contrast, the AtTuB6 line showed an almost temperature- invariant elongation between 17 °C to 26 °C, which increased steeply at 30 °C.

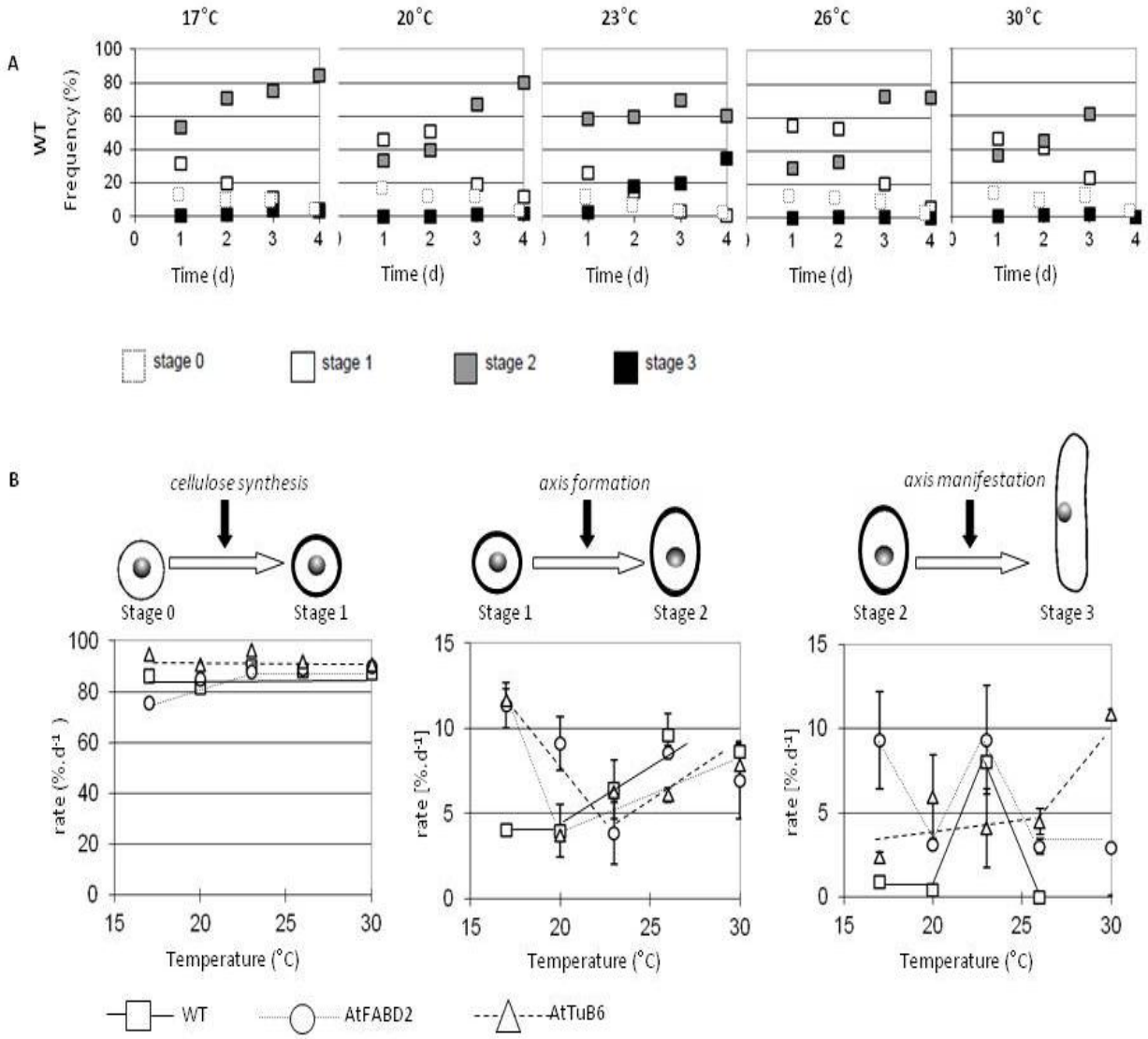

Figure 3.9.: Effect of temperature on the temporal pattern of regeneration stages.

(A) Time course for the incidence of individual stages at different temperatures from 17 °C to 30 °C in non- transformed wild-type cells (WT).

(B) Temperature dependency for the rates of transition between the different stages in non-transformed BY-2 cells (WT), cells expressing GFP in fusion with the actin marker AtFABD2 under control of the CaMV- 35S promoter (AtFABD2), and cells expressing GFP in fusion with the microtubule marker AtTuB6 under control of the CaMV-35S promoter (AtTuB6). Rates and standard errors were fitted based on a linear regression of relative frequencies over time (as shown for the WT in A) from populations ranging from 1.250 to 3-000 individual cells.

To gain further insight into these patterns, mortality was scored at the transition between stage 1 to stage 2 and the transition between stage 2 to stage 3. For the non- transformed WT cell line, mortality was modest for temperatures below 26 °C, but increased drastically at higher temperatures (Figure 3.10.). The AtTuB6 line showed a parallel pattern with generally reduced mortalities at day 2. The AtFABD2 line contrasted with these results, exhibiting high mortalities at 17 °C and 20 °C for the transition from stage 2 to stage 3.

These data suggest that the transition from stage 0 to stage 1, i.e. the regeneration of a cellulosic wall, is mostly independent of temperature, whereas the subsequent transition from stage 1 to stage 2, i.e. axis induction, requires a minimal temperature to proceed efficiently. Here, the expression of the AtTuB6 and the AtFABD2 marker accelerates axis induction at low temperatures. However, this acceleration effect disappears when the temperature is raised up to 23 °C. The transition from stage 2 to stage 3, i.e. axis manifestation and cell elongation, is sensitive to low and high temperatures. In the case of the AtFABD2 line this is accompanied by a high mortality rate at temperatures below 23 °C. In contrast, the expression of the AtTuB6 marker seems to stabilize cell elongation against fluctuations of temperature, which is also mirrored by reduced mortality.

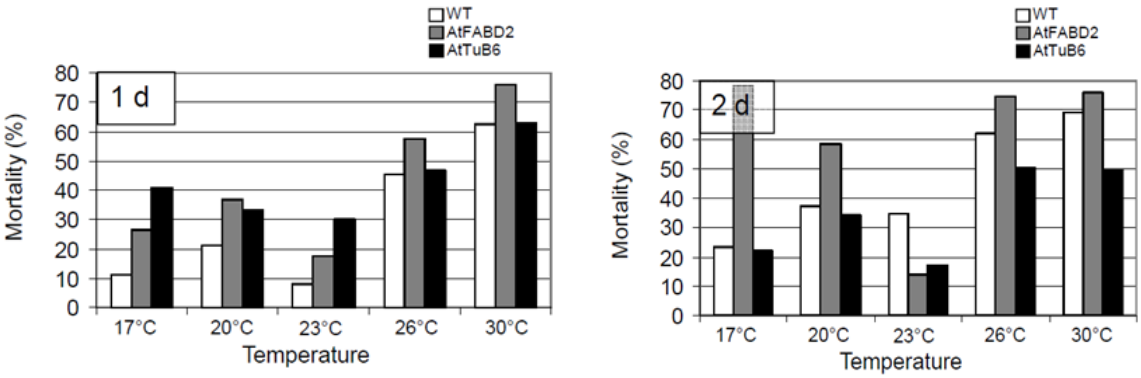

Figure 3.10.: Temperature sensitivity of the protoplast mortality in non- transformed BY-2 cells (WT, white bars), cells expressing GFP in fusion with the actin marker AtFABD2 under control of the CaMV-35S promoter (AtFABD2, grey bars), and cells expressing GFP in fusion with the microtubule marker AtTuB6 under control of the CaMV- 35S promoter (AtTuB6, black bars). Mortality is shown for day 1 (left graph) and day 2 (l graph), i.e. before divisions of temperature-adapted cells can occur. Mortality was determined from populations of 500 till 2.000 individual cells.

3.2.3. RGD– peptides promote axis formation and manifestation

The heptapeptide YGRGDSP (termed “RGD”) mimics the adhesive motif of fibronectin and vitronectin recognized by animal integrins. It has been shown to interact with unknown plant components that mediate interactions of cytoplasmic strands with the extracellular matrix (Canut et al. 1998). Since axis formation (stage 2) is preceded by the deposition of a new cellulosic wall (stage 1), which points to an interaction between the cytoskeleton and extracellular components (Wyatt and Carpita 1993), the questions is whether it would be possible to titrate this putative interaction with RGD- peptides.

As a control, the heptapeptide YGDGRSP (termed “DGR”) was employed, which has been reported to be inactive (Canut et al. 1998).

In non- transformed cells, treatment with 1 ng/ml of RGD peptides promoted the transition from stage 1 to the subsequent stage 2 and stage 3 (Figure 3.11. A). This leads to a reduced frequency of cells in stage 1 and increased frequencies of cells in stage 2 and stage 3. Treatment with the same concentration of DGR peptides produced an intermediate behavior: During the initial phase of the experiments (up to day 1), values were close to those observed in controls without peptides. From day 2 onward, the values obtained for treatment with DGR peptides approached those of treatment with the RGD peptides. Compared to RGD peptides, DGR was even more effective in enhancing the frequency of stage 3 cells. In a preparatory study, the concentration of peptides from 1 ng/ ml to 10 ng/ml was varied, but it failed to trigger a stronger effect. This suggests that 1 ng/ ml had already saturated the effect.

Furthermore it was observed that for concentrations exceeding 3 ng/ml, the difference between RGD and DGR peptides merged progressively until (at 10 ng/ml) the effect was identical and independent of the peptide sequences, suggesting a non- specific interaction.

Protoplasts treated with RGD peptides tended to aggregate, flattening at the domains of contact. Neither untreated controls nor DGR-treated protoplasts showed this phenomenon. When this study was extended to AtTuB6 (Figure 3.11. B) and AtFABD2 cells (Figure 3.11. C), the same effect pattern as in the non- transformed cells was observed: The incidence of cells in stage 1 decreased, whereas cells in stages 2 and 3 became more frequent, and the DGR produced intermediate effects.

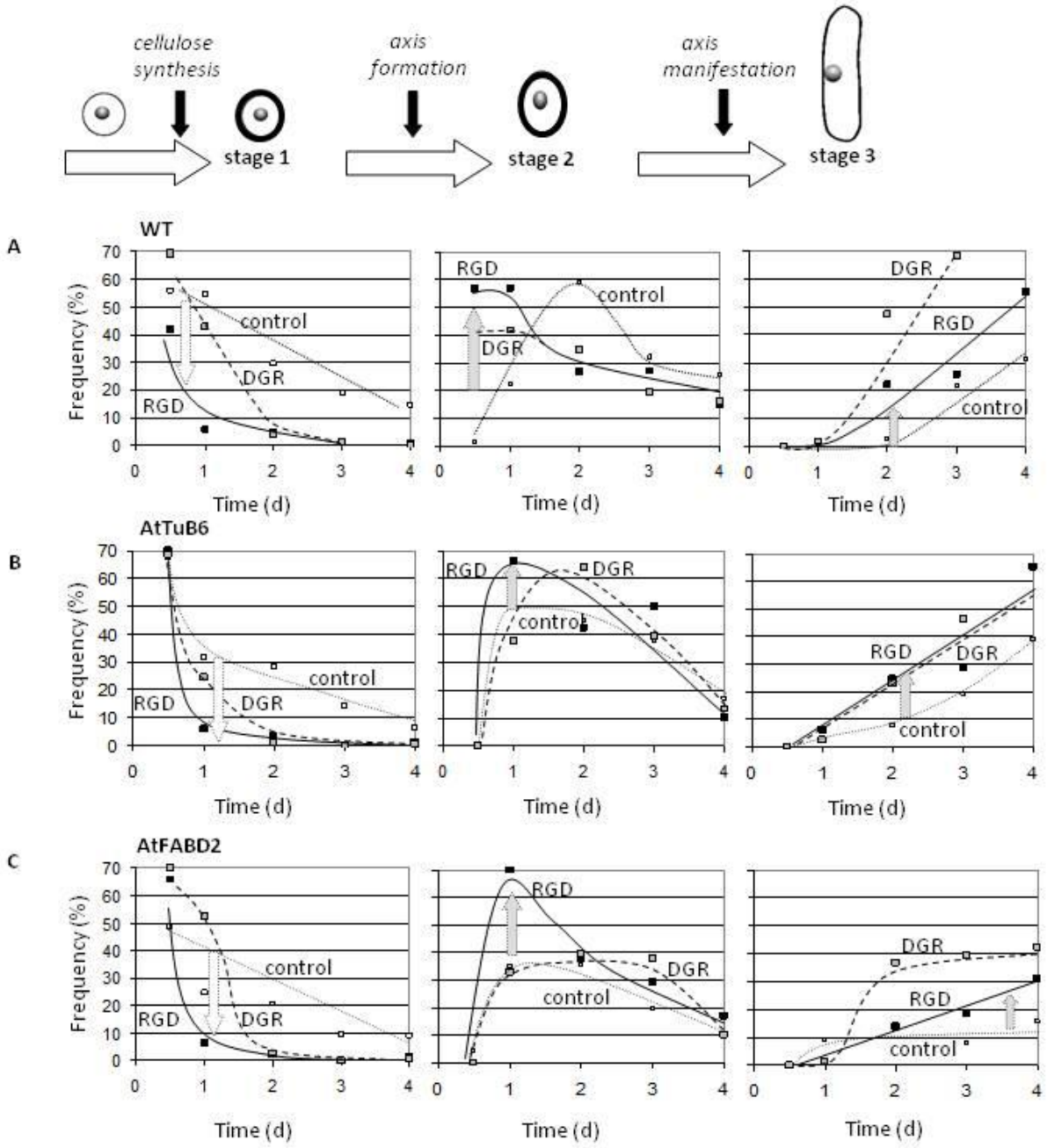

Figure 3.11.: Effect of the heptapeptide YGRGDSP on the temporal pattern of regeneration stages. *Stages 1* to *3* in non-transformed BY-2 cells (wild-type, WT, A), cells expressing GFP in fusion with the microtubule marker AtTuB6 under control of the CaMV-35S promoter (AtTuB6, B), and cells expressing GFP in fusion with the actin marker AtFABD2 under control of the CaMV-35S promoter (AtFABD2, C). Open squares, non- treated cells; black squares, 1 ng/ml of the pentapeptide YGRGDSP; grey squares,1 ng/ml of the pentapeptide YGDGRSP added at time 0. The data represent populations of 300- 2.000 individual cells.

3.3. Geometry sensing

The previous two sections described scalar (non- directional) influences on polarity regeneration. These included changes observed upon overexpression of the actin- binding FABD2 marker, or the overexpression of GFP- tubulin (part 3.1), as well as manipulation of regeneration by cytoskeletal drugs, induced expression of actin- bundling proteins, temperature, and RGD- peptides (part 3.2). In the following, a novel approach is described, where the *tabula rasa* system is integrated into a microfluidic platform, which allows for vectorial manipulations.

To impose vectorial chemical or mechanical cues to the regenerating protoplasts, a microfluidic system was designed. It consisted of a Y- shaped channel, allowing the influx of medium, and rectangular microvessels, which were inserted into the bottom of the channel such that the long axis of the microvessel was oriented perpendicular with the flow of medium (Figure 3.12. A).

First, the technical prerequisites, like the accessibility for microscopic inspection, the suppression of protoplast floating, the homogeneity of the microvessels, sterility, and the exclusion of template auto fluorescence as well as the possibility of leakage of the microvessels had to be considered for the procession of the channel design. The biological requirements, like sufficient supply of nutrients and the possibility for keeping the cells at a high viability, were regarded in the fabrication strategy, the selection of material, size and depth of vessels as well as width and depth of the channels. Furthermore the speed of flow and viscosity of the medium had to be adjusted during lengthy preparatory experiments. This optimization procedure led to a system, where around 90% of loaded protoplasts were found viable even after 7 days of culture in the microvessels.

The protoplasts passed through the characteristic sequence of axis formation (Figure 3.12. B), starting from a spherical protoplast (stage 0), over a radial symmetric cell with a cell wall that can be fluorescently stained by Calcofluor White (stage 1). These stages were followed by a break of radial symmetry and appearance of axiality (stage 2) and finally directional cell expansion (stage 3). Only 12% of the cells did not regenerate a wall and remained arrested in stage 0, but they maintained their viability. Although this fraction of non- regenerating cells is higher than the 5- 7% found for axis regeneration outside of a microfluidic environment (Zaban et al. 2013), the fact that almost 90% of viable cells underwent normal axis formation shows that the conditions, which have been tuned, are close to the technically possible optimum.

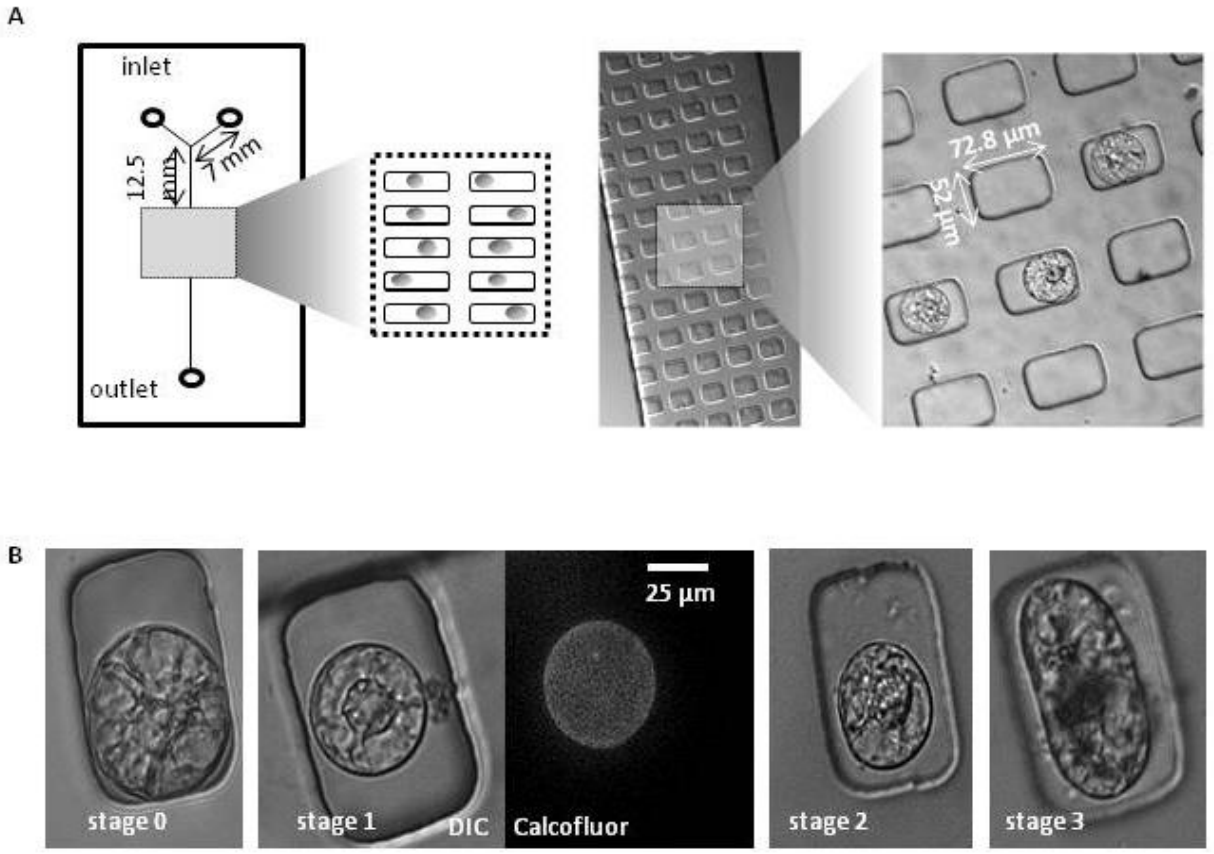

Figure 3.12.: Microfluidic chamber for regeneration of protoplasts in microvessels. (A) Design of channel and microvessels and representative images of microvessels prior to (left) and subsequent to (right) filling with protoplasts. (B) Representative images for different stages of protoplast regeneration following the classification given in (3.1, Figure 3.1, page 44). Stage 0 (days 0-1) protoplast with central nucleus, from which numerous fine cytoplasmic strands emanate, nuclear position is vividly changing during that stage (days 0- 1), stage 1 (around day 1) symmetrical cell with central nucleus apparently tethered to few, massive strands, a cellulosic wall is present at this stage and can be labelled by Calcofluor White, stage 2 (around day 2) first appearance of axiality manifest as ovoid shape, stage 3 (from day 3) rapid cell expansion parallel to this axis.

3.3.1. The cell axis aligns with the vessel geometry before touching the vessel's wall

For the majority of regenerating protoplasts, cell axis aligned with the longer axis of the rectangular micro vessel. This case of alignment is subsequently termed as "longitudinal orientation" (Figure 3.13. A). Only a smaller fraction produced an axis parallel with the shorter axis of the chamber, subsequently termed as "transverse orientation" (Figure 3.13. B).

When these transversely oriented cells touched the wall of the micro vessel, they progressively tilted over an oblique intermediate state (Figure 3.13. C) into a longitudinal orientation, such that the fraction of these cells further drops between day 4 and day 7 (Figure 3.13. D). At day 4 the most of the transversely oriented cells already have touched the wall, but then some of these cells reorientated their position regarding to the cell axis.

Interestingly, the majority of cells that were correctly aligned with the micro vessel axis expressed this axis long before touching the wall (Figure 3.13. F).

3.3.2. Cell axis alignment can be blocked by NPA

The phytotropin 1-N-naphthylphthalamic acid (NPA) is a compound that specifically inhibits auxin- efflux carriers (Petrášek et al. 2006).

To gain insight into the cellular mechanisms underlying axis alignment, the regeneration of protoplasts was followed under the same conditions like in the previous experiments, but with adding a low concentration of NPA (1 µM) via one inlet to the microfluidic stream. This concentration was based on a previous study, where already 3 µM of NPA were sufficient to block division synchrony between the individual cells of a file (Maisch and Nick 2007).

It was observed that the alignment of the regenerating cell axis with the chamber geometry is initiating under control conditions at day 3 (Figure 3.13. D). This was eliminated in presence of NPA at day 4 (Figure 3.13. E), when the majority of cells had already touched the wall. Only at day 7, a slight preponderance of longitudinal alignment with a frequency of 45% over transverse (40%) alignment became detectable. This was produced by cells that had tilted their orientation after being squeezed against the side walls. Thus, the alignment of cell axis is blocked by low concentrations of NPA.

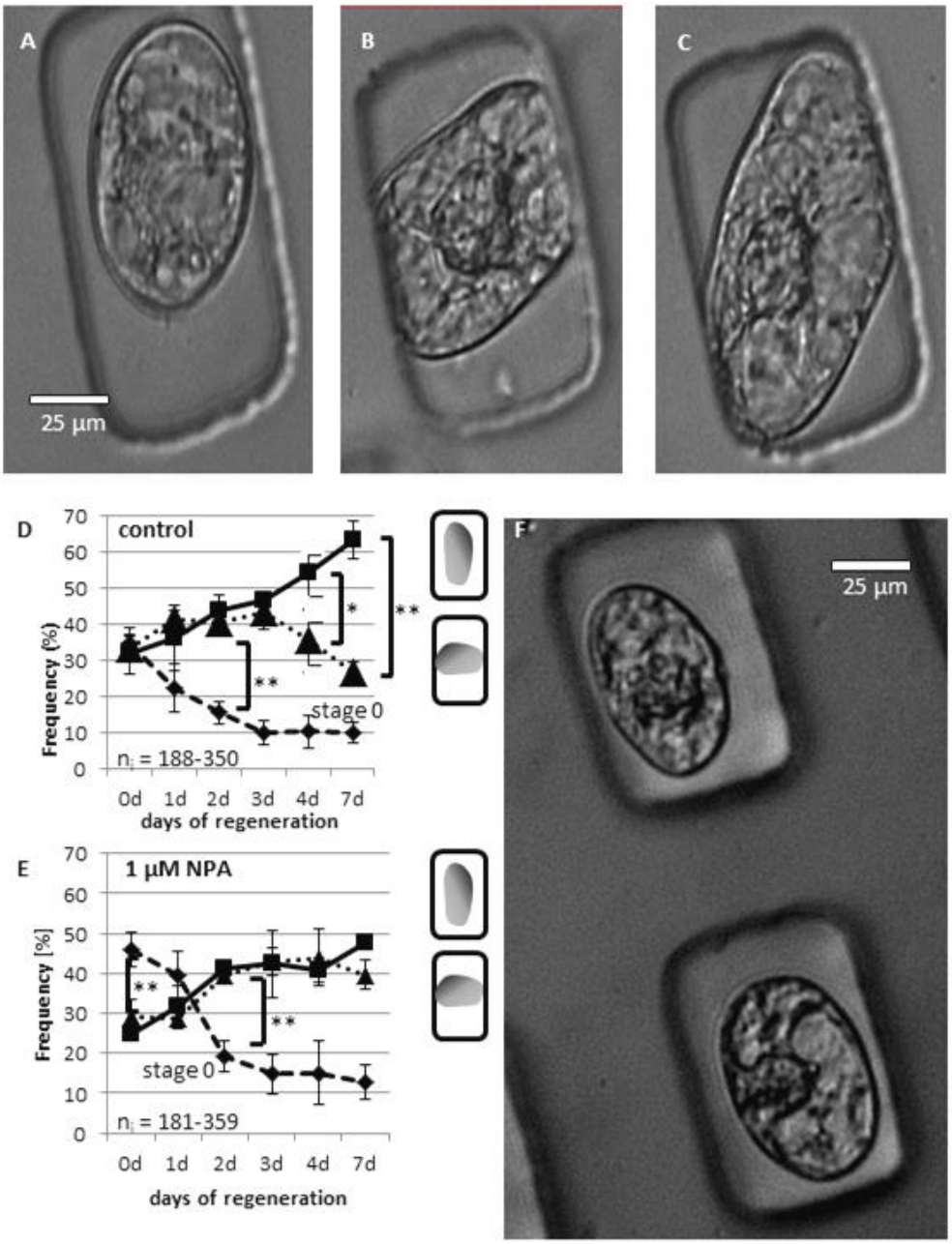

Figure 3.13.: Cell axis aligns with vessel geometry before touching the wall.

(A- C) Different orientations of cell axis with respect to microvessel geometry: (A) longitudinal, (B) transverse, (C) cell during tilting from transverse to longitudinal orientation. (D and E) Temporal change in the incidence of longitudinal (squares) and transverse (triangles) cells, as well as protoplasts that have not initiated regeneration (stage 0, diamonds) under control conditions (D) or in presence of 1 µM of the auxin efflux inhibitor 1-N-napthylphthalamic acid (NPA, E). Data represent average values and standard errors from three independent biological replicas. Brackets represent statistical significance of the indicated differences as tested by a paired, two-sided t-test (* *P*<5 %, ** *P*<1 %). (F) Representative image for the longitudinal alignment of cells in stage 2 that are aligned prior to touching the wall of the microvessel.

3.3.4. Geometrical alignment can be overrun by a flux of NAA, but not by 2, 4- D

In the next step a gradient of the artificial stable auxins 1-naphthaleneacetic acid (NAA) and 2, 4- dichlorophenoxyacetic acid (2, 4- D) was imposed. These two auxins differ with respect to their transport properties (Delbarre et al. 1996 and Hošek et al. 2012): NAA is efficiently transported through the auxin efflux carrier, which can be blocked by NPA, but 2, 4- D is transported through the efflux carrier only poorly.

To exclude potential influence of shear forces, the gradient was administered through mere diffusion by adding 2 µl of 1µM auxin to one of the inlets. In the following step, after it has been taken up into the channel, the flow was stopped.

Due to the fact that, so far, no method is available that would allow to measure the local concentration of auxin, the spread of the gradient of NAA and 2, 4 D and its subsequent dissipation was calculated based on the parameters of the microfluidic device (Figure 3.15.).

The gradient of auxins along the channel was predicted to be maximal at half a day after loading and to be decayed subsequently. Directly after loading, the front of auxins was estimated to be around 5 mm upstream of the first row of microvessels, i.e. 7 mm downstream of the joint, such that transverse gradients of auxin were negligible.

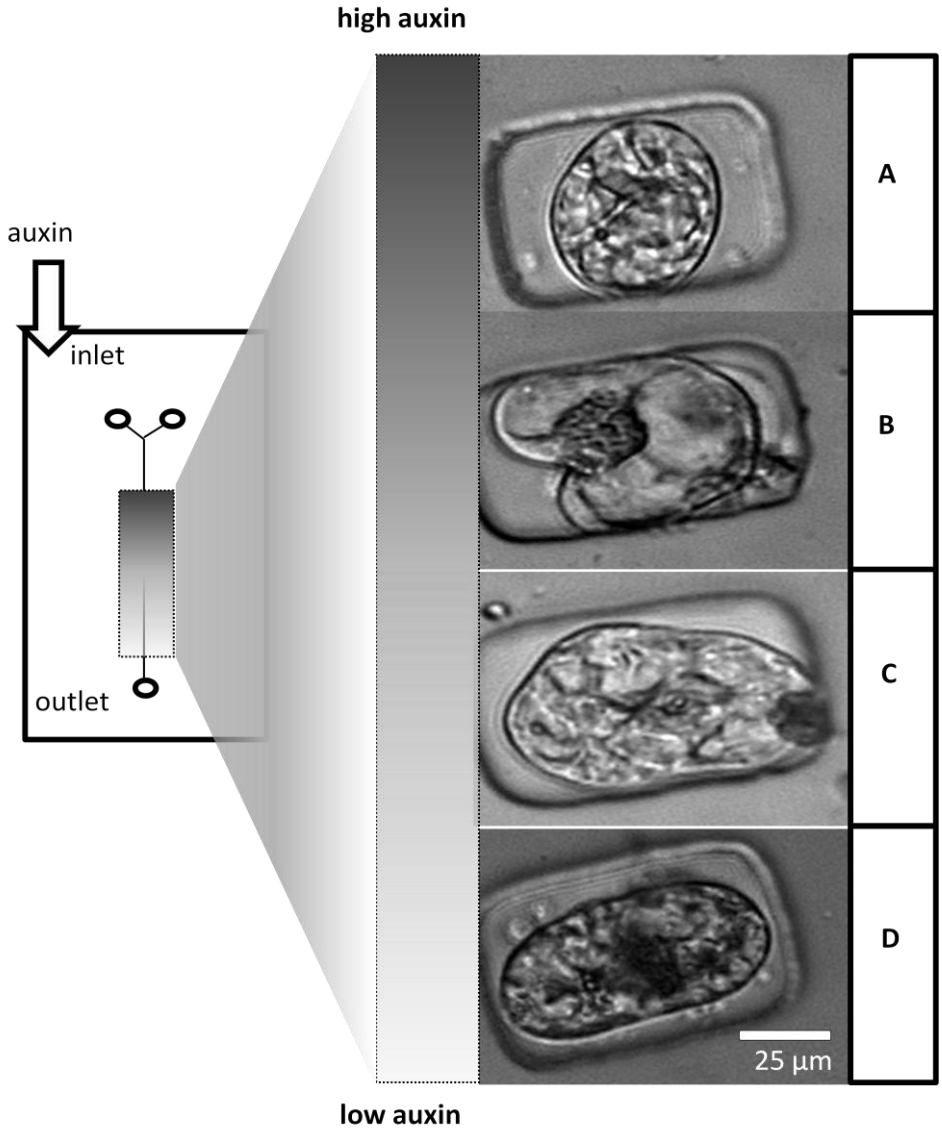

Figure 3.14.: Longitudinal gradients of auxins interfere with geometrical alignment. Set- up of the experiment: The artificial stable auxins 1-naphthaleneacetic acid (NAA) or 2,4-dichlorophenoxyacetic acid (2, 4- D) where administered to one of the inlets (8 µl, 1 µM) after filling the channel with protoplasts. Flux through the channel was stopped, such that the applied auxin dissipated into the channel by diffusion. The resulting gradient was calculated to become maximal around 0.5 days after application and to weaken subsequently slowly approaching a final concentration of around 0.2 µM auxin. Cellular responses were observed and scored (Figure 3.15. and 3.16.) in four domains (A- D) of the gradient as indicated in the figure. Representative images for the cellular responses in these domains are shown for treatment with NAA.

When the response of the cells to the gradient of NAA was screened, a marked difference along the channel was observed (Figure 3.14.):

Close to the inlet, at the anterior end of the channel, the majority of cells aligned transversely, that means parallel to the short axis of the channel. In contrast, at the posterior end of the channel, most cells aligned longitudinally, i.e. parallel with the long axis of the channel. Due to this difference in orientation, the cells near the inlet were rounder, whereas the cells near the outlet appeared more elongate. In the central regions of the channel, cells developed discrepant alignments, where an originally transverse axis was overlaid by subsequent alignment in longitudinal orientation. Thus, the cells oriented parallel to the NAA gradient in the upstream regions of the microfluidic channel, whereas in the downstream regions the geometry of the microvessels dominated.

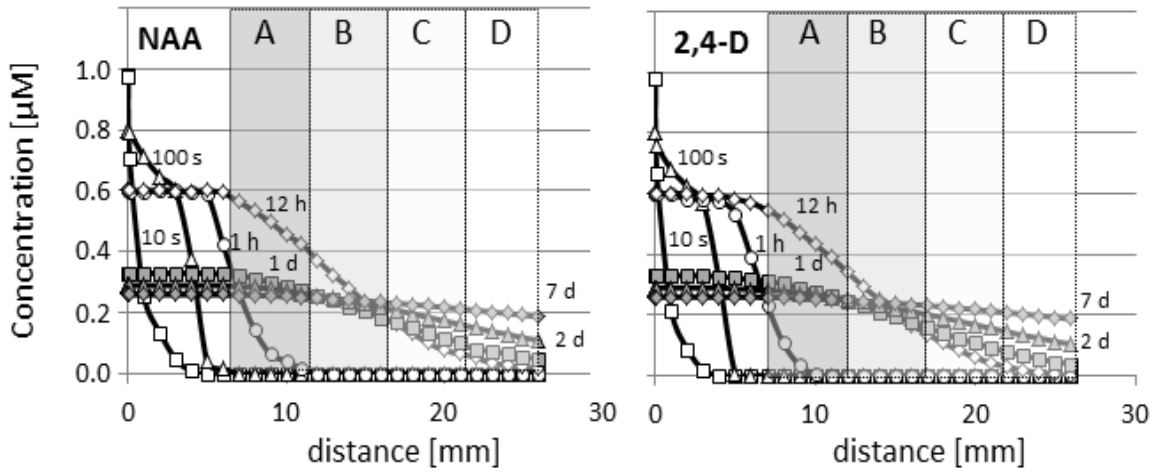

Figure 3.15.: Longitudinal gradients of auxins interfere with geometrical alignment. Predicted temporal dynamics of the auxin gradient.

To quantify this response, the channel was subdivided into four areas from A, most upstream, to D, most downstream, and the frequencies of transverse versus longitudinal alignment were scored over time (Figures 3.14 and 3.16.).

There was a clear gradient in the frequency of transverse alignment with higher incidences in area A and a steady decrease over areas B and C to minimal values in the downstream area D. This gradient was detectable from day 3 on and became more prominent reaching 55% in area A and over 38% in area D, if scored at day 7. Conversely, the frequency of longitudinal alignments increased from the upstream area A (42%) to the downstream area D (52%).

The frequency of non-regenerating protoplasts arrested in stage 0 was lower than 10% throughout. The comparison with the control values in the absence of additional auxin (Figure. 3.16. E) shows clearly that the geometrical alignment was strongly reduced in presence of an auxin gradient even in the most remote area D. In the most upstream area A, geometrical alignment was even overrun by the effect of the auxin gradient.

For comparison, the same set-up replacing NAA by 2, 4- D (Figures. 3.16. C, D), was repeated. Again, there was a gradient of geometrical alignment with a progressive dominance of longitudinal over transverse orientation from areas A over B, C till area D.

However, the reduction of this geometrical alignment by 2, 4- D was less pronounced and was not able to overrun the geometrical alignment, in contrast to NAA. Thus, although both artificial auxins could weaken the impact of microvessel geometry, the effect of a gradient of NAA was stronger and even able to override the impact of geometry, whereas the effect of 2, 4- D was more limited to a reduction of geometrical alignment.

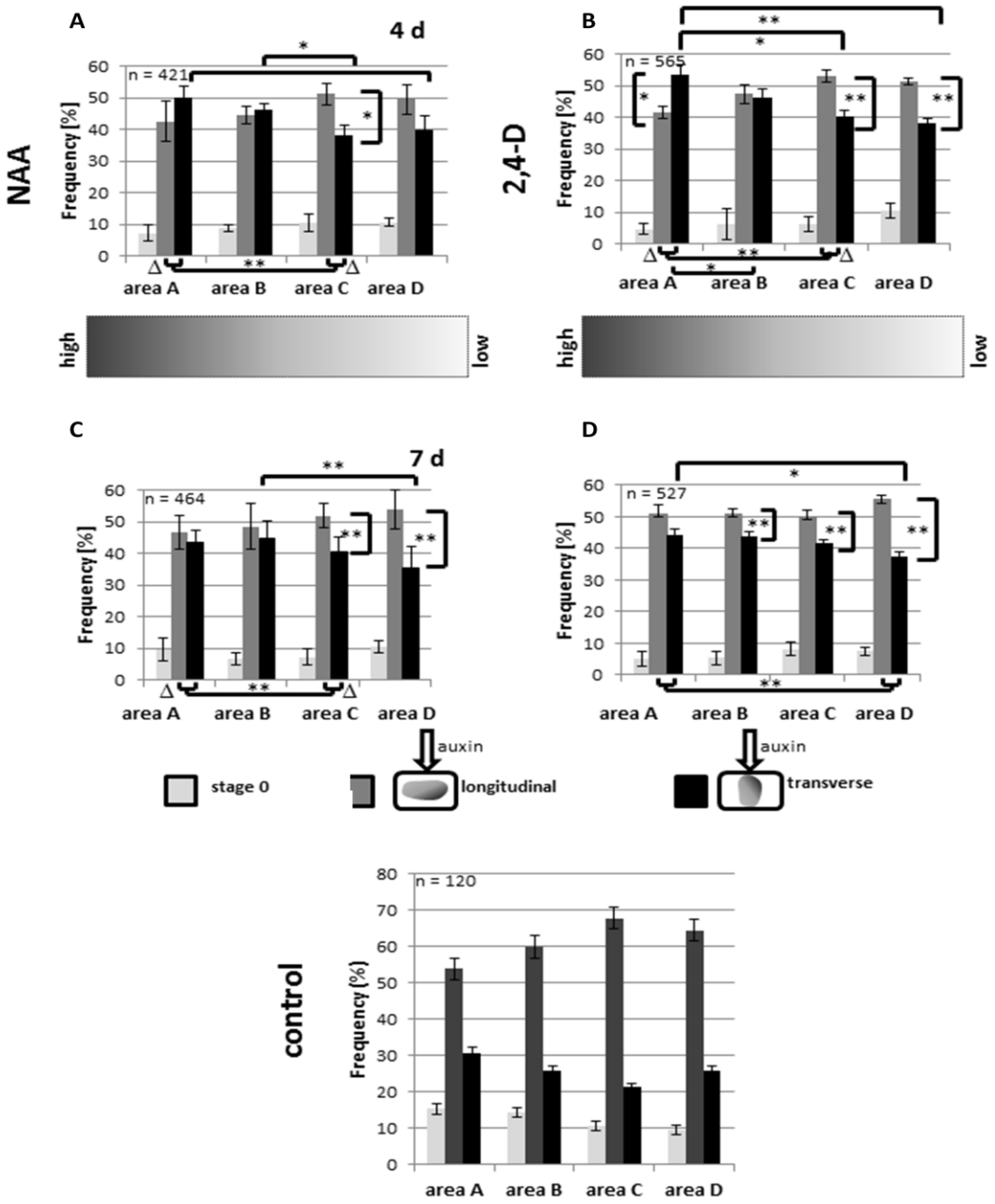

Figure 3.16.: Quantification of the interference by gradients of auxins with geometrical alignment. The incidence of longitudinal (grey bars) and transverse (black bars) cells, as well as protoplasts that have not initiated regeneration (stage 0, light grey bars) in the different domains (A- D, see Figure 3.14.) of a gradient imposed by 1 µM of the artificial stable auxins 1-naphthaleneacetic acid (NAA) (A, B) or 2, 4- dichlorophenoxyacetic acid (2, 4- D) (C, D) at days 4 (A, C) and 7 (B, D) as compared to controls in the absence of auxins (E) assessed shown for the final time point (day 7). Data represent mean values and standard errors of five independent biological replicas. Brackets represent statistical significance of the indicated differences as tested by a paired, two-sided t-test (* *P*<5 %, ** *P*<1 %), the brackets labelled by asterisks represent statistical significance for the difference between transverse and longitudinal alignment in a given domain.

3.4 Summary

In this dissertation a new system for studying polarity establishment and geometry sensing in tobacco BY-2 protoplasts was worked out. With this system it was possible to collect quantitative and qualitative aspects of the polarity induction *de novo* in protoplasts and to integrate this data into a model regarding the protoplast regeneration process.

For the polarity induction *de novo* and also for the geometry sensing in plant cells a lot of factors are closely linked and interacting. With the *tabula rasa* approach it was shown that the configuration of the cytoskeleton is important for the establishment of polarity and the new cell axis. If microtubules were bundled, the regeneration process was accelerated whereas the bundling of actin filaments causes slower kinetics for the regeneration process. It was shown that dynamic actin is necessary for polarity induction *de novo*, especially for the formation of the new cell axis. Furthermore, the actinfilaments- mediated vesicle transport of cellulose synthases towards the membrane of the protoplasts and their integration into the membrane along cortical microtubules is essential for the regeneration of the new cell wall. In addition, the *tabula rasa* approach showed that there is an optimal temperature for the regeneration process and that it is possible to influence the system by using different temperatures, cytoskeletal drugs or RGD- peptides.

Other factors influencing this process are mechanical constraints and chemical signals. To investigate these factors, the *tabula rasa* approach was integrated into a microfluidic platform. The microfluidic channels used in this study contain microvessels and due to the shape of the vessels protoplasts are forced to align their cell axis with the long axis of the vessel. This dissertation showed that this alignment initiated *before* the protoplasts touched the wall, and that protoplasts use auxin efflux for sensing their environment and that the new established cell axis is orientated towards the surrounding geometry. Furthermore, it was demonstrated that an orthogonally added auxin gradient can overrun tissue limitations like the vessel geometry and with addition of artificial auxin the regeneration process was accelerated.

4. DISCUSSION

Because of the sessile lifestyle of plants, plant development has to adapt to the environment. Plants have evolved numerous mechanisms to adjust their shape and their responses to environmental conditions. These responses require that the innate directionality (axis and polarity) of the plant are aligned with directional cues from the environment. In contrast to animals, plant polarity is not systemic, but based on a pronounced polarity of each single cell, which will establish the polarity of the whole plant organism. Thus, the induction of polarity in a single cell marks the first step in plant development and thus in adaptation. In this work, the establishment of cell polarity was investigated by using an experimental system, where cells are stripped from their innate polarity and subsequently induced to regenerate a new cell polarity. This experimental system is based on protoplast of the tobacco cell line BY-2, a model system for molecular plant cell biology. In this system, it was possible to assess the roles of directional signal flow (such as the directional transport of the plant hormone auxin), cytoskeletal organization (i.e. actin filaments and microtubules), and the formation of the new cell wall for polarity induction. Moreover, it was possible to ask, whether the new cell axis is formed *de novo* or whether it is brought about by reorientation of a preexisting axis. As third question, this work investigated how geometrical cues from the environment (for instance, the neighboring cells) are integrated into axis formation.

4.1. The search for the pacemaker of polarity induction

The formation of a new cell wall (leading to stage 1) represents a crucial step in regeneration. With the duration of around 1 day, it limits the rate of the entire process. The newly regenerated walls lack the directional texture characteristic of axially growing plant cells. Their synthesis is preceded by intensive dynamics of cytoplasmic architecture, which includes the active migration of the nucleus. Interestingly, cell wall synthesis does not proceed gradually, but becomes manifested as a sudden and saltatory transition, happening within a few minutes. The time point of this transition differs widely over the population of cells, but for a given cell it proceeds within a very short window of time.

The role of microtubules was probed in this event and it was observed that cell wall regeneration is promoted in the AtTuB6 marker line, which could be phenocopied in the non-transformed wild- type by treatment with the microtubule stabilizer taxol. Conversely, the promotion of cell wall formation in the AtTub6 line could be reverted by treatment with

oryzalin, a compound that sequesters tubulin heterodimers and thus causes a destabilization of dynamic microtubules. The data not only suggest that microtubule stability promotes the synthesis of a new cell wall, but also that the expression of the ectopic tubulin AtTuB6 confers a slight but significant stabilization to microtubules.

The situation for actin filaments is similar: Cell wall regeneration is promoted in the AtFABD2 marker line, which was phenocopied in the non- transformed wild-type by treatment with the actin stabilizer phalloidin. Conversely, the promotion in the AtFABD2 line can be reverted by treatment with latrunculin B, sequestering actin monomers and thus destabilizing dynamic actin filaments. Similar to microtubules, actin filament stability promotes the synthesis of a new cell wall. Again, the expression of the fluorescent actin marker (FABD2, the actin-binding domain of plant fimbrin) confers a slight stabilization of actin filaments consistent with the published record for this probe (Holweg 2007; Wang et al. 2008). Since the cortical actin array is extremely dynamic with filament lifetimes in the range of 30 s (Staiger et al. 2009), any function dependent on this actin array is expected to be extremely sensitive to actin stabilization. At the transition from stage 0 to stage 1, neither microtubules nor actin filaments show any significant alignment, which is mirrored by the absence of directional texture in the deposited cellulose.

RGD- peptides promote the transition to stage 1, and at the same time this transition is well buffered against changes in temperature. These observations can be incorporated into a working model for the cellular events driving induction of axis and polarity in the regenerating protoplast (Figure 4.1.).

The enzyme complexes synthesizing cellulose are transported from the Golgi apparatus to the plasma membrane in exocytotic vesicles (Haigler and Brown 1986), but can only function upon integration of these vesicles into the plasma membrane. The sudden appearance of cellulose within a few minutes (Figure 3.2., p. 46) suggests that these vesicles are not continuously inserted into the membrane. First, they accumulate beneath the membrane and remain in place until they are released simultaneously. This is consistent with a previously proposed model (Emons and Mulder 1998), whereby cell wall synthesis is confined to so-called activation zones, where the constrained fusion of the exocytotic vesicles loaded with the cellulose synthetase is released by a signal, which is probably a calcium wave.

In the regenerating protoplast, this releasing signal correlates with the positioning of the nucleus that undergoes intensive movements prior to cell wall resynthesis (Figure 3.2., p. 46). Since both, cellulose and vesicle transport, require the addition of chemical energy, they should depend strongly on temperature. In this background, the pronounced temperature compensation for the transition from stage 0 to stage 1 is unexpected at first sight. However,

cellulose synthesis is not the rate- limiting process here, because it can proceed within a few minutes, once the vesicles containing the cellulose syntetases have fused with the plasma membrane. However, these vesicles have accumulated over a time span that seems to be sufficiently long to reach saturation, even for the lower temperatures leading to the observed and apparent temperature compensation.

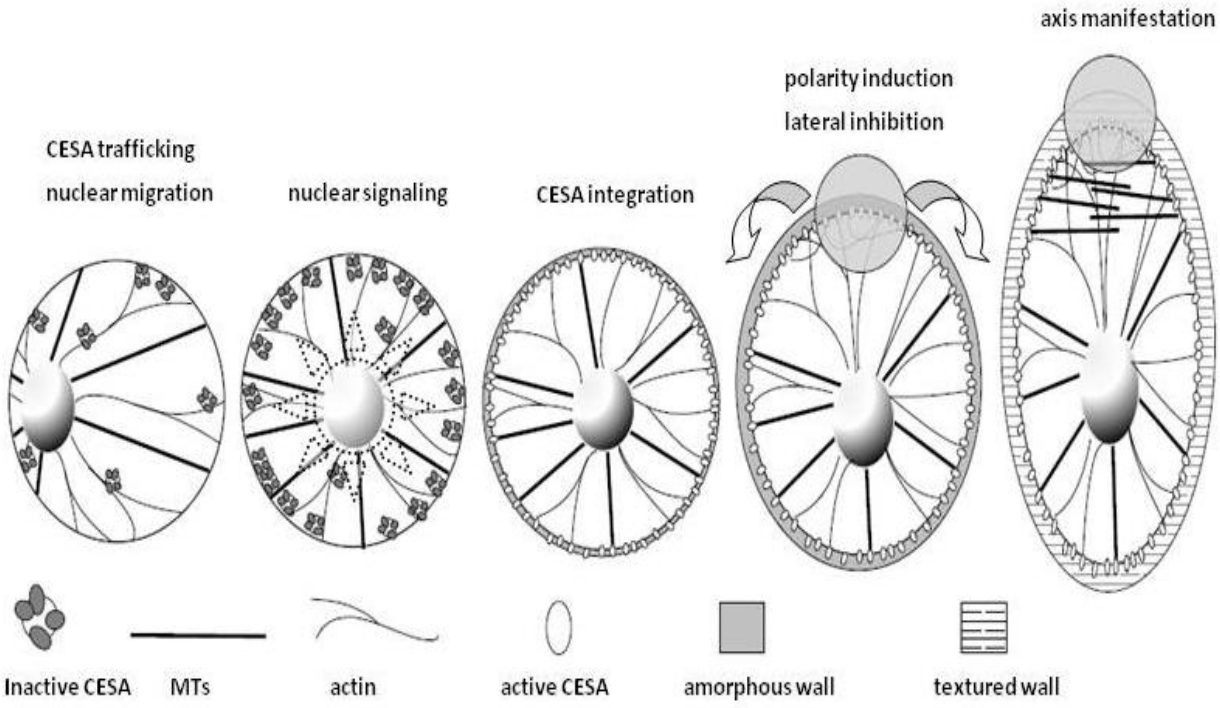

Figure 4.1.: Working model for polarity induction in regenerating protoplasts. During stage 0, vesicles containing cellulose- synthetases (CESAs) are transported towards the membrane, but they are not inserted. Simultaneously, the nucleus is repositioned by the cytoskeleton. When the nucleus has reached the cell center, a signal is released that will trigger integration of CESAs into the membrane followed by rapid synthesis of amorphous cellulose. A cell pole is defined that will laterally inhibit the formation of ectopic competitors. This inhibition requires dynamic actin. Cortical microtubules align in perpendicular orientation reinforcing cell elongation.

Why is the transition toward stage 1 supported by cytoskeletal stability? The efficiency of exocytosis depends on the motility of the endoplasmic reticulum, which in turn is dependent on myosin activity and actin organization (Ueda et al. 2010). This dependency would explain why the transition to stage 1 is promoted by the stabilization of actin and is delayed by its destabilization. It would also account for the effect of RGD- peptides. RGD- peptides can modulate cytoskeletal organization by interfering with the so- called cytoskeleton plasma membrane cell wall continuum (for reviews see Baluska et al. 2003; Pickard 2007), and therefore are expected to modulate the transition to stage 1 as well.

The role of microtubule stability is less evident. The cellulase- interacting protein CSI has been shown to bind microtubules directly *in vitro* (Li et al. 2012), adding further molecular proof to the so- called microtubule- microfibril hypothesis proposed half a century ago (Green 1962). However, this hypothesis dealing with the oriented deposition of cellulose microfibrils does not address why microtubules should stimulate the synthesis of cellulose *per se*, although the microtubule- microfibril hypothesis is relevant for the subsequent stages of regeneration as will be discussed below. It is a second function of microtubules that has to be considered in this context: Microtubules control through unconventional, plant- specific, minusend- directed KCH kinesins (Klotz and Nick 2012) the positioning and tethering of the nucleus, preceding the appearance of a new cell wall. Nuclear positioning, in turn, has been found to act as pacemaker for mitosis (Frey et al. 2010). The nuclear positioning is accompanied by extensive remodeling of cytoplasmic streaming (Figure 3.2.). This leads to the question of whether nuclear movements act as pacemakers for polarity induction.

The mechanism seems to act in a classical case of polarity induction, like the gravimorphosis of germinating fern protonemata: the direction of protonema outgrowth is determined by the gravity vector during a defined time window preceding germination, but cannot adjust its direction once it has germinated (Edwards and Roux 1994). During the time of gravity responsiveness, the nucleus of the spore undergoes vigorous movements that, as concluded from inhibitor studies, are driven by microtubules (Edwards and Roux 1997). In fact, the geometry of cell division is defined by microtubules emanating from the moving nucleus. These microtubules deposit a belt of endosomes that later, upon the completion of mitosis, are read out by a different set of “exploratory” microtubules (Dhonukshe et al. 2005). The observations of this dissertation are consistent with the working hypothesis that the nucleus “explores” its position using microtubules. The nucleus might convey positional information through microtubules to the cell periphery and thus trigger the release of cellulose synthase-containing vesicles underneath the cell membrane (Figure 3.2.).

4.1.1. The formation of the new cell axis requires dynamic actin, whereas the symmetry of axis manifestation depends on microtubule dynamics

A small, but not negligible fraction of cells deviated from the standard path of regeneration. Some of these cells were disturbed in axis manifestation leading to sausage- shaped bending, whereas in other cases, tripolar cells were generated. These deviations were markedly more frequent in the AtFABD2 line, where the lifetime of actin filaments is slightly, but significantly increased (Holweg 2007; Wang et al. 2008).

In fact, axis formation and manifestation could be perturbed by inducible expression of the actin- stabilizing LIM domain, and the high frequency of deviating cells in the AtFABD2 line (about 60%) could be reduced by application of latrunculin B (to 32%) leading to a partial rescue of correct axis formation and manifestation. These findings lead to the conclusion that axis formation and consequently, axis manifestation requires the extremely dynamic population of actin filaments subtending the plasma membrane (Staiger et al. 2009). A conceptual base for this observation (Figure 3.6.) might be the dynamic repartitioning of auxin- efflux carriers required to establish cell polarity (Dhonuskhe et al. 2008; for review see Peera et al. 2011), which in turn depends on dynamic actin (for review see Nick 2010).

However, other actin- related processes such as anchoring of calcium channels or localized secretion proposed for zygote polarity in *Fucus L*. (Brawley and Robinson 1985) should be kept in mind (Figure 4.2.).

The promotion of stage 2 by RGD- peptides can be explained by the accelerated formation of a new cell wall discussed above and suggests that the regeneration of a new cell wall is a prerequisite for polarity induction. The observed pronounced temperature optimum for the transition to stage 2, which might arise from an antagonistic interaction between membrane fluidity and actin filaments, is similar to the situation reported for cold acclimation (Örvar et al. 2000). The tripolar cells resemble the structures observed in *Fucus*, when the zygotes were irradiated with strong plane polarized blue light (Jaffe 1966). These tripolar structures call for a critical discussion of terminology.

Polarity can be expressed in two versions (Nick and Furuya 1992): As complex polarity, where both poles along an axis are explicitly defined by molecules or activities, or as simple polarity, where only one pole is defined explicitly, whereas the opposite pole is merely defined by the absence of the respective molecules or activities.

The animal- vegetative polarity of sea- urchin eggs (Boveri 1901), the prestalk- prespore polarity of *Dictyostelium discoideum* (Williams 1988), or the head- foot polarity of *Hydra* (Bode and Bode 1984) provide classical examples for complex polarities. As pointed out

more than a century ago by the plant physiologist Julius Sachs during a scientific debate with his opponent Vöchting (1878), any reorientation of complex polarities should result in a quadripolar situation (Sachs 1880). However, tripolar situations as those observed here are indicative of perturbations of simple polarities, when a second, competing pole is ectopically laid down. In *Fucus L*., it is the site of prospective rhizoid outgrowth, which is explicitly defined by the accumulation of calcium influx channels and the actin cap. On the other hand the opposite thallus "pole" is not defined positively, but simply follows a default pathway proceeding in the absence of calcium influx and membrane- associated actin (Brawley and Robinson 1985; Goodner and Quatrano 1993).

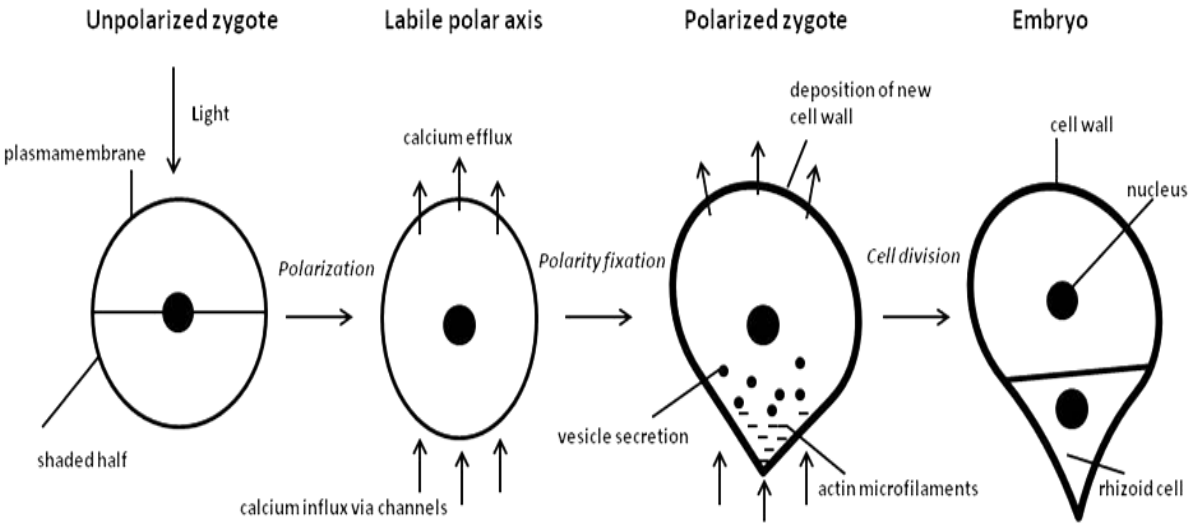

Figure 4.2.: Model of polarity induction in the *Fucus* zygote.
By an asymmetric stimulus from the environment, such as light pulse, the zygote is polarized. Current-charged calcium ions move through the polarized but still spherical zygote at the site at which the rhizoid will emerge. Cell polarity is fixed when actin microfilaments assemble at the site of the rhizoid pole and the cell wall assembles around the zygote. After that, the zygote divides, and the rhizoid cell grows at its tip. Model modified from Plant Physiology online, Chapter 16.3.

Irradiation with plane polarized light will activate the already oriented and therefore dichroitic photoreceptor to a similar extent in two sites of the zygote such that two competing rhizoid sites will develop. The thalloid pole, which is actually just a “none-pole”, will remain undivided, leading to the observed tripolar structures. For complex polarities, a body axis appears concomitantly with or even prior to polarization.

In contrast, simple polarities have to be established and read out as morphogenetic gradients before a body axis can be laid down. The tripolar structures, which were observed when actin dynamics are impaired during the initial phases of regeneration, suggest that it is the polarity induction rather than the axis formation that drives the transition from stage 1 to stage 2.

Following the polarity induction and axis formation, cortical microtubules are progressively ordered into parallel arrays, accompanied by cell elongation in a direction perpendicular to microtubule orientation and a progressive alignment of cellulose texture along microtubules. The actin network is repartitioned in favour of perinuclear bundles that are interconnected with the cortical actin prevalent during the preceding stages. The AtTuB6 line, although promoted in the early transitions (up to stage 2), was trapped in stage 2 and subsequently produced a high fraction of characteristic sausage- shaped aberrations. This phenotype could be partially phenocopied by taxol, and partially rescued by oryzalin.

Axis manifestation (leading to stage 3) is based on elongation growth, which requires anisotropic cell expansion (Sijacic and Liu 2010). In expanding cylinders, mechanic tension is anisotropic with transverse doubled over longitudinal tension, such that cylindrical plant cells are expected to widen rather than to elongate (Preston 1955). By transverse deposition of cellulose microfibrils, plant cells can override this mechanic anisotropy and reinforce elongation growth (Green 1980). Cortical microtubules can align cellulose orientation either by physical coupling with cellulose- synthase subunits through proteins such as CSI1 (Li et al. 2012) or by influencing cellulose self-organization through a control of cellulose crystallinity (Fujita et al. 2011). The setup of parallel microtubule arrays (transition from stage 1 to stage 2) might be caused by disassembly of the randomly-oriented network found in stages 0 and 1, followed by a directional reassembly. Alternatively, microtubules might co-align by mutual sliding. Directional reassembly would be impaired when microtubules are stabilized by taxol or overexpression of the AtTuB6 marker.

However, it is observed that under these conditions, stage 2 was advanced in time consistent with a model of mutual sliding. A promotion of microtubule alignment after treatment with taxol has also been reported by Kuss- Wymer and Cyr (1992). However, the readout of the cell axis from these microtubule arrays requires dynamic microtubules, since AtTuB6 cells

are trapped in stage 2 and exit with a high frequency into aberrant sausage- shaped aberrations. This aberration is accompanied by asymmetric deposition of the cell wall, very often linked with a strong asymmetry of nuclear positioning which is shifted towards the concave flank where the wall is thicker (Figure 3.4.). This phenotype indicates that microtubule dynamics are necessary to balance cell elongation at the two flanks of the elongating cell. It is not straightforward to derive the observed thickness of the cell wall from altered orientation of cortical microtubules. However, the model already proposed for the transition from stage 0 to stage 1 might also account for the role of dynamic microtubules in axis manifestation (stage 3).

A signal from the nucleus, conveyed through microtubules, might promote the integration of cellulose- synthase complexes into the membrane (Figure 4.1.). The symmetry of this signal would be established depending on the dynamic instability of competing microtubule populations at the two flanks stabilizing microtubules. This geometrical cross- talk would be impaired such that cellulose synthesis at the cell wall adjacent to the nucleus would be uncoupled from the events at the opposite flank, resulting in the observed sausage phenotype. The promotion of axis manifestation by RGD- peptides indicates a stabilizing function of the cytoskeleton plasma membrane cell wall continuum consistent with the model of a regionally differentiated membrane (Baluska et al. 2003; Pickard 2007). The feedback from the cell wall relies on dynamic actin filaments that are found to align with the elongation axis, consistent with the published record on elongating plant cells (Smertenko et al. 2010). It should be mentioned that in this study similar sausage- shaped aberrations were observed under conditions of sustained auxin depletion.

4.2. A technical “tissue” allows to separate mechanical from chemical cues

Plant cells process chemical and mechanical cues for alignment of their axis of growth and division to minimize mechanical tensions in the turgescent tissue. As illustrated by the phyllotaxis model, which describes the regular arrangement of lateral organs around the stem (Bayer et al. 2009, Scarpella et al. 2006), the individual roles of these cues are difficult to be separated in the complex context of organs and tissues. This was the motivation for the strategy to mimic both cues by a technical simulation of a plant tissue.

Here, the chemical cue, auxin flux, was administered as microfluidic gradient, whereas the directional mechanical cue was achieved by rectangular microvessels of a size that are corresponding to the dimensions set by cell walls in a natural tissue. Plant protoplasts as symmetrical cells that had been stripped from their innate directionality by the digestion of the cell wall were integrated into this technical framework. Although the idea of a biomimetic array of “artificial cells” that are arranged in a flow of a chemical signal may seem straightforward, the technical realization of this approach was far from being trivial.

A long preparatory phase was required to reconcile the technical with the biological requirements and to establish a system that could be handled. It must preserve biological functionality allowing at the same time a high degree of reproducibility.

Biomimetic microfluidic devices inspired by plant tissues have been generated previously by parallel channel networks embedded in a polymeric material layer and used to investigate the optimal pattern for maximal flow in order to understand the biophysical constraints shaping venation patterns in real leaves (Noblin et al. 2008) or by generating a microfluidic system in a hydrogel to study biophysical aspects of transpiration (Wheeler and Stroock 2008). However, these approaches remained merely technical and did not integrate cells. There are two reports, where plant cells, more precisely protoplasts from tobacco leaves, have been kept alive in a microfluidic channel over several days (Ko et al. 2006, Wu et al. 2011). However, in both cases, cells were floating freely in a large compartment of around 1 mm width without any possibility to administer directional cues to the regenerating protoplasts. In contrast, the system described in the current work successfully integrates living, developing plant cells into a technical realization of a tissue, where either mechanical or chemical cues can convey directional information.

To the current state of knowledge, the setup in this dissertation represents the first example where this has been achieved for plant cells.

4.3. Regenerating protoplasts use auxin efflux to explore geometry

As mentioned above, the role of the cytoskeleton for the symmetry break in the regenerating protoplast was followed (chapter 3.1, p.43-51). Interestingly, the first phase of regeneration is characterized by extensive nuclear movements. Only when the nucleus has been positioned to the cell center in a long preparatory phase that usually lasts an entire day, the symmetrical cell produces a new cell wall by a rapid process completed in a few minutes. This walled cell is still perfectly symmetric. Following that stage, symmetry break is observed by alignment of actin in a gradient followed by microtubular alignment perpendicular to this gradient.

This scenario supports a model, where mechanical constraints of the cell wall are used as spatial input for cytoskeletal reorganization similar to phyllotaxis in the developing apical meristem (Hamant et al. 2008). The observation that the cells align with the longer chamber axis, are congruent with this model.

However, a closer look revealed that the alignment with the longer chamber axis became evident, before the cells were touching the wall, i.e. before there was any mechanic input from pressure of the expanding cell against a mechanic constraint. This indicates that the cells use a non- mechanical signal to explore the geometry of the surrounding space. This signal might be auxin. This idea was tested by inhibition of the auxin efflux by the well established and specific inhibitor NPA (Thompson et al. 1973).

4.3.1. Auxin flux *versus* local auxin concentration

In fact, it was observed that the alignment of cell axis with the longer chamber axis was lost in presence of NPA. The expanding protoplasts use auxin efflux to explore the geometry of their environment and subsequently use differences in the local concentration of auxin to align their axis in such a way that during later expansion the resulting mechanical tension will be minimized.

The discovery of auxin- dependent alignment leads to question on the nature of the input. Principally, the cells might respond to the local concentration of auxin at the different flanks of the regenerating cell. Alternatively, they might respond to the flux of auxin that has passed through them. The debate on these two models has been quite controversial since Tsvi Sachs (Sachs, 1969) proposed that the auxin, which is transported through a given cell in the regenerating tissue, will act as signal promoting the capacity for polar auxin transport in a positive feedback loop. This so- called auxin canalization can be seen as the core mechanism for the flexible architectural self organisation of vascular land plants (Figure 4.3.).

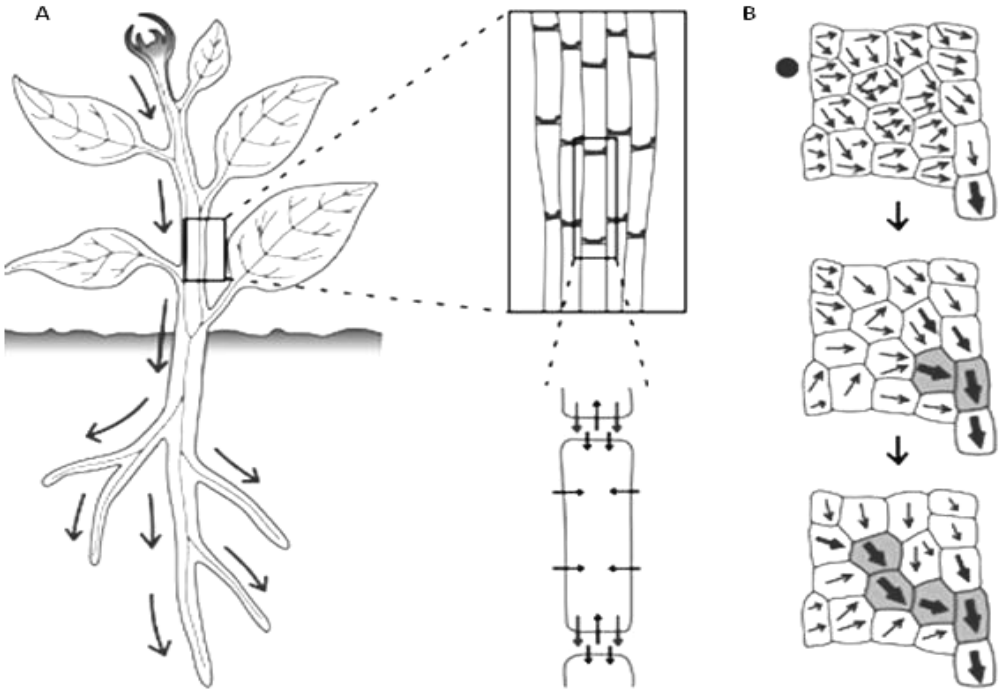

Figure 4.3.: Auxin transport and canalization hypothesis. (A) Auxin is produced in large amounts in immature shoot-organs and is transported to the roots by vascular strands. The apical- basal polarity of auxin transport derives from the polar localization of efflux carriers of the PIN proteins at the basal plasma-membrane of vascular cells. Specialized efflux carriers are required for auxin to leave the cell (black arrows) as auxin is negatively charged at intracellular pH; by contrast, auxin is electrically neutral at extracellular pH and can thus diffuse into the cell. (B) Stages of vascular strand formation in response to lateral application of auxin (black circle) according to the “auxin canalization hypothesis”. The positive feedback between cellular auxin efflux (black arrows) and the localization of efflux carriers is shown. At the cellular site of auxin gradually polar auxin transport exits (thicker black arrows). This occurs first in the cells in contact to the pre- existing vasculature. They transport auxin along the original, apical-basal polarity of the tissue. Large polar-auxin-transport capacity in selected cells leads to vascular differentiation (grey fill) and drains auxin away from neighboring cells. The process forms a continuous vascular strand that connects the applied auxin to the pre- existing vessel. Figure modified from Sawchuk and Scarpella (2013)

.

This mechanism channels the auxin flux in regenerating tissues into distinct pathways that later will differentiate into vascular bundles such that new organs as young leaf primordia or buds will be optimally connected. But it also can be bypassed through interruptions by wounds inflicted onto the pre- existing vasculature. Microscopical details of fossil wood suggest that this canalization has been used back to 400 million years ago (Rothwell and Lev-Yadun 2005).

4.3.2. Mystery of the PIN- Proteins: Do the auxin transporters also act as receptors for auxin?

A conceptual problem of this flux canalization model has been the need to explain, how a cell could measure the flux of auxin (a “holistic feature”). Therefore, alternative mechanisms have been searched that would sense local concentrations of auxin as input rather than fluxes of auxin through the cell (Merks et al. 2007).

The polarity of auxin flux is brought about by a transcellular gradient in the activity of auxin efflux carriers such as the PIN transporters. This gradient of PIN activity has been shown to arise from a gradient in the PIN cycling between the plasma membrane and intracellular stores (Dhonukshe et al. 2008). This cycling, in turn, depends on the concentration of auxin in the environment (Paciorek et al. 2005) and on dynamic actin filaments that are remodelled in response to auxin (for review see Nick 2010). When the cycling of PINs would differ as a function of local auxin concentration, this would explain in principle, why the cell axis aligns with auxin gradients and would circumvent the need to sense fluxes of auxin. Since the gradient is maximal at 0.5 d after loading and dissipates later, the induction of a cell axis in parallel to auxin is determined during the first day of regeneration. This is consistent with the other experiments, where polarity in regenerating BY-2 protoplasts was disturbed by inducible expression of actin- bundling proteins at different time points (Zaban et al. 2013). Interestingly, this axis becomes manifest only from 2 d later.

For answering the question if the “artificial tissue” designed in this work might contribute to the debate a gradient of two (artificial) auxins that differ with respect to their transport features was administered: NAA is transported in a polar manner, which is very similar to the natural auxin IAA, whereas 2, 4- D is transported only very poorly (Delbarre et al. 1996, Hošek et al. 2012). The auxin gradient was oriented perpendicular with the long axis of the microvessels, and the consideration was, whether this gradient could affect or possibly overrun the directional cues derived from microvessel geometry. For NAA, this was exactly what was observed. In contrast, a gradient of 2, 4- D failed to overrun the effect of microvessel geometry. This indicates that directional transport of a given auxin species

promotes the alignment of cell axis with the auxin gradient. Interestingly, NAA, but not 2, 4-D, were found to be effective in triggering the actin remodelling required to sustain polar auxin transport as shown for tobacco BY-2 (Maisch and Nick 2007) and rice coleoptiles (Nick et al. 2009).

There is a second argument in favour of the auxin flux mechanism: The local sensing mechanism predicts that PIN transporters would accumulate at the sites of elevated auxin concentration such that auxin is pumped up into local maxima (Merks et al. 2007). When the expanding protoplast approaches the wall of the microchamber, this should cause a local increase of the secreted auxin in the limited space between membrane and chamber wall, such that PIN transporters would be expected to accumulate there, which should result in axis alignment parallel to the shorter axis of the microchamber – opposite to the observation. Therefore, one could not neglect the microchamber geometry and should keep in mind that there might be other factors e.g. mechanical or other hormonal stimuli, which influence the induction of polarity beyond the effects of auxin efflux.

4.4. Future prospects

The microfluidic system used in this dissertation is, of course, still a very rough approximation of the situation in a tissue, where local maxima and minima convey positional information. Further improvements regarding the microchannels, e.g. minimization of the microchannel leakage, must be developed for an easier handling of the preliminary work steps and the following loading processes.

Another new channel design, based on the present microchannels, should be developed. This would make the implementation of the gradients easier and the areas within the channels could be distincted more effectively. With the further processing of the channel design one could set up new designs of technical plant tissues prospectively with a specialized function by using single cells and the manipulation of those via microfluidics. E.g. studying the cell cell interaction and communication in such a technical tissue could be possible through the development of artificial Plasmodesmata by the insert of small channel connections between the single microchambers.

As experimental approach to discriminate between different sensing mechanisms, the auxin-reporter line DR5::GFP could be integrated into the gradient. However, it should be kept in mind that gradients potentially visualized by this reporter would not necessarily monitor local concentrations of auxin, but the temporal integral of auxin- dependent transcriptional activation. To map the auxin effects in a high spatio- temporal resolution, it would be possible to integrate the novel sensor DII Venus into the system described in this work. It is a versatile tool to analyze dynamics of auxin distributions and signaling during development. This tool was already used to follow dynamic changes in cellular auxin distributions within different tissues of *Arabidopsis thaliana* (Brunoud et al. 2012).

A further strategy would be to use 2- NAA as well transportable, but biologically inactive auxin analogue, as well as other inhibitors such as CPD (l-(2-carboxyphenyl)-3-phenyl-propane-l,3-dione), PBA (1-pyrenoylbenzoic acid), TIBA (2,3,5-triiodobenzoic acid), or Brefeldin A. CPD, PBA and TIBA are auxin transport inhibitors whereas Brefeldin A is inhibiting vesicle trafficking and just mimics physiological effects of auxin transport inhibitors.

Whether the explorative signal is auxin itself, or whether, alternatively, a signal that interferes with auxin passage through the membrane (an interesting candidate would be apoplastic protons) will be a topic for future experiments. New experiments by changing the intercellular auxin flux rates should be considered to get a deeper insight into the polarity establishment taking place in an apolar cell. Therefore, the integration of the patterning information by

feeding caged IAA and the release of locally active auxin by means of microirradiation (Kusaka et al 2009) would be a future aim. This can then be combined with transgenic cell lines, where either cytoskeletal components or components of auxin transport, like PIN Proteins, and signal components are visualized by fluorescent proteins.

4.4.1. Long term aim and vision

Since of a rising number of cancer and other diseases of mankind, a great need for the development and production of cancer drugs and other medicine arises in the pharmaceutical field. In some cases the production is quite costly e.g. for taxol (Paclitaxel ®), which is used in many treatments for cancer combat (Kaye, 1996). Due to this it is not astonishing that the need for new sources in cancer pharmaceutica is extremely promoted. Even in the sea, rare animal species are investigated for the discovery of usable substances like makrolides for instance, and their effects on cancer diseases (Yeung and Paterson, 2002).

It is known that many plants produce rare and expensive chemical substances which can be used for disease treatment. The current method to get those substances is the chemical isolation via tissue extraction. The extraction and purification for taxol (patent US6452024 B1, 2002) is costly, needs big amounts of dried plant material of Pacific yew (*Taxus brevifolia*) and it is time consuming.

With the further processing of the technical plant tissue it could be one day possible to exploit rare and expensive chemical substances like taxol or withanoloides in a simpler and cheaper way by using plant cells in a microfluidic system. Examples for the use of withanoloides are the salpichrolids, which are used in the agricultural field as an insecticide and ixocarpalacton A, which is a promising agent for the prevention of cancer.

The microfluidic system developed in this thesis might be used to put integrate specialized plant cells with the capability to produce the desired chemical substance into a microfluidic channel, feed them with a cheap precursor or inducer A via one inlet and obtain the desired, expensive substance B through the outlet, for instance.

However, to develop this, a lot of cooperative work and interactive research between biochemists, pharmacists and microfluidic experts must take place.

4.5. Conclusion

In plant cells polarity induction *de novo* can be investigated and understood by using BY-2 tobacco protoplasts. By the definition of subsequent regeneration stages it was possible to quantify and qualify the regeneration progress. By the use of different cytoskeletal inhibitors the role of actin filaments and microtubules for polarity induction could be assessed. Moreover, the influence of temperature and RGD- peptides acting on unknown plant analogues of integrins, were also tested. The results have identified microtubule- driven nuclear movements and cytoskeleton- membrane- cell wall interaction as important factors for polarity and axis induction *de novo*. Microtubules as mechanically rigid structures can convey compression forces, whereas actin as flexible elements can convey traction forces. When both elements are linked by proteins such as the KCH- kinesins (Klotz and Nick 2012), a tensegrial network emerges that can collect and integrate mechanic forces, which allows the cell to explore geometry (for review see Nick 2011).

Using a microfluidic based technical simulation of a tissue and regenerating protoplasts it was investigated, how plant cells adjust their axis in a way that resulting mechanical tensions in the tissue will be minimized. It was shown that the regenerating protoplasts formed a new axis in harmony with the geometry of their environment. To explore geometry, they use auxin efflux as chemical cue, before even facing constraints from physical contact with the wall of the vessel or, in real tissues, the counterforce from a cell wall. This chemical sensing of geometry required auxin efflux with input from local auxin concentration. A gradient of NAA could overrun the geometry of the microvessel regarding the axis formation in the regenerating cell. A gradient of 2, 4- D, although less efficient than NAA, could reduce to a certain extent the input from microvessel geometry.

5. APPENDIX

5.1. Comparison of two independent non- transformed BY-2 WT cell lines regarding the regeneration process

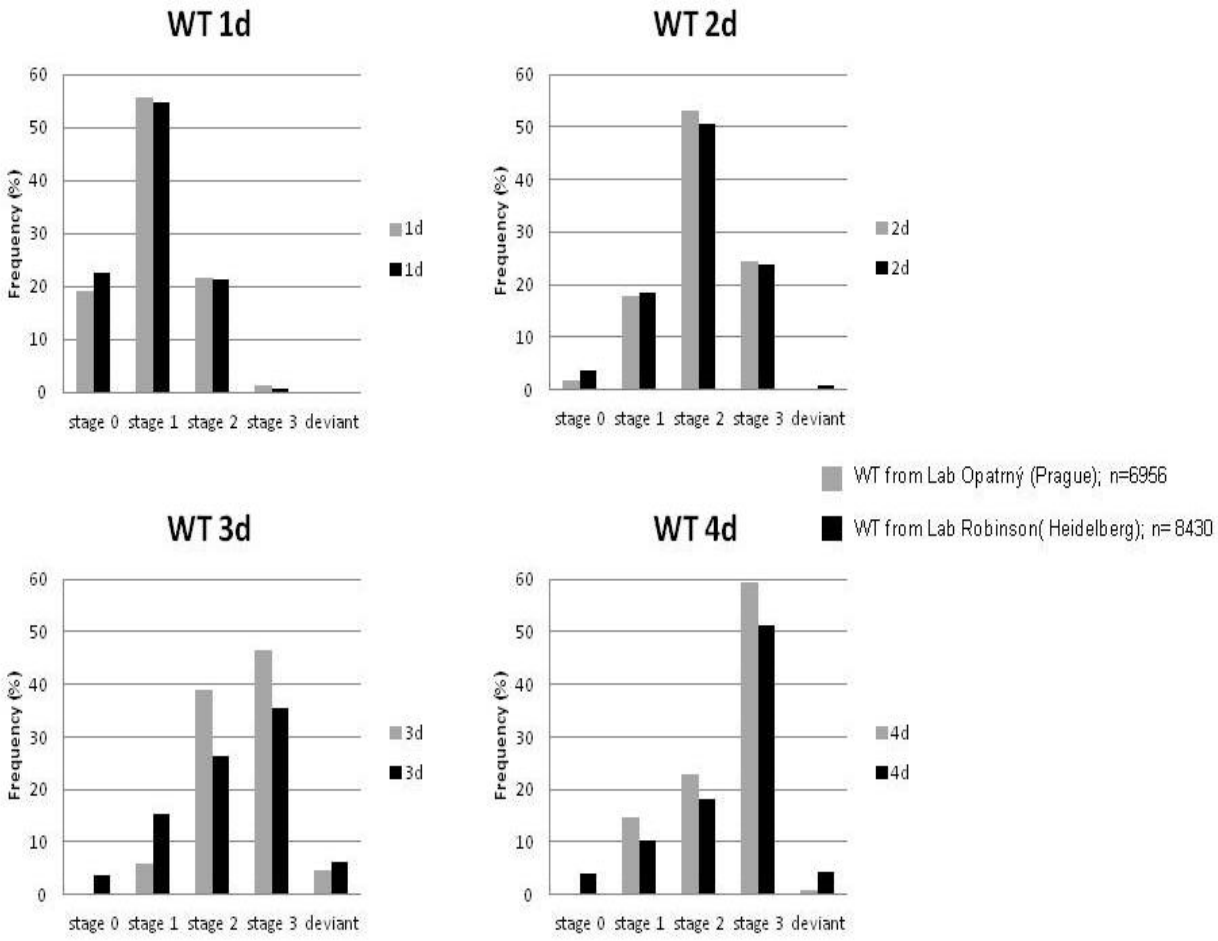

Both non- transformed BY-2 WT cell lines are not significant different in their frequencies of regeneration stages observed on day 1 and day 2. Note that the grey marked BY-2 WT cell line from Prague differs at day 3 but align again on day 4 with the black BY-2 WT cell line originated from the Robinson lab.

5.2. RGD and DGR treatment of non- transformed BY-2 WT protoplasts

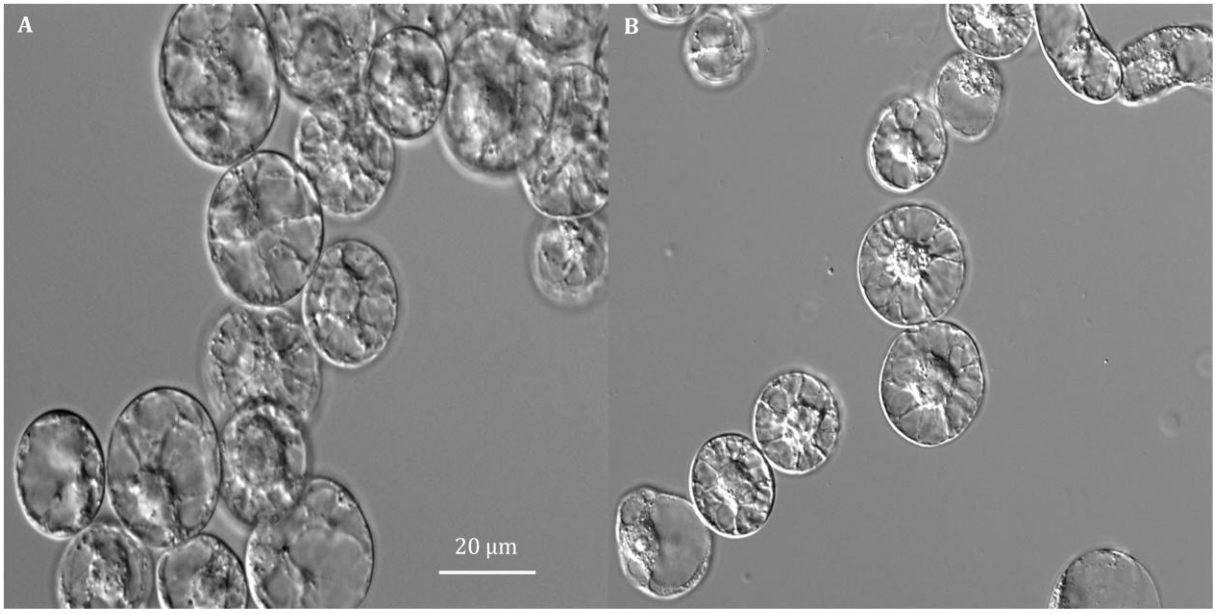

After 1d the regenerating BY- 2 WT protoplasts treated with 10 ng RGD- peptide (A) are closer together than Protoplasts treated with 10 ng DGR-peptide (B). In (A) more cells are already in stage 2 (compared to (B)). The total percentage of the number of cells is similar, but with RGD treatment the cells are forming conglomerates.

5.3. Cell viability of non- transformed BY-2 WT cells within the microfluidic channels

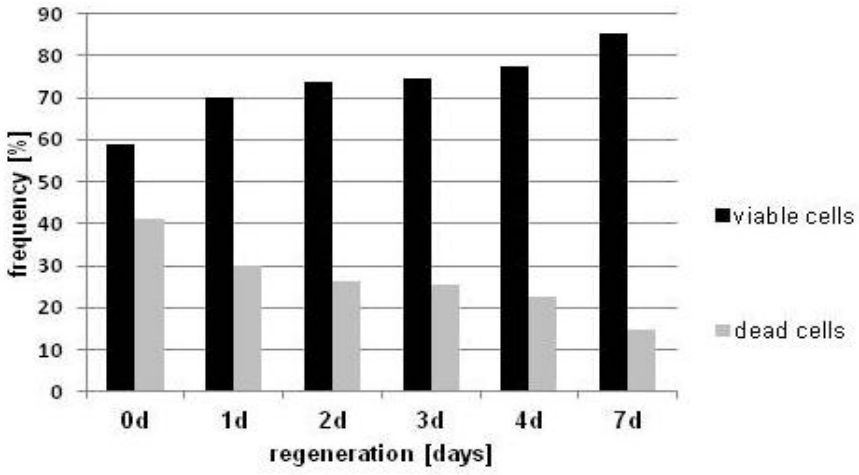

Within the microfluidic channels the cell viability is comparable to the viability of regenerating cells in an autonomous environment. The percentage of dead cells descends continuously until day 7 of the regeneration process. While on the first observation day the frequency of dead cells is around 40%, on day 7 just around 10% of dead cells were counted.

5.4. Frequency of BY-2 WT cells in areas A-D

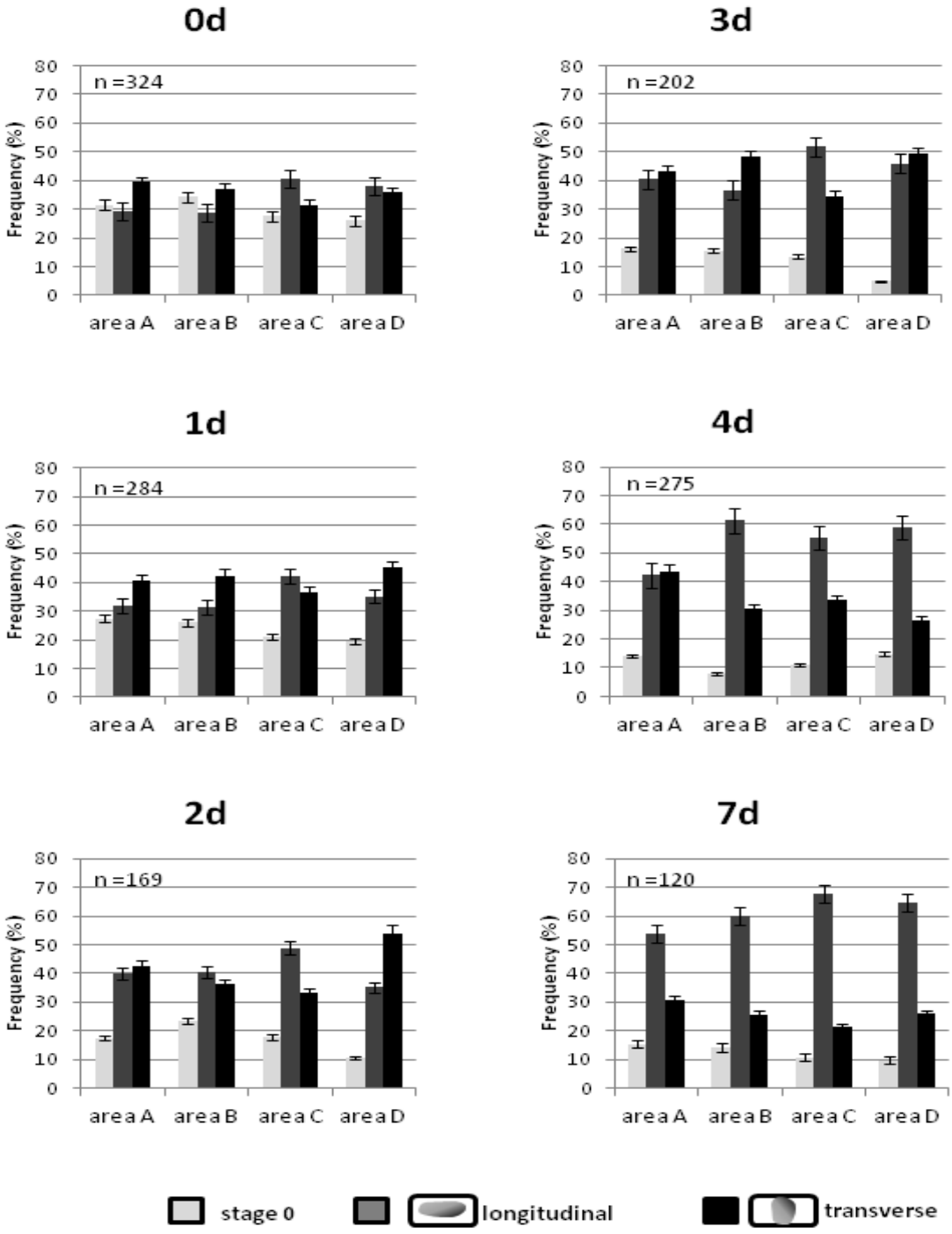

Complete data set of the frequency of BY-2 WT cells from day0- day 7 in the areas A-D. Countings were done in experiments without adding auxin gradients.

5.5. Effect of 1 µM NAA on regenerating BY-2 WT cells in the microfluidic channels

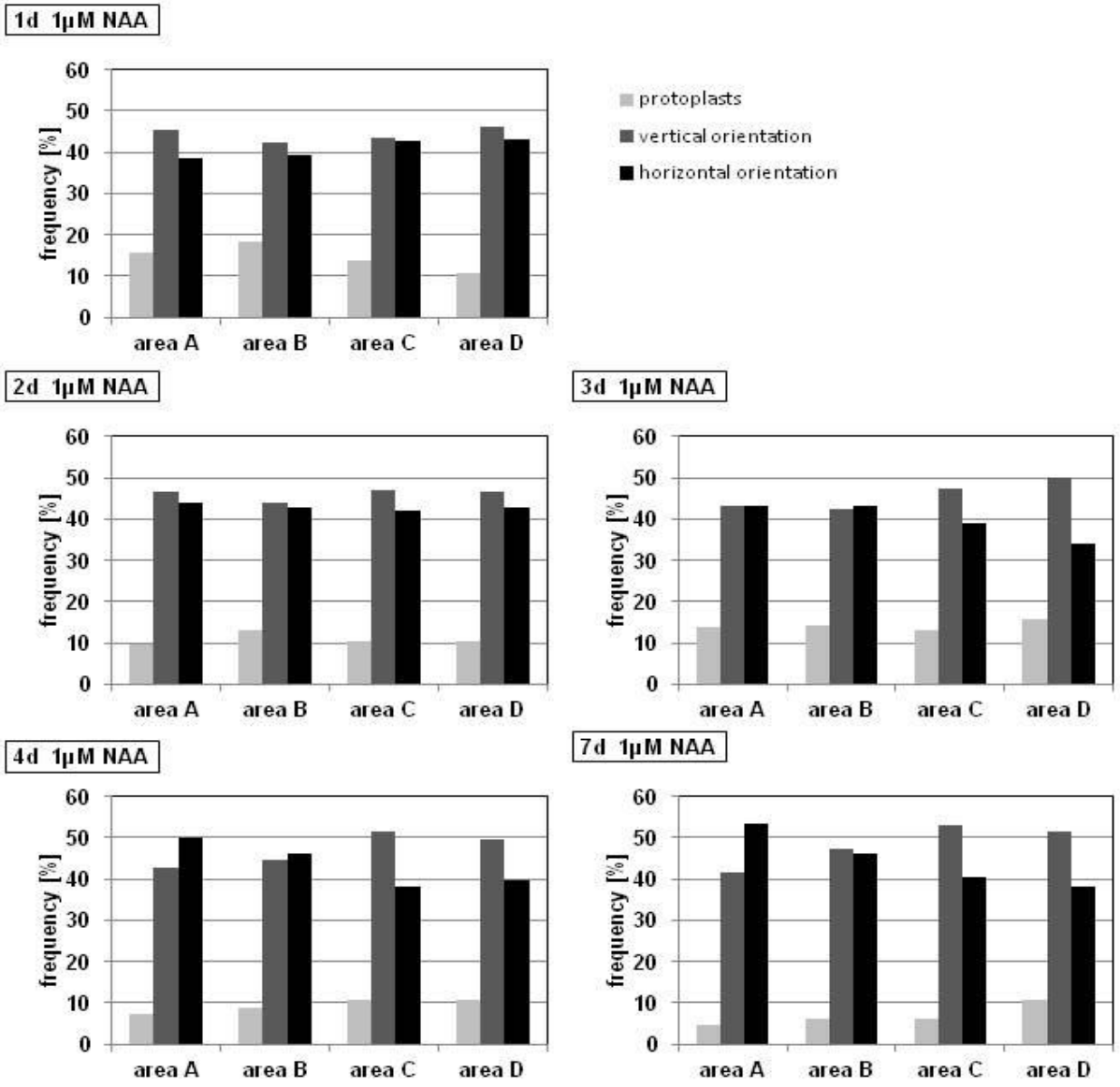

Complete data set on the NAA- treatment of non- transformed BY-2 WT cells within the microfluidic channels. The difference of the frequencies of the cell axis orientation on day 2 and day 3 is not significant different in the areas A and B. From day 3 on one can see that cell with vertical orientation of the cell axis are more frequent in the areas C and D.

5.6. Effect of 1 µM 2, 4- D on regenerating BY-2 WT cells in the microfluidic channels

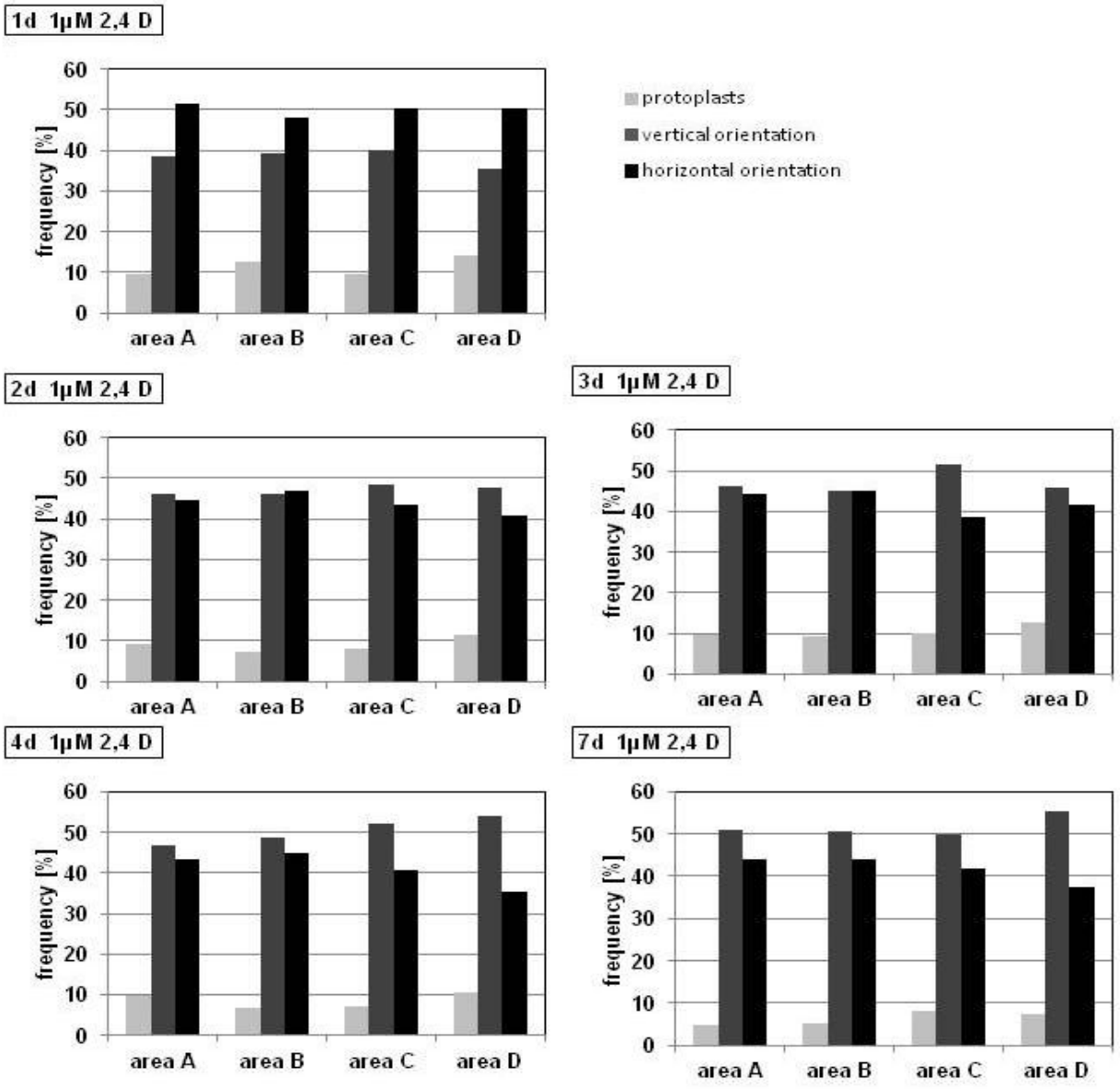

Complete data set on the 2, 4- D treatment of non- transformed BY-2 WT cells within the microfluidic channels. The difference of the frequencies of the cell axis orientation on day 2 and day 3 is not significant different in the areas A and B. From day 3 on one can see that cell with vertical orientation of the cell axis are more frequent in the areas C and D. Compared to the data set of the NAA treatment the differences in the frequencies of vertical and horizontal orientated cells at day 2 and day 3 are less obvious.

REFERENCES

- Akashi T, Kawasaki S, Shibaoka H (1990) Stabilization of cortical microtubules by the cell wall in cultured tobacco cells. Effects of extensin on the cold-stability of cortical microtubules. *Planta* 182:363–369
- Baluska F, Samaj J, Wojtaszek P, Volkmann D, Menzel D (2003) Cytoskeleton plasma membrane-cell wall continuum in plants. Emerging links revisited. *Plant Physiol.* 133:482-491
- Bayer EM, Smith RS, Mandel T, Nakayama N, Sauer M, Prusinkiewicz P, Cris Kuhlemeier C (2009) Integration of transport-based models for phyllotaxis and midvein formation. *Genes & Dev*. 23: 373-384
- Bayly R & Axelrod JD (2011) Pointing in the right direction: new developments in the field of planar cell polarity. *Nature Reviews Genetics* 12:385-391
- Bhatla SC, Kießling J, Reski R (2002) Observation of polarity induction by cytochemical localization of phenylalkylamine-binding receptors in regenerating protoplasts of the moss *Physcomitrella patens. Protoplasma* 219:99–105
- Bloch R (1965) Polarity and gradients in plants. A survey. In: Ruhland W, ed. *Encyclopedia of Plant Physiology. vol. 15. Springer- Verlag,* Heidelberg. pp. 234–274
- Bode PM, Bode HR (1984) Patterning in *Hydra. In: Malacinski GM,* Bryant SV, eds. *Pattern Formation. MacMillan, London New York.* pp. 213–241
- Boveri T (1901) Über die Polarität des Seeigeleies. *Verhandlungen der physikalisch-medizinischen Gesellschaft Würzburg* 34:145–175
- Brawley SH, Robinson KR (1985) Cytochalasin treatment disrupts the endogenous currents associated with cell polarization in fucoid zygotes: Studies of the role of F-actin in embryogenesis. *J. Cell Biol.* 100:1173–1184
- Brunoud G, Wells DM, Olivera M, Larrieu A, Mirabet V, Burrow AH, Beeckman T, Kepinski S, Traas J, Bennett MJ, Vernoux T (2012) A novel sensor to map auxin response and distribution at high-temporal resolution. Nature 482: 103-108

- Canut H, Carrasco A, Galaud JP, Cassan C, Bouyssou H, Vita N, Ferrara P, Pont-Lezica R (1998) High affinity RGD-binding sites at the plasma membrane of *Arabidopsis thaliana links the cell wall. Plant J.* 16:63–71
- Delbarre A, Meller P, Imhoff V, Guern J (1996) Comparison of mechanisms controlling uptake and accumulation of 2,4-dichlorophenoxy acetic acid, naphthalene-1-acetic acid, and indole-3-acetic acid in suspension cultured tobacco cells. *Planta* 198:532–541
- Dhonukshe P, Kleine-Vehn J, Friml J (2005) Cell polarity, auxin transport, and cytoskeleton-mediated division planes: Who comes first? *Protoplasma* 226:67–73
- Dhonukshe P, Tanaka H, Goh T, Ebine K, Mähönen AP, Prasad K, Blilou I, Geldner N, Xu J, Uemura T, Chory J, Ueda T, Nakano A, Scheres B. and Friml J. (2008) Generation of cell polarity in plants links endocytosis, auxin distribution and cell fate decisions. 0456:962–966
- Duan CQ, Zhang YM, Gao ZN (2012) Electrochemical Behaviors and Electrochemical Determination of 1-naphthaleneacetic Acid at an Ionic Liquid Modified Carbon Paste Electrode. Proc Natl Acad Sci USA 78:976–980
- Edwards ES, Roux SJ (1994) Limited period of graviresponsiveness in germinating spores of Ceratopteris richardii. Planta 195:150–152
- Edwards ES, Roux SJ (1997) The influence of gravity and light on developmental polarity of single cells of *Ceratopteris richardii* gametophytes. *Biol. Bull.* 192:139–140
- Emons AMC, Mulder BM (1998) The making of the architecture of the plant cell wall: How cells exploit geometry. *Proc. Natl. Acad. Sci. USA* 95:7215–7219
- Fischer R, Zekert N, Takeshita N (2008) Polarized growth in fungi- interplay between the cytoskeleton, positional markers and membrane domains. *Mol. Mbio.*68:813-826
- Fleming AJ, McQueen-Mason S, Mandel T (1997) Induction of Leaf Primordia by the Cell Wall Protein Expansin. *Science* 276:1415–1418
- Frey N, Klotz J, Nick P (2010) A kinesin with calponin-homology domain is involved in premitotic nuclear migration. *J. Exp. Bot.* 61:3423–3437
- Fu Y, Wu G, Yang Z (2001) ROP Gtpase–dependent dynamics of tip-localized F-actin controls tip growth in pollen tubes. *JCB* 152:1019-1032

- Fujita M, Himmelspach R, Hocart CH, Williamson RE, Mansfield SD, Wasteneys GO (2011) Cortical microtubules optimize cell-wall crystallinity to drive unidirectional growth in *Arabidopsis. Plant J.* 66:915–928
- Geitmann A, Ortega JK (2009) Mechanics and modeling of plant cell growth. *Trends Plant Sci.* 14:467–478
- Goldsmith MHM, Goldsmith TH, Martin MH (1981) Mathematical analysis of the chemosmotic polar diffusion of auxin through plant tissues. *Proc Natl Acad Sci USA* 78:976–980
- Goodner B, Quatrano RS (1993) *Fucus* embryogenesis: A model to study the establishment of polarity. Plant Cell 5:1471–1481
- Green PB (1962) Mechanism for plant cellular morphogenesis. *Science* 38:1404–1405
- Green PB (1980) Organogenesis – a biophysical view. *Annu. Rev. Plant Physiol.* 31:51–82
- Guenot B, Bayer E, Kierzkowski D, Smith RS, Mandel T, Zádníková P, Benková E, Kuhlemeier C (2012) PIN1-Independent Leaf Initiation in Arabidopsis. *Plant Physiol* 159:1501–1510
- Hable WE, Hart PE (2010) Signaling mechanisms in the establishment of plant and fucoid algal polarity. *Mol. Repr. Develop.* 77:751–758
- Haigler CH, Brown RM (1986) Transport of rosettes from the Golgi apparatus to the plasma membrane in isolated mesophyll cells of *Zinnia elegans during differentation to tracheary elements in* suspension culture. *Protoplasma* 134:111–120
- Hamant O, Heisler MG, Jönsson H, Krupinski P, Uyttewaal M, Bokov P, Corson F, Sahlin P, Boudaoud A, Meyerowitz EM, Couder Y, Traas J (2008) Developmental patterning by mechanical signals in Arabidopsis. *Science*, 22:1650–1655
- Hohenberger P, Eing C, Straessner R, Durst S, Frey W, Nick P(2011) Plant actin controls membrane permeability. *BBA Membranes* 1808:2304–2312
- Holweg CL (2007) Living markers for actin block myosin-dependent motility of plant organelles and auxin. *Cell Motil. Cytoskel*. 64:69–81
- Hošek P, Kubeš M, Laňková M, et al. (2012) Auxin transport at cellular level: new insights supported by mathematical modelling. *J Exp Bot* 63:3815–3827

- Jaffe LF (1966) Electrical currents through the developing *Fucus* egg.*Proc. Natl. Acad. Sci. USA* 56:1102–1109
- Kaye SB (1996) Paclitaxel in Cancer Treatment. *Br J Cancer* 73(3):414
- Klotz J, Nick P (2012) A novel actin-microtubule cross-linking kinesin, NtKCH, functions in cell expansion and division. *New Phytol. 193:*576–589
- Ko JM, Ju JI, Lee SH, Cha HC (2006) Tobacco protoplast culture in a polydimethylsiloxane-based microfluidic channel. *Protoplasma* 227:237–240
- Kranz E, Lörz H (1993) In vitro fertilization with isolated, single gametes results in zygotic embryogenesis and fertile maize plants. *Plant Cell* 5:739–746
- Kusaka N, Maisch J, Nick P, Hayashi KI, Nozaki H (2009) Manipulation of Intercellular Auxin in a Single Cell by Light with Esterase-Resistant Caged Auxins. *ChemBioChem* 10:2195–2202
- Kuss-Wymer CL, Cyr RJ (1992) Tobacco protoplasts differentiate into elongate cells without net microtubule depolymerization. *Protoplasma* 168: 64–72
- Li S, Lei L, Somerville CR, Gua Y (2012) Cellulose synthase interactive protein 1 (CSI1) links microtubules and cellulose synthase complexes. *Proc. Natl. Acad. Sci. USA* 109:185–190
- Lintilhac PM (1999) Towards a theory of cellularity − speculations on the nature of the living cell. *Bioscience* 49:60–68
- Lintilhac PM, Vesecky TB (1984) Stress-induced alignment of division plane in plant tissues grown *in vitro*. *Nature* 307:363–364
- Lomax TL, Muday GK, Rubery PH (1995) Auxin transport. *PJ Davies ed, Plant hormones: physiology, biochemistry, and molecular biology* 509-530
- Maeda H, Ishida N (1967) Specificity of binding of hexopyranosyl polysaccharides with fluorescent brightener. *J Biochem* 62:276–278
- Maisch J, Nick P (2007) Actin is involved in auxin-dependent patterning. *Plant Physiol* 143:1695–1704
- Maung SM & Jenny A (2011) Planar cell polarity in Drosophila. *Organogenesis* 7:165-179

- Merks RMH, Van de Peer Y, Inzé D, Beemster GTS (2007) Canalization without flux sensors: a traveling-wave hypothesis. *Trends Plant Sci* 12:384–290
- Murata T, Wada M (1991) Effects of centrifugation on preprophase Nagata T, Nemoto Y, Hasezawa S (1992) Tobacco BY-2 cell line as the “HeLa” cell in the cell biology of higher plants. *Int. Rev. Cytol.* 132:1–30
- Nagata T, Nemoto Y, Hasezawa S (1992) Tobacco BY–2 cell line as the "HeLa" cell in the cell biology of higher plants. *Int Rev Cytol* 132:1–30
- Nagata T, Takebe I (1970) Cell wall regeneration and cell division in isolated tobacco mesophyll protoplasts. *Planta* 92:301–308
- Nick P (1999) Signals, Motors, Morphogenesis -the Cytoskeleton in Plant Development. *Plant Biol* 1:159-169
- Nick P (2010) Probing the actin-auxin oscillator. Plant Signaling Behav 5:4–9
- Nick P (2011) Mechanics of the cytoskeleton. In: P. Wojtaszek, ed. *Mechanical Integration of Plant Cells and Plants. Springer-Verlag,* Berlin-Heidelberg. pp. 53–90
- Nick P, Furuya M (1992) Induction and fixation of polarity – Early steps in plant morphogenesis. *Dev. Growth Differ.* 34:115–125
- Nick P, Han M, An G (2009) Auxin stimulates its own transport by actin reorganization. *Plant Physiol* 151:155–167
- Niklas KJ, Spatz HC (2004) Growth and hydraulic (not mechanical) constraints govern the scaling of tree height and mass. *Proc Natl Acad Sci USA* 101:15661–15663
- Noblin X, Mahadevan L, Coomaraswamy IA, Weitz DA, Holbrook NM, Zwieniecki MA (2008) Optimal vein density in artificial and real leaves. *Proc Natl Acad Sci USA* 105:9140–9144
- Orvar BJ, Sangwan V, Omann F, Dhindsa RS (2000) Early steps in cold sensing by plant cells: The role of actin cytoskeleton and membrane fluidity. *Plant J.* 23:785–794
- Paciorek T, Zažimalová E, Ruthardt N, Petrášek J, Stierhof YD, Kleine-Vehn J, Morris DA, Emans N, Jürgens G, Geldner N, Friml J (2005) Auxin inhibits endocytosis and promotes its own efflux from cells. *Nature* 435:1251–1256

- Paredez AR, Somerville CR, Ehrhardt DW (2006) Visualization of cellulose synthase demonstrates functional association with microtubules. *Science* 312:1491–1495
- Peera WA, Blakeslee JJ, Yang H, Murphy AS (2011) Seven things we think we know about auxin transport. *Mol. Plant* 4:487–504
- Pel HJ, de Winde JH, Archer DB, Dyer PS, Hofmann G, Schapp PJ (2007) Genome sequencing and analysis of the versatile cell factory Aspergillus niger CBS 513.88. *Nat Biotechnol* 25:221-231
- Petrášek J, Mravec J, Bouchard R, BlakesleeJ.J, Abas M, Seifertová D, Wiśniewska J, Tadele Z, Kubeš M, Čovanová M, Dhonukshe P, Skůpa P, Benková E, Perry L,Křeček P, Lee O.R, Fink G.R, Geisler M, Murphy A.S, Luschnig C, Zažímalová E and Friml J (2006) PIN proteins perform a rate-limiting function in cellular auxin efflux. *Science* 312:914-918
- Pickard BG (2007) Delivering force and amplifying signals in plant mechanosensing. Curr. Top. Membr. 58:361–392
- Pickard BG (2008) “Second extrinsic organizational mechanism” for orienting cellulose: Modeling a role for the plasmalemmal reticulum. *Protoplasma* 233:1–29
- Preston RD (1955) Mechanical properties of the plant cell wall. In: W. Ruhland, ed. *Handbuch der Pflanzenphysiologie vol. 1. Springer-* Verlag, Berlin-Göttingen-Heidelberg. pp. 745–751
- Reinhardt D, Mandel T, Kuhlemeier C (2000) Auxin regulates the initiation and radial position of plant lateral organs. *Plant Cell* 12:507–518
- Reinhardt D, Pesce ER, Stieger P, Mandel T, Baltensperger K, Bennett M, Traas J, Friml J, Kuhlemeier C (2003) Regulation of phyllotaxis by polar auxin transport. *Nature* 426:255–260
- Rothwell GW, Lev-Yadun S (2005) Evidence of polar auxin flow in 375 million-year-old fossil wood . *Am J Bot* 92:903–906
- Sachs J (1880) Stoff und Form der Pflanzenorgane. *Arb. Bot. Inst. Würzburg 2,* 469–479
- Sachs T (1969) Polarity and the induction of organized vascular tissues. *Ann Bot* 33:263

- Sano T, Higaki T, Oda Y, Hayashi T, Hasezawa S (2005) Appearance of actin microfilament 'twin peaks' in mitosis and their function in cell plate formation, as visualized in tobacco BY-2 cells expressing GFP-fimbrin. *Plant J.* 44:595–605
- Sawchuk M. G. and Scarpella E. (2013) Polarity, Continuity, and Alignment in Plant Vascular Strands. J Int Plant Biol 55:824–834
- Saxena SK, Boersma L, Lindstrom FT, Young JL (1974) The Self-Diffusion Coefficients of 45Ca and 2,4-Dichlorophenoxyacetic Acid. Soil Science 117:14–20
- Scarpella E, Marcos D, Friml J, Berleth T (2006) Control of leaf vascular patterning by polar auxin transport. *Genes & Dev.* 20:1015–1027
- Sijacic L, Liu Z (2010) Novel insights from live-imaging in shoot meristem development. J. Integr. Plant Biol. 52:393–399
- Smertenko AP, Deeks MJ, Hussey PJ (2010) Strategies of actin reorganisation in plant cells. J. Cell Sci. 123:3019–3028
- Staiger CJ, Sheahan MB, Khurana P, Wang X, McCurdy DW, Blanchoin L (2009) Actin filament dynamics are dominated by rapid growth and severing activity in the Arabidopsis cortical array. JCB 184:269–280
- Sun Y, Liu Y, Qu W, Jiang X (2009) Combining nanosurface chemistry and microfluidics for molecular analysis and cell biology. *Anal Chim Acta* 650:98–105
- Takeshita N & Fischer R (2011) On the role of microtubules, cell end markers, and septal microtubule organizing centres on site selection for polar growth in *Aspergillus nidulans*. *Fungal Biology* 115:506-517
- Thomas C, Moreau F, Dieterle M, Hoffmann C, Gatti S, Hofmann C, Van Troys M, Ampe C, Steinmetz A (2007) The LIM Domains of WLIM1 define a new class of actin bundling modules. *J. Biol. Chem.* 282:33599–33608
- Thompson KS, Hertel R, Müller S, Tavares JE (1973) 1-N-naphthylphthalamic and 2, 3, 5-triiodobenzoic acids: in vitro binding to particulate cell fractions and action on auxin transport in corn coleoptiles. *Planta* 109:337–352
- Turing AM (1952) The chemical basis of morphogenesis. Phil Trans R Soc London 237: 37-72

- Twell D, Park SK, Lalanne E (1998) Asymmetric division and cell-fate determination in developing pollen. Trends Plant Sci. 3:305–310
- Ueda H, Yokota E, Kutsuna N, Shimada T, Tamura K, Shimmen T, Hasezawa S, Dolja VV, Hara-Nishimura I (2010) Myosindependent endoplasmic reticulum motility and F-actin organization in plant cells. *Proc. Natl. Acad. Sci. USA* 107:6894–6899
- Vöchting H (1878) Über Organbildung im Pflanzenreich. Cohen, Bonn
- Wang YS, Yoo CM, Blancaflor EB (2008) Improved imaging of actin filaments in transgenic *Arabidopsis plants expressing a green* fluorescent protein fusion to the C and N-termini of the fimbrin actinbinding domain 2. *New Phytol.* 177:525–536
- Weismann A (1892) The Germ Plasm: A theory of heredity. *Charles Scribners Sons*
- Wheeler TD, Stroock AD (2008) The transpiration of water at negative pressures in a synthetic tree. *Nature* 455:208–212
- Williams JG (1988) The role of diffusible molecules in regulating the cellular differentiation of *Dictyostelium discoideum. Development* 103:1–16
- Wu H, Liu W, Tu Q, Song N, Li L, Wang J, Wang J (2011) Culture and chemical-induced fusion of tobacco mesophyll protoplasts in a microfluidic device. *Microfluid Nanofluid* 10:867–876
- Wyatt SE, Carpita NC (1993) The plant cytoskeleton – cell wall continuum. *Trends Cell Biol.* 3:413–417
- Wymer C, Wymer SA, Cosgrove DJ, Cyr RJ (1996) Plant cell growth responds to external forces and the response requires intact microtubules. *Plant Physiol.* 110:425-430
- Yeung K & Paterson I (2002) Actin-bindende marine Makrolide: Totalsynthese und biologische Bedeutung. Angewandte Chemie 114:4826-4847
- Zaban B, Maisch J, Nick P (2013) Dynamic actin controls polarity induction de novo in protoplasts*. J Int Plant Biol* 55:142-159
- Zaban B, Liu W, Xiang J, Nick P (2014) Plant cells use auxin efflux to explore geometry. *Scientific Reports* 4:5842